

FINAL PUBLISHABLE REPORT

Grant Agreement number	14IND04
Project short name	EMPRESS
Project full title	Enhancing process efficiency through improved temperature measurement
Period covered:	From 1 May 2015 To 30 April 2018
Coordinator:	
Name, title, organisation:	Jonathan Pearce, NPL
Tel:	+44 (0)20 8943 6886
Email:	jonathan.pearce@npl.co.uk
Website address:	https://www.strath.ac.uk/research/advancedformingresearchcentre/whatwedo/collaborativeprojects/empressproject/
Other partners:	<ul style="list-style-type: none"> 1 NPL, United Kingdom 2 BRML, Romania 3 CEM, Spain 4 CMI, Czech Republic 5 DTI, Denmark 6 DTU, Denmark 7 INRIM, Italy 8 JV, Norway 9 PTB, Germany 10 Elkem, Norway 11 GF, Italy 12 MUT, Germany 13 STRATH, United Kingdom 14 UC3M, Spain 15 UCAM, United Kingdom 16 UOXF, United Kingdom 17 BAE, United Kingdom 18 CCPI, United Kingdom

TABLE OF CONTENTS

Glossary	3
1 Executive summary	4
2 Need for the project	5
3 Objectives	8
4 Results	8
4.1 Low-drift contact sensors to above 2000 °C	8
4.1.1 Development of new and optimised Pt-Rh thermocouples	9
4.1.2 Development of a sapphire tube thermometer	11
4.1.3 Development of carbon thermocouples	12
4.2 Zero-drift contact temperature sensors to 1350 °C	15
4.2.1 Development of self-validating thermocouples	15
4.2.2 Evaluation of mineral-insulated ultra-stable high temperature thermocouples	17
4.3 Traceable surface temperature measurement with contact sensors	21
4.3.1 Development of phosphor thermometers – NPL	21
4.3.2 Development of phosphor thermometers – INRIM	28
4.3.3 Development of phosphor thermometers – in-process trials at Gamma Forgiati (GF)	30
4.3.4 Development of phosphor thermometers – in-process trials at BAE Systems	32
4.3.5 Heat flux compensated probe and block calibrator	35
4.3.6 Surface temperature probe calibrator at DTI	37
4.4 Traceable combustion temperature measurement	38
4.4.1 Development of a portable standard flame system	38
4.4.2 Development of a FTIR flame thermometry system	39
4.4.3 Development of a UV flame thermometry system	42
4.4.4 Development of the DFWM and LIGS laser based thermometers	43
4.5 Overall summary of results	44
5 Impact	45
5.1 Summary of dissemination activities	45
5.2 Impact on industrial and other user communities	47
5.3 Impact on the metrological and scientific communities	49
6 List of publications	51
7 Website address and contact details	51
8 References	52

Glossary

AFRC	Advanced Forming Research Centre, part of the University of Strathclyde (STRATH)
ASME	American Society of Mechanical Engineers
ASTM	American Society for Testing and Materials
BIPM	International Bureau for Weights and Measures
BS	British Standard
CARS	Coherent anti-Stokes Raman spectroscopy
CCT	Consultative Committee for Thermometry, part of the BIPM
DFWM	Degenerate Four-Wave Mixing, a type of flame thermometry
EC	European Commission
EU	European Union
FTIR	Fourier Transform Infrared Spectroscopy
IEC	International Electrotechnical Commission
InstMC	Institute of Measurement and Control
IoP	Institute of Physics
IPCC	Integrated Pollution Prevention and Control
IR	Infrared
ISAT	Instrument Science and Technology Committee, part of the IoP
ISO	International Standards Organisation
ITS-90	International Temperature Scale of 1990
LIGS	Laser induced grating spectroscopy
MI	Mineral insulated, metal sheathed, a specific type of flexible thermocouple assembly
Nadcap	National Aerospace and Defence Contractors Accreditation Program
NMI	National Measurement Institute
NOx	Generic term for nitrogen oxides that are most relevant for air pollution
NPL STD	NPL standard
PRT	Platinum resistance thermometer
Pt-Rh	Platinum-rhodium alloy
RMG	EURAMET Researcher Mobility Grant
SAE	SAE International, a global association of technical experts
TC-T	EURAMET Technical Committee for Thermometry
UKAS	United Kingdom Accreditation Service
UN	United Nations
UV	Ultraviolet

1 Executive summary

The overall objective of the project is to significantly enhance the efficiency of high value manufacturing processes by improving temperature measurement capability. High value manufacturing is heavily reliant on accurate, traceable temperature measurement. Traceability of temperature measurements to the International Temperature Scale of 1990 (ITS-90) is a critical factor in establishing low measurement uncertainty and reproducible, consistent process control, and introducing such traceability *in-situ* (i.e. within the industrial process) is a theme running through this project.

For applications above 1300 °C (e.g. casting, forging and sintering) there is a need for more stable sensors and standardisation of at least one new thermocouple type to fill the gap between 1500 °C and 1800 °C. Above 1800 °C, only tungsten-rhenium (W-Re) thermocouples are widely available, but their erratic performance renders them very unsatisfactory for long-term measurement. At lower temperatures below 500 °C, reliable welding of high strength steel requires specific heat treatment processes pre- and post-weld. This is subject to a range of standards, but manufacturers often experience extreme difficulty with compliance in obtaining sufficiently low uncertainties due to the limitations of surface temperature measurement (by contact sensors). Forming of metal and composites to 500 °C is also subject to these issues, which is holding back uptake of new, more efficient furnace technology. Measurement of combustion temperature is extremely difficult and prone to large errors, e.g. thermocouple measurements of flame temperatures can be in error by hundreds of degrees. Traceability of flame and combustion thermometry is non-existent. What is needed is a portable 'standard flame' whose temperature is traceably calibrated, which may be used to calibrate other combustion temperature sensors or measurement methods.

To address these difficulties, a four-fold approach was taken. To **reduce the uncertainty of temperature measurement in-process**, more stable thermocouples have been developed and evaluated; these include the identification of a Pt-Rh thermocouple (Pt-40%Rh vs. Pt-6%Rh) optimised with respect to thermoelectric stability (i.e. minimised calibration drift) for use to 1800 °C, development of a sapphire tube based blackbody sensor for use in silicon processing to 1600 °C, development of a carbon thermocouple for use to over 2000 °C (which ultimately exhibited good stability up to 1500 °C, but could not be stabilised at higher temperatures). To implement **in-situ traceability of temperature measurement in-process**, ultra-low drift sensors have been developed and assessed. The two key developments here are a) a mineral-insulated, metal-sheathed thermocouple with a double wall construction which has exhibited stability a factor of 10 better than conventional equivalent thermocouples, and b) a self-validating thermocouple which uses a built-in traceably calibrated fixed point cell to provide *in-situ* self-calibration. To implement **traceable surface temperature measurement in-process**, a suite of thermometry techniques has been developed which are based on phosphor thermometry, as well as a contact probe which automatically compensates for heat flows; a key output is a surface probe calibrator based on phosphor thermometry. To introduce **traceability to combustion temperature measurement**, a portable standard flame has been commissioned and thoroughly characterised; this is now an artefact which can be transported to end-users' facilities to traceably calibrate flame and combustion thermometry instrumentation. All these developments have been subjected to trials in a wide range of industrial processes to demonstrate their viability, including, but not limited to silicon processing, heat treatment furnaces for aerospace components, ceramic manufacturing, welding of large scale marine steel components, and forging of automotive components.

Early impact looks promising. CCPI and UCAM have entered a commercial partnership during the lifetime of the project and the validation performed during EMPRESS will play a key role in bringing the benefits of the new double wall MI thermocouple technology to end-users. Presentation of the results to the IEC committee responsible for IEC 61515, and the SAE committee responsible for NADCAP standards e.g. AMS2750E will facilitate uptake in critical applications in aerospace manufacturing. The phosphor thermometry developments are the subject of great interest and the consortium has been approached by several companies looking to license the know-how on two fronts: a) for direct application to processing challenges and b) for calibration equipment e.g. surface probe calibrators. It is also being used in trials in high temperature mechanical testing (critical for gas turbine development) and is underpinning further developments in the follow-on EMPRESS2 project; examples include combination with fibre-optics, and combination with thermography (thermal imaging) to overcome the problem of unknown emissivity; this is applicable to a wide range of process challenges in high value manufacturing. The portable standard flame is now an artefact available to end-users; its use is already envisaged for waste incineration/power generation applications and development of economical flame imaging instrumentation.

2 Need for the project

Manufacturing contributes over €8 trillion of value added to the global economy [1], of which 22 % is due to the European Union (EU). Modern high value manufacturing is a vital part of the economy of numerous EU countries; e.g. aerospace, which employs more than 500,000 people distributed throughout the EU and has a turnover of more than €105 billion [2, page 32]. Key areas of research and development in the aerospace sector are improving engine efficiency by maximising the temperature rise through the combustor and reducing airframe weight by using new materials¹ and implementing more efficient production processes. All of these key areas require improved temperature measurement. Facilitating links between the EU Member States and their collaboration on matters of aviation research has been identified as a priority by the Advisory Council for Aeronautics Research in Europe (ACARE) [3, page 92], who in particular called for a 50 % reduction of greenhouse gas emissions per passenger kilometre by reducing airframe weight and increasing engine fuel efficiency in equal measure [4]. Many challenges associated with improving aircraft engine fuel efficiency stem from the requirement to maximise the temperature rise through the combustor² [6, page 8]. More generally, most industrial processes need to be maintained at a specific temperature to maximise efficiency. Accurate control of temperature ensures process efficiency; by improving temperature measurement techniques for selected applications, this project has enhanced the efficiency of high value manufacturing processes, in terms of reduced wastage, improved yield, more consistent processing, increased intervals between sensor checks and maintenance, increased reliability, improved energy efficiency, and reduced greenhouse gas emissions.

The EC Efficiency Plan [7] outlines the importance of enhancing efficiency to increase the competitiveness of European manufacturing industry, which accounts for about 25 % of the EU's energy consumption. The need for better process control has been brought to the fore by the EU's introduction of a legislative framework to enforce emissions levels of new vehicles [8] by imposing fuel efficiency targets [9] in recognition of this sector's vast contribution (20 %) to overall EU emissions.

Low-drift contact sensors

Important gaps exist in temperature measurement capability in the aerospace and energy sectors, particularly in heat treatment and forging of components, casting of exotic single-crystal alloys and combustion temperature measurement. Challenges remain for manufacturers in mitigating drift of thermocouples, which are used almost exclusively for process control. Processing of refractory materials, such as ceramics and nuclear fuel, is still inefficient above 1800 °C due to inaccuracies in temperature control. Semiconductor processing is not always amenable to the use of thermocouples for process control, so to address this gap, an optical solution is needed.

The current state of the art for contact thermometry measurements between 1300 °C and 1600 °C comprises noble metal thermocouples, Type R (Pt-13%Rh vs. Pt), Type S (Pt-10%Rh vs. Pt), and Type B (Pt-30%Rh vs. Pt-6%Rh). These are known to drift, often by several degrees, and in an unpredictable manner, so their performance is limiting the efficiency of a number of advanced manufacturing processes such as specialist casting and heat treatment of critical aerospace components, so much so that zero waste manufacture in-process is currently unobtainable. Above about 1600 °C only the W-Re thermocouple contact sensor is routinely available; this is subject to drift of > 10 °C and an uncertainty when new of 1 % of temperature (20 °C at 2000 °C). A key standard for the aerospace manufacturing supply chain is AMS 2750 E [10] which specifies the temperature measurement and control requirements for a number of aspects of manufacturing. Importantly, Clause 3.1.2.3 of AMS2750E states that although the standard specifies calibration intervals for particular thermocouple types, the user is responsible for ensuring that excessive drift has not occurred during the process. For example, Class 1 Types R, S and B thermocouples used for controlling a process may not be recalibrated (Table 1 of AMS2750E [10]), and the maximum permitted error is of the order of 1 °C. Achieving greater confidence in compliance is an urgent need. To address this, it is necessary to identify and characterise Pt-Rh alloys with superior thermoelectric stability (to 1800 °C) to the standard Type R, S and B thermocouples, which, although in widespread use, for historical reasons are not necessarily optimal in performance³ [11], and

¹ The Airbus A350 XWB airframe is 53% composite, and 33 % Al and Ti alloys. The wings are nearly 100 % composite.

² To see the effect of temperature on efficiency e of a heat engine operating in ambient temperature $T_c = 298$ K, a temperature increase of 10 °C of an engine operating at $T_h = 873$ K results in an efficiency increase of 0.8 %. Note the achievable efficiency is significantly lower than the commonly cited Carnot efficiency due to irreversible processes involved in real systems. A modified Carnot expression should be used, $e = 1 - (T_c / T_h)^{1/2}$ [5, page 127].

³ For example, the Pt-13%Rh vs. Pt (Type R) thermocouple arose because Pt-10%Rh vs. Pt (Type S) thermocouples of English manufacture accidentally included about 0.34 % iron in the early 20th century, giving a significantly higher emf (voltage) than that of Type R. By the time this was discovered, the thermocouples were in widespread use. The Pt-13%Rh thermocouple (Type R) was then developed to give the same output as that of Type S thermocouples contaminated with iron. No optimisation at all was involved in its development.

develop a reference function⁴ using the techniques established in WP6 of the EMRP project IND01 HiTeMS to supplement the current provisions of relevant standards e.g. ASTM E1751 [12]⁵. For temperatures above 1800 °C an alternative such as carbon thermocouples must be investigated. In some processing environments thermocouples are not suitable, such as silicon and semiconductor processing applications; for these, optical-based sensors such as those using single-crystal sapphire light guides are needed, with an uncertainty of less than 1 °C as demonstrated in-process.

Zero-drift contact temperature sensors

For long-term measurements, e.g. heat treatment and creep testing, the unknown drift of the control or monitoring thermocouples can cause serious errors in the reading, leading to loss of product. The principal mitigation method is to replace the sensors at frequent intervals, which is costly and potentially disruptive to the process. This needs to be addressed by a) developing and trialling in-process self-validating thermocouples, eliminating the cost and time penalties incurred by continual process interruption; and b) trialling, in-process, new mineral-insulated metal-sheathed (MI) cable as a more stable substitute for Type K or N thermocouples. Self-validating thermocouple prototypes, which make use of a high temperature fixed-point reference with invariant melting temperature mounted on the tip of a thermocouple to provide traceable in-situ calibration, have been successfully used with refractory thermocouples in a space application [13]. They have been further developed in the EMRP project IND01 HiTeMS and industrial users have shown strong interest, but the general feedback is that they are still too large to employ in most industrial applications. There is an urgent need to reduce the dimensions of the fixed-point artefacts to a size commensurate with use in industrial environments i.e. without requiring new sensor placements. The temperature measurement uncertainty, in-process, for Pt-Rh thermocouples needs to be reduced to less than 1 °C up to 1500 °C for at least 6 months use.

Below about 1300 °C the ‘work horse’ of industrial temperature measurement in industry is the Type N MI cable thermocouple. While not as stable or accurate as noble metal thermocouples, it is generally a factor of about 100 less expensive. A novel MI cable formulation has been developed by UCAM [14] with an extra wall to protect the thermoelements from the Mn and Cr contaminants which cause instability. In addition, this new thermocouple type can operate at temperatures as high as 1370 °C, currently not achievable with conventional Type N thermocouples. Early indications are that this MI cable is about 10 times more stable than conventional MI cable, but there is an urgent need for independent, impartial assessment of the metrological performance of this new device. In addition, trials have been performed in real-world industrial processing environments such as heat treatment of high-value single-crystal alloy turbine blades.

Surface temperature

An area of growing importance in advanced manufacturing is surface temperature measurement where uncertainties are unacceptably large. Growing use of light composite materials and aluminium alloys introduces new challenges associated with welding, forging and forming; placing high demands on surface temperature measurement techniques to ensure adequate pre- and post-welding/forming heat treatment. Improved forming techniques are identified as a priority in the EU publication ‘Factories of the Future’ [15]. The demand for ever stronger steel structures in marine and submarine applications, including offshore structures for e.g. renewable energy and oil/gas platforms, is also growing [16], which places high demand on welding quality and strength.

For temperatures up to about 500 °C, surface temperature measurement by contact thermometry is very problematic, and yet critical for a wide range of industrial processes. In marine construction for example (ships, submarines, oil, gas and renewable energy platforms) the use of temperature sensitive crayons to determine pre-weld temperature range is widespread, but the results are very subjective and non-traceable. Surface contact sensors are used but poorly characterised and also prone to subjectivity. Infra-red thermometry is beset with emissivity problems which often give rise to readings in error by tens or even hundreds of degrees, and is not robust enough for routine use in the marine manufacturing sector. More advanced techniques such as phosphor thermometry and dynamically compensating sensors (which compensate errors due to stray heat flows) are difficult to obtain commercially and are often not suitable for use by process engineers, so a simplified ‘turn-key’ system needs to be developed.

These new techniques need to be adapted for use in high value manufacturing processes. Post-weld heat treatment is an essential variable in all of the key welding procedure specifications. For example, heat

⁴ Characteristic relationship between thermocouple emf and temperature.

⁵ The ASTM E1751 standard [12] defines the relationship between thermocouple emf and temperature for non-letter designated thermocouples, permitting the use of this group of thermocouples to measure temperatures either directly or following calibration.

treatment temperatures for carbon steel welds made in accordance with the requirements of BS EN 13445:2009 [17], ASME VIII [18] and PD 5500 [19] are between 550 °C and 600 °C. ISO 15614-1 (2004) Clause 8.412 [20] specifies that post-weld heat treatment should be within ± 20 °C of the specified temperature. It is specified in BS EN 13445-4:2009 Clause 10.4.4 [17] that thermocouples shall be used for temperature sensing; direction in this standard are given which assume a precision/accuracy in temperature sensing of much better than 10 °C. This is unrealistic: despite sensors having a manufacturer stated accuracy of the order of 0.3 °C [21, pages 18-21], actual errors of tens of degrees may arise, for a variety of reasons, varying widely with surface type [22]. Thus any new surface calibration techniques should permit the insertion of the actual material of interest e.g. marine steel as the calibrator plate against which the surface temperature probe can be contacted.

Preparation of steel surfaces for application of coatings means ensuring the temperature of the steel is at least 3 °C above the dew point prior to applying the coating, which requires accurate surface temperature measurement. For this, many steel structure construction processes (e.g. marine and nuclear) are subject to the BS EN ISO 8502-4:2000 standard [23], which requires surface thermometers accurate to ± 0.5 °C. This accuracy, for this type of thermometer, is currently unachievable.

In forging and forming, the lack of suitable temperature sensors is limiting replacement of gas-fired convection furnaces with more modern, energy efficient infra-red (IR) furnaces. Rapid heating using IR furnaces can substantially reduce preheating and heat treatment cycle times, and is inherently more energy efficient, thus reducing energy consumption and increasing process productivity. Furthermore rapid pre-heating of billets in forging using IR furnaces reduces the final grain size (hence improving strength) in some aluminium alloys by an order of magnitude [24]. The new surface temperature sensors in this project will directly enable wider uptake of the new furnace technology.

Two new techniques have been developed for traceably calibrating contact surface temperature probes based on phosphor thermometry which is free of heat flow and emissivity problems, and additionally a dynamically compensated probe has been developed and proven. The project has also developed a practical phosphor thermometer, and directly applied this to industrial problems, specifically welding of large marine steel components and forging of automotive components, with an uncertainty of better than 5 °C.

Combustion thermometry

Accurate temperature measurement is also required in combustion and flame processes, which is important for manufacturing (e.g. steel and cement) and for heat engines (e.g. internal combustion engines and gas turbines) used in transport. Currently, traceability of combustion thermometry to the International Temperature Scale (ITS-90) [30] does not exist. Combustion is the prime source of the world's energy, whether for industrial production e.g. blast furnaces, transport, electricity generation, or space heating. Hydrogen remains an important fuel alternative in the automotive and power generation sectors, and combustion temperature measurement is a key aspect of syngas⁶ and other hydrogen-enriched gas combustor designs [25]. Currently, the most accurate means of measuring temperatures of combustion processes are generally optical methods such as Coherent Anti-Stokes Raman Spectroscopy (CARS), Degenerate Four Wave Mixing (DFWM) or more recently Laser Induced Grating Spectroscopy (LIGS). Thermographic phosphors are also sometimes deployed to measure the temperature of the flame. However, despite the sophistication of these optical methods the absolute temperatures have uncertainties of typically between 5 % and 10 % of temperature. This situation limits the efficiency of combustion processes, makes efforts to improve efficiency extremely difficult [26], and hinders the improvement of heat engines and other combustion processes. The high temperatures generated by combustion processes have a direct influence on a variety of factors including chemical reaction rates, process efficiency, pollutant levels, product quality, and rate of failure mechanisms [27]. It is therefore of great importance to determine the temperature with the best possible accuracy. Thermocouples are still widely used in this context due to their simplicity and low cost, and a large proportion of traceability in the combustion industry is via corrected thermocouples. However, thermocouple gas thermometry is subject to numerous errors resulting from the complex interaction between the thermocouple and its environment [28]. Non-contact laser diagnostic techniques avoid these problems but are generally technically complex, and none have traceability to temperature standards. To advance the state of the art, a standard flame needs to be commissioned, that has a known temperature traceable to ITS-90, and that can be transported to an end-user's site and used to validate the optical temperature measuring methods. This portable standard flame must be validated against a suite of complementary flame characterisation techniques. The uncertainty of flame temperature measurement needs to be reduced by a factor of 10 when compared to current methods.

⁶ Syngas is a hydrogen-rich fuel gas comprising a mixture of H, CO, CO₂, and diluents such as steam and N₂.

Summary

The range of temperature measurement improvements in this project have the potential to reduce energy consumption, improve yield, improve consistency and reliability, reduce emissions, and enhance overall process efficiency. Helping improve process efficiency for high value manufacturing is identified as a priority target in the EURAMET TC-T roadmap [29]: the route is via new thermocouples and self-validating sensors for harsh environments. Many modern industries have a global presence: parts are manufactured and brought together from diverse locations for assembly; assured in-process traceability of measurements to the ITS-90 is essential for product consistency and reproducible processes: this is built-in to all the solutions generated in this project. In summary there is a well-documented industrial need for:

- Better traceable process control of heat treatment and casting applications
- Better traceable contact surface temperature measurement for welding, joining, forging and forming
- Better traceable combustion temperature measurement for industrial processing and heat engines

3 Objectives

The overall objective of the project is to significantly enhance the efficiency of high value manufacturing processes by improving temperature measurement capability. The specific technical objectives of the project were to:

1. Develop novel low drift temperature sensors for enhanced production and temperature control by developing novel sensors suitable for high data capture rate in the same format as current sensors, with in-process traceable uncertainty of better than 3 °C at temperatures around 1450 °C and better than 5 °C at temperatures > 2000 °C.
2. Develop non-drift contact sensors optimised for heat treatment applications to temperatures around 1350 °C. The aim is for the sensors to remain in service, with a stability of better than 1 °C, for at least 6 months and be implemented in-process in at least one industrial setting.
3. Develop traceable surface temperature measurement methods to enhance materials/chemical processing to around 500 °C, with a target uncertainty of better than 5 °C. The methods aim to allow the calibration of surface temperature sensors using at least one novel surface temperature approach; and will be used to demonstrate improved temperature measurement in at least two industrial settings.
4. Develop an *in-situ* combustion standard of known temperature for the validation of flame temperatures. The combustion standard aims to have an uncertainty of less than 1 %, a factor of 10 lower than current methods and be tested in at least two industrial settings.
5. Ensure that the outputs from the project are effectively disseminated to, and exploited by, the high value manufacturing sector (e.g. automotive, aerospace, casting, heat treatment and sensor manufacturers). The take up of the novel sensor and sensing methods developed in the project will be facilitated to support the development of new, innovative products and services, enhancing the competitiveness of EU industry.

4 Results

In this section the project's technical outputs are presented against each of the objectives, on an objective by objective basis.

4.1 Low-drift contact sensors to above 2000 °C

State of the art

The current state of the art for contact thermometry measurements between 1300 °C and 1600 °C comprises noble metal thermocouples, Type R, S and B. These are known to drift, often by several degrees, and in an unpredictable manner, so their performance is limiting the efficiency of a number of advanced manufacturing processes such as specialist casting and heat treatment of critical aerospace components, so much so that zero waste manufacture in-process is currently unobtainable. Above about 1600 °C only the W-Re

thermocouple contact sensor is routinely available; this is subject to drift of $> 10\text{ }^{\circ}\text{C}$ and an uncertainty when new of 1 % of temperature ($20\text{ }^{\circ}\text{C}$ at $2000\text{ }^{\circ}\text{C}$).

The state of the art has been advanced by identifying Pt-Rh alloys with superior thermoelectric stability (to $1800\text{ }^{\circ}\text{C}$) to the standard Type R, S and B) by means of a pan-European determination of the reference function using the complementary calibration facilities of a number of NMIs. Above $1800\text{ }^{\circ}\text{C}$, the state of the art has been advanced by developing carbon thermocouples with a stability of better than $5\text{ }^{\circ}\text{C}$ above $2000\text{ }^{\circ}\text{C}$, as demonstrated by trials in an industrial process. For processing environments where thermocouples are not suitable, such as those involving silicon, a sensor based on a single-crystal sapphire light guide with a blackbody at the tip has been developed.

4.1.1 Development of new and optimised Pt-Rh thermocouples

Optimisation

Thermocouples based on alloys of Pt and Rh are in widespread use. Their chief advantage is their excellent thermoelectric stability and the fact that, with appropriate compositions, they can be used up to about $1800\text{ }^{\circ}\text{C}$. However, to the authors' knowledge the selection of Pt-Rh alloys in common use (i.e. Type R, S, B [31] and Land-Jewell [32,33]) have not been subjected to optimisation [11]. A new technique for determining an optimal pair of Pt-Rh wires to minimise thermoelectric drift is demonstrated based on two factors. Firstly, a recent demonstration that the high-temperature thermoelectric stability of Pt-Rh alloy wires improved with the mass fraction of Rh [34]. Secondly, the likelihood that, barring significant contamination, the most important factor governing thermoelectric stability and homogeneity of Pt-Rh wires is oxide vapour transport [35-38]. We report on the results of a multi-wire thermocouple continuously exposed to high temperature and repeatedly calibrated in-situ. A key benefit of the advent of high temperature fixed points based on metal-carbon eutectic alloys (HTFPs) [39,40] is the ability to quantify the stability of thermocouples above $1100\text{ }^{\circ}\text{C}$ with unprecedented accuracy. In these measurements, in-situ calibrations were performed using the Co-C [41] and Pd-C [42] fixed points at temperatures of $1324\text{ }^{\circ}\text{C}$ and $1492\text{ }^{\circ}\text{C}$ respectively [43].

In the NPL measurement, seven wires (Pt-5%Rh, Pt-8%Rh, Pt-10%Rh, Pt-13%Rh, Pt-20%Rh, Pt-30%Rh and Pt-40%Rh) were used to construct a multi-element thermocouple, again having a common measurement junction. This thermocouple was held at $1315\text{ }^{\circ}\text{C}$ and calibrated repeatedly at $1324\text{ }^{\circ}\text{C}$ in-situ, providing extremely accurate measurements of the stability of each of the large number of pairs of wires. The procedure followed by PTB was the same as that of NPL, except that the pairs measured were Pt-40%Rh/Pt-10%Rh (denoted 40/10), 30/10, 25/10, 20/10, 17/10, 30/17, 40/13, 30/13, 25/13, 20/13, 40/20, 40/17, and 25/17, and calibrations were performed in a dedicated calibration furnace. The stability of the 7-wire thermocouple as measured by repeated calibrations at the Co-C and Pd-C fixed points (NPL) is shown in Figure 4.1.1. An analysis of the stability and resulting optimal thermocouple using these measurements has been presented in depth in [43]. From these measurements the optimum thermocouple composition can be obtained, i.e. that corresponding to zero drift; in this case, the most stable composition was identified as the Pt-40%Rh versus Pt-6%Rh. A draft reference function was evaluated for this thermocouple by CEM, NPL, PTB and the Republic of Korea NMI, KRISS. The thermocouple was then trialled in industrial processes to assess its usability.

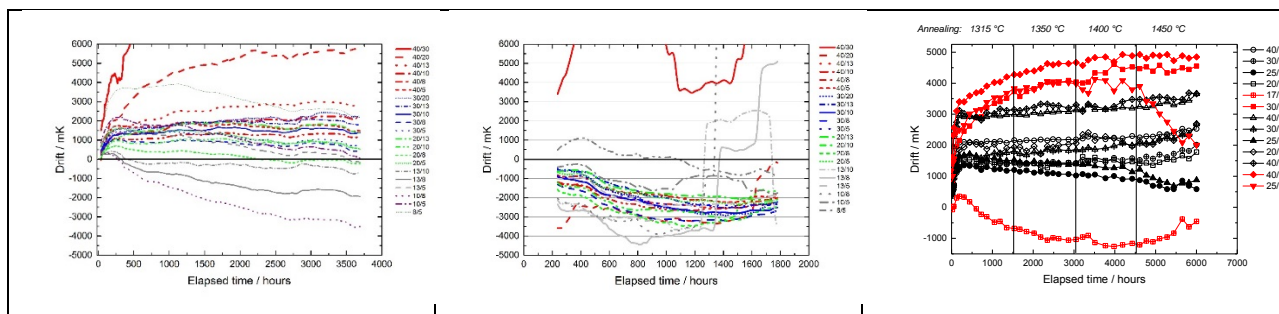


Figure 4.1.1: Drift of the NPL Pt-Rh thermocouples at $1324\text{ }^{\circ}\text{C}$ (left), NPL at $1492\text{ }^{\circ}\text{C}$ (middle) and PTB at $1315\text{ }^{\circ}\text{C}$ (right).

AFRC measurements

At the Advanced Forming Research Centre (AFRC, University of Strathclyde) a Pt-40%Rh/Pt-6%Rh thermocouple calibrated at NPL before, was tested in an industrial furnace up to $1200\text{ }^{\circ}\text{C}$. Figure 4.1.2 shows a schematic of the installation of the thermocouple. It should be noted, that no cold junction compensation was applied, because the Seebeck coefficient at room temperature is very low ($S < 0.5\text{ }\mu\text{V/K}$ in the temperature range $0\text{ }^{\circ}\text{C}$ to $30\text{ }^{\circ}\text{C}$). The connections between the thermocouple wires and copper wires were kept in an enclosure with air bubble packing to provide a suitable insulation. The furnace temperature was measured

separately by using a type N thermocouple of 6 mm outer diameter inserted inside two protection sheaths of dissimilar material: a ceramic sheath of 15.3 mm external diameter placed within a large Inconel 600 metal enclosure of 21.3 mm diameter. This thermocouple was located below the Pt40%Rh-Pt6%Rh thermocouple and at the same distance from the internal refractory wall as Figure 4.1.2 shows.

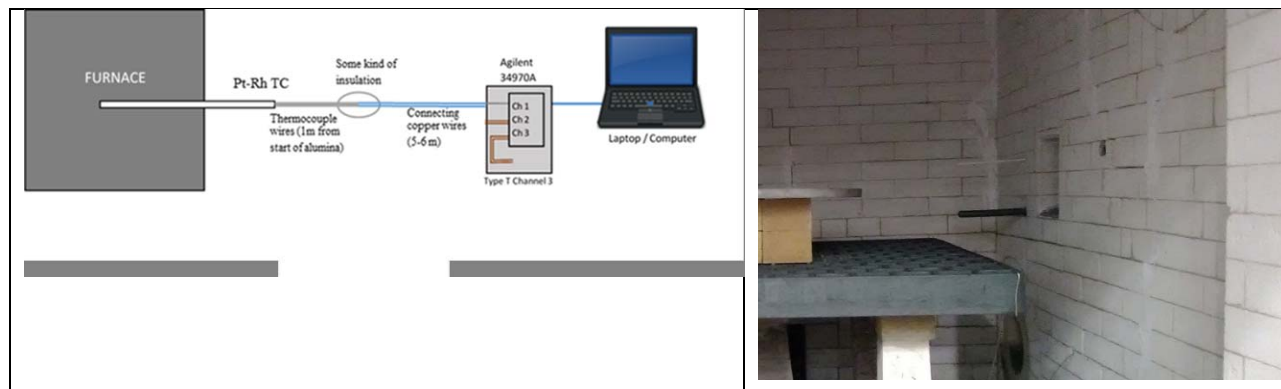


Figure 4.1.2: Left: Measurement arrangement at AFRC. Right: Arrangement of the Pt40%Rh/Pt6%Rh thermocouple (top) and the Type N furnace thermocouple (bottom) in the furnace chamber.

The results of one measuring run over a period of about 9 days are presented in Figure 4.1.3. Here, the temperature of the Pt-40%Rh/Pt-6%Rh thermocouple against the furnace temperature is presented. The first temperature was calculated on basis of the thermovoltage (emf)⁷ measured and by using the preliminary coefficients of the draft reference function. Above about 1100 °C this temperature difference increased to a value of about 25 °C which was stable at 1169 °C for the whole measurement period. During the cooling-process the temperature indicated by the Pt-40%Rh/Pt-6%Rh thermocouple was lower than the furnace temperature. Some emf values measured by using the Pt-40%Rh/Pt-6%Rh thermocouple deviate significantly from the furnace temperature and can be considered as outliers.

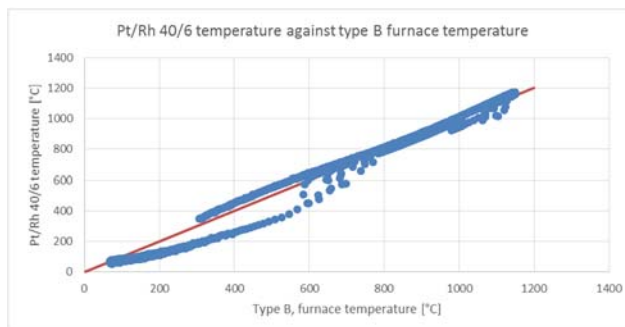


Figure 4.1.3: Pt-40%Rh/Pt-6%Rh thermocouple temperature against furnace temperature up to 1200 °C.

The main reason of the indicated temperature differences within the furnace might be the furnace mode of operation based on flames coming out from the burners to increase the temperature, which gives rise to temperature gradients within the nominally uniform temperature volume of the furnace. Furthermore, the three years old type N thermocouple might suffer on unknown drift effects which could explain the temperature difference between the temperature measured by using the Pt40%Rh-Pt6%Rh thermocouple and the furnace temperature (type N thermocouple). The larger differences found during the heating and cooling processes especially at lower temperatures are due to the fact, that at low temperatures the furnace refractory walls are not in thermal equilibrium and therefore larger temperature differences could be indicated by the both thermocouples placed near the wall.

MUT measurements

A new Pt-40%Rh/Pt-6%Rh thermocouple was tested at MUT Advanced Heating GmbH (Jena) in an industrial furnace with a nitrogen atmosphere up to about 1605 °C. The temperature of the furnace was controlled and measured by using a Type B thermocouple. The results of two measurements are presented in Figure 4.1.4 (whole measurements, and constant temperature at 1605 °C of the first run for 140 minutes). The mean emf of the Pt40%Rh-Pt6%Rh thermocouple at the holding temperature of 1605 °C of about 12.743 mV, measured in both runs, corresponds to a temperature of about 1602 °C calculated on basis of the preliminary coefficients

⁷ EMF: Electromotive force, effectively the voltage developed by a thermocouple which represents the measurand

of the function for the Pt40%Rh-Pt6%Rh combination. Both temperatures measured by using the Type B and the Pt-40%Rh/Pt-6%Rh thermocouple agree very well within the uncertainty of the Type B thermocouple of about $\pm 5^\circ\text{C}$. During the heating and cooling period deviations between the both temperatures of the Type B and the Pt-40%Rh/Pt-6%Rh thermocouple were within about $\pm 30^\circ\text{C}$.

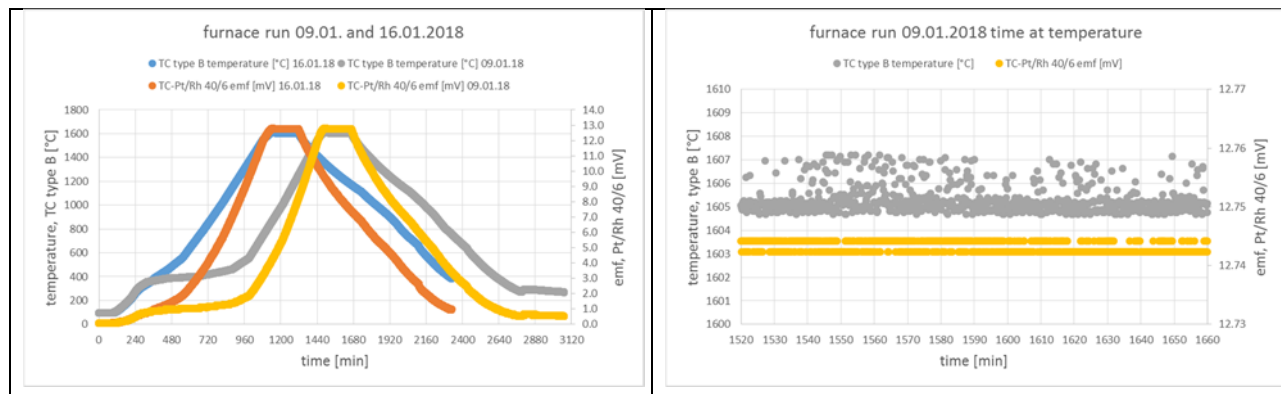


Figure 4.1.4: Left: Measured emf/temperature using the Pt-40%Rh/Pt-6%Rh thermocouple and the Type B thermocouple at MUT during ramping procedure. Right: Temperature stability at about 1605 °C.

4.1.2 Development of a sapphire tube thermometer

JV and Elkem carried out tests of a custom built sapphire tube thermometer in a production furnace at Elkem, Kristiansand, in September and October 2017. The device consists of a long single-crystal sapphire tube with a small tungsten filament at one end and an optical detection system at the other. The thermally generated light from the filament is detected, and can be converted to a temperature from calibration points and a mathematical model derived from the Planck law. The optical readout system consists of a wide-band Si detector, an objective lens, a field stop, a collimation lens, and a Lyot stop.

The furnace used at Elkem is a silicon solidification facility which subjects molten silicon to a specific cycle of controlled cooling designed to localise foreign species in a relatively small region. When the slab of Si finally reaches room temperature the pure Si may be separated from the impurity rich part mechanically. The furnace consists of a large inner chamber surrounded by water-cooled insulation. A small number of feed-throughs can be used to mount sensors inside the chamber, and the sapphire tube was mounted in a vertical feedthrough from the top of the furnace. While the sapphire tube used was almost 1 m long the tip still only just reached the hot zone, and the immersion depth was about 100 mm.

The production process involves a complete temperature cycle roughly once every 24 hours. Within that time the furnace is heated from room temperature to an initial pre-heating stage at 1420 °C before a further warm-up to the maximum temperature of around 1600 °C and a subsequent cooling cycle which eventually takes the temperature back down to ambient. The sapphire tube went through 23 such cycles.

The cooling process is proprietary and Elkem will not disclose the details. However, the recordings during the preheating stage are available, and contain important observations. The data are shown in Figure 4.1.5. The main feature is a uniform drift towards lower temperature from cycle to cycle, which amounts to about 110 °C from start to finish. Also shown in Figure 4.1.5 is the appearance of the sapphire tube after the measurements in the production furnace, showing a white, almost misty layer in the lowest 10 cm which is partly transparent; initially the entire tube was completely clear. The layer appears to be AlON (aluminium oxynitride), probably formed by a reaction between the sapphire and air at high temperatures. It is thought that this may have a bearing on the drift. The calibration on return of the device to JV was almost identical to the calibration before, but the immersion profiles were different by several degrees Celsius.

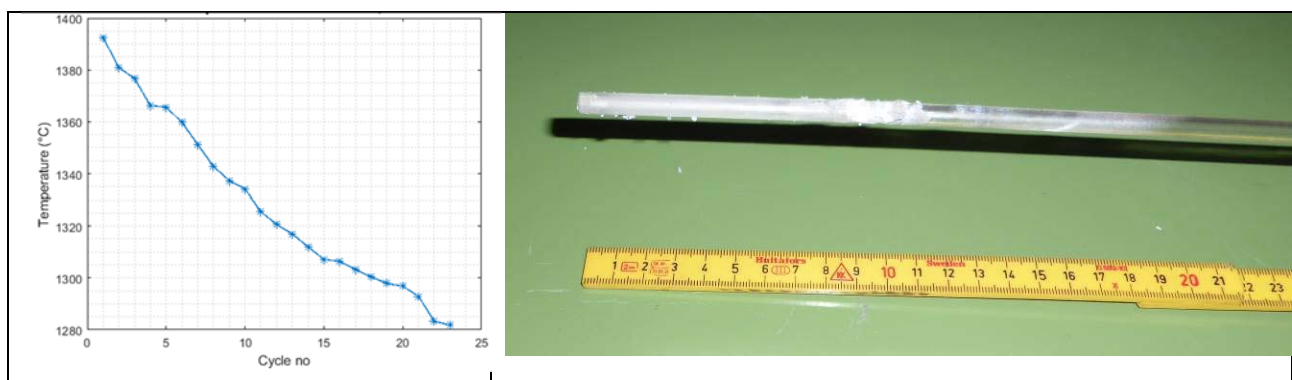


Figure 4.1.5: Left: drift during in-process trial at Elkem. Right: The appearance of the sapphire tube after the measurements in the production furnace.

At present the cause of the in-process drift is unknown, but there are three hypotheses:

- Impeded optical heat transfer. The change in transparency could affect the heat transfer to the tungsten filament. The heating of the tungsten filament is dominated by radiation. In equilibrium, the filament radiates thermally at the same power as it receives from the environment. Some of the radiated energy is lost, however into the optical system and into the surrounding walls. This loss of energy means the tungsten filament must cool slightly compared with its environment: just enough so that the mismatch in emitted and received radiation matches the loss. If the radiation on the tungsten filament is somehow restricted its temperature will fall. A change in the transmission properties of the sapphire is observed, but it is not simple to quantify the effect on the radiative transfer.
- Changes in surface properties of the tungsten. A gradual change in the surface properties of the tungsten could affect the emissivity, in turn modifying how strongly it radiates. A higher emissivity of the surface will predominantly affect the front surface because multiple reflections between the surrounding enclosure and the other tungsten faces will increase the absorption of radiation. The increased self-radiation increases the heat losses and may reduce the temperature of the filament.
- Mechanical bending: Mechanical load on the sapphire tube may have displaced the tungsten filament, in turn weakening the detected signal because the light from the tungsten first reflects off the sapphire wall before reaching the optical detector. The light path from the detector to the filament must reflect from the sapphire wall at very high angles of incidence, for which the reflection coefficient is high. It remains a possibility that the detected intensity is affected, however. The sapphire tube was protected by a stiff and fairly wide jacket of SiC during the measurements. It would take considerable force to bend it, but the mechanical connection between the SiC tube and the furnace wall might yield slightly and perhaps enough to displace the tip by a few centimetres.

4.1.3 Development of carbon thermocouples

Development at PTB

The graphite-based thermocouples are formed by rigid elements, such as tubes and rods of suitable dimensions, which have been screwed together with the aid of additional graphite plugs to form the measuring junction. The electrical contacts of the graphite items with copper wires for the emf measurements were realised by mechanical clamping by means of graphite screws or nuts which takes place in the head of the thermocouples. Due to the compactness and high thermal conductivity of the graphite materials, high temperatures ($T > 100\text{ }^{\circ}\text{C}$) can occur at these reference points, so that a separate measurement of this reference junction temperature with a Pt100 resistance thermometer is indispensable to correct the thermal voltage of the measurement accordingly. Figure 4.1.6 shows the basic structure of a graphite-based thermocouple. The length of the tubes and rods used was about 600 mm, the diameters of the tubes were 12 mm for the outside and 8 mm for the inside. The diameters of the solid rods were 4 mm (for Sigradur®G (glassy carbon) 3 mm). Figure 4.1.6 also shows photos of the measuring junction and the head of a thermocouple with the insulation plug made of boron nitride and the copper leads to the Pt100 resistance thermometer and the copper lines for measuring the thermal voltage.

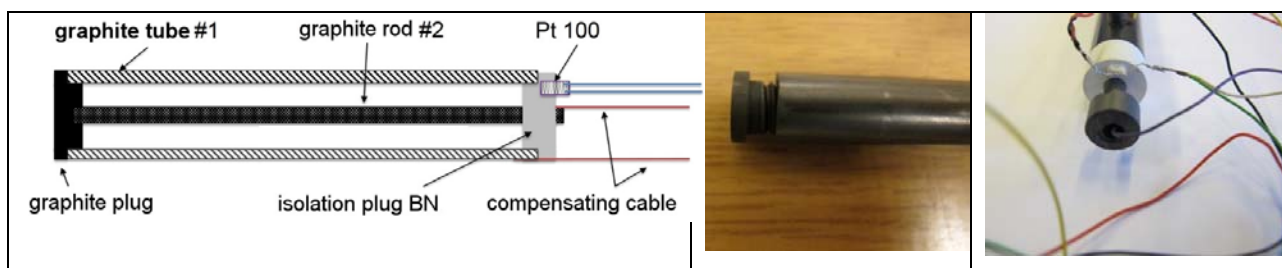


Figure 4.1.6: Left: Schematic of the graphite-based thermocouples. Middle: Measuring junction. Right: Measuring head with a Pt100 resistance thermometer.

Initial results were not sufficiently good; the measured high thermal voltage drifts did not allow an application for reliable temperature measurements. Therefore, some of the graphite tubes and rods of the two different graphite materials (R7510, R7660) from SGL Carbon were subjected to an additional cleaning / aging at SGL Carbon at a maximal temperature of 2200 °C for 24 h. The remaining tubes and rods of SGL Carbon were subjected to thermal treatment for 2.5 hours at 2300 °C under vacuum and in an Ar / Cl₂ atmosphere at KGT Graphit Technologie GmbH. With this additional thermal treatment, improved thermoelectric stabilities could be achieved. Figure 4.1.7 shows the stability that was finally achieved the combination of Sigradur®/R7660 at 1500 °C. Thermoelectric stability above 1500 °C could not be achieved yet.

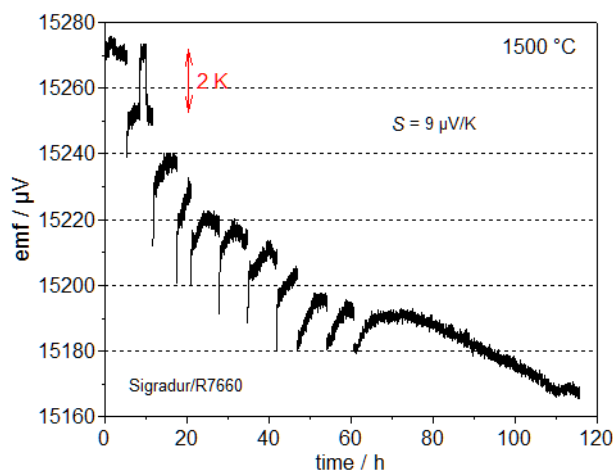


Figure 4.1.7: Thermal voltage during daily cycling and of a final long-term measurement of the thermocouple Sig/7660 at 1500 °C.

Measurements at MUT

At MUT Advanced Heating GmbH in Jena a thermocouple constructed from Sigradur®G/R7660 (rod/tube, KGT-aging) was tested in an industrial vacuum furnace at a pressure of about 0.7 mbar. The temperature of the furnace was controlled with a pyrometer. The design of the MUT thermocouple differs from the thermocouple constructed at the PTB through a shorter length and a bigger head due to the need of a KF40 flange. Figure 4.1.8 shows a schematic and a photo of the graphite thermocouple. In this first configuration, the temperature of the thermocouple head could not be measured. A further improvement of the design allowed the measurement of the temperature of the reference junction, the connection of the graphite materials to the copper lines. The furnace with the incorporated graphite thermocouple is also shown in Figure 4.1.8.

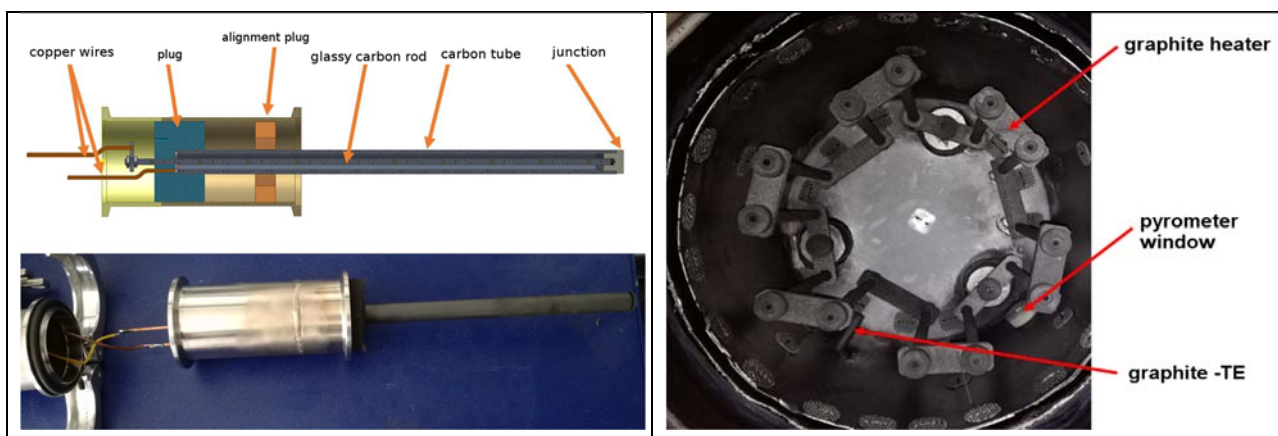


Figure 4.1.8: Left: Schematic and picture of the graphite-based thermocouples constructed by MUT. Right: the vacuum furnace with graphite thermocouple at MUT.

For a long-term measurement with the thermocouple Sig/7660 the head of the thermocouple was equipped with a Type K thermocouple to measure the temperature of the copper graphite transitions. The thermocouple Sig/7660 was measured for about 100 h at 1500 °C, the thermal voltage and the temperature of the head is displayed in Figure 4.1.9. The emf of thermocouple at 1500 °C showed a substantial drop at the beginning, starting at about 16.3 mV and decrease to about 15.93 mV. The thermal voltage of the graphite thermocouple becomes stable at a value of (15.93 ± 0.03) mV after the drop in the first 24 h of the measurement. It should be noted, that the measured emf of 15.93 mV agrees well with the first emf of 15.91 mV measured at PTB at 1500 °C.

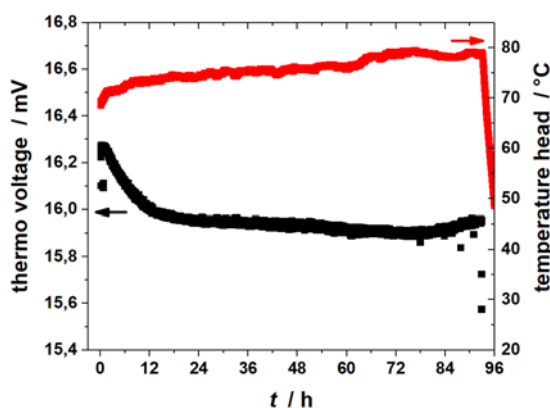


Figure 4.1.9: Thermal voltage (black) and temperature of the head (red) of the MUT thermocouple Sig/7660 for about 100 h at 1500 °C.

The temperature of the head increases during the measurements to about 80 °C (red curve in Figure 4.1.9), which is about 25 °C higher than the head temperature measured at PTB. The reason is probably the shorter length of the thermocouple used at MUT which results in a shorter distance of the head to the high temperature of the furnace at MUT. These preliminary results indicate that graphite glassy-carbon based thermocouples can be used at 1500 °C but further investigations are needed to study the long-term stability and to estimate the thermal voltage profile as well as the highest possible application temperature.

Summary of results

- Optimised Pt-Rh thermocouple between 1324 °C and 1492 °C identified at Pt-40%Rh/Pt-6%Rh and trialled in-process with satisfactory results in term of stability; preliminary reference function developed; trialled at AFRC and MUT
- Development of stable carbon thermocouples to 1500 °C has been achieved for the first time; trialled at MUT
- Development of a sapphire tube blackbody based sensor for silicon processing, and trialled in-situ at ELKEM. Robustness was excellent, but in-process calibration drift is so far unexplained

4.2 Zero-drift contact temperature sensors to 1350 °C

State of the art

The current state of the art for long-term process temperature control with contact sensors comprises mainly of the Pt-Rh thermocouples described in the preceding sections and the MI thermocouples Type K and N. These types are all susceptible to calibration drift, the unknown magnitude and direction of which can cause serious errors in the reading, leading to loss of product or inefficiency. The principal mitigation is frequent replacement, which is costly and disruptive. The state of the art has been advanced in two ways. Firstly, by developing and trialling in-process self-validating thermocouples (abbreviated to 'inseva') with, for the first time, an external form factor which is indistinguishable from existing process control sensors, and which allow periodic *in-situ* re-calibration traceable to ITS-90. Temperature measurement uncertainty of less than 1 °C in-process has been achieved over a timescale of months. Secondly, by performing metrological characterisation of the drift performance of the new double-walled MI cable of UCAM, superior drift performance has been demonstrated, and the new devices have been trialled in industrial heat treatment applications.

4.2.1 Development of self-validating thermocouples

In general, thermocouples used at high temperatures (>1000 °C) will drift from their initial calibration state, resulting in an incorrect temperature reading which becomes worse with time [44]. In industrial applications this can result in large process temperature errors with associated efficiency losses [45]. Self-validating thermocouples can take laboratory-based artefacts such as high temperature fixed points [46,47] into the industrial setting. Typically, a miniature fixed point containing a phase-change ingot is integrated with the measurement junction of a thermocouple [48-53], allowing in-situ calibration [54,55]. In EMPRESS, a slim-line self-calibrating thermocouple with outer diameter of 7 mm, i.e. the same as that used in many heat treatment processes, has been developed and trialled in-process at AFRC (aerospace heat treatment) and ICPE-CA (ceramic manufacturing).

The design of the cell, and a typical melting curve from the phase-change cell used for in-situ self-validation, is shown in Figure 4.2.1.

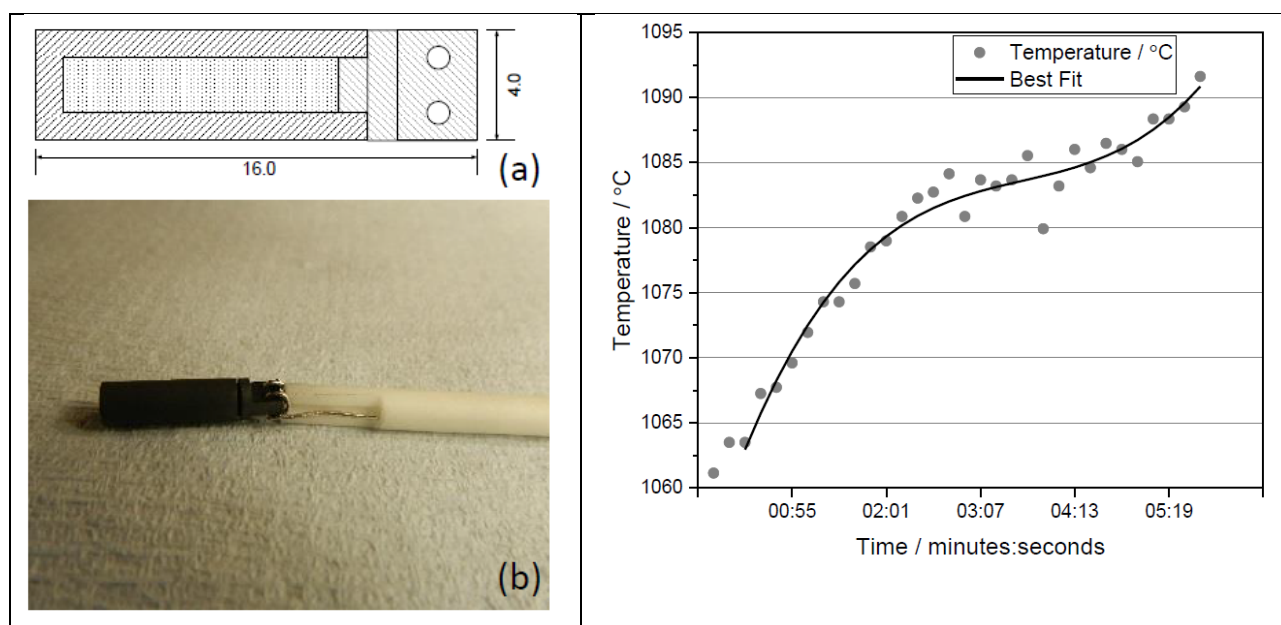


Figure 4.2.1: Left: The self-validating fixed-point cell. Right: Temperature measured by a Cu self-validating thermocouple as the furnace is heated through 1084 °C (melting point of copper) plotted together with the best-fit polynomial used to determine the point of inflection (i.e. the calibration point).

Four sets of tests were performed to evaluate the robustness of the self-validating thermocouples: Tests at NPL (copper, 1084 °C); industrial trials at ICPE-CA (BRML) (copper, 1084 °C); industrial trials at AFRC (STRATH) (copper, 1084 °C); tests at NPL (Co-C, 1324 °C and Ni-C, 1329 °C).

Tests at NPL (copper)

The stability of four different cells, all having the same design, was assessed by repeatedly cycling the thermocouple through the melting and freezing point of copper (1084 °C). Three of the cells showed a tendency to break relatively early on; the cause of the breakage was identified as contamination of the Pt-based wires with graphite from the crucible, as shown in Figure 4.2.2. The addition of an inert coating on the graphite crucible greatly extended the lifetime. The results of the long-term exposure, in terms of calibration as a function of time, are shown in Figure 4.2.2.

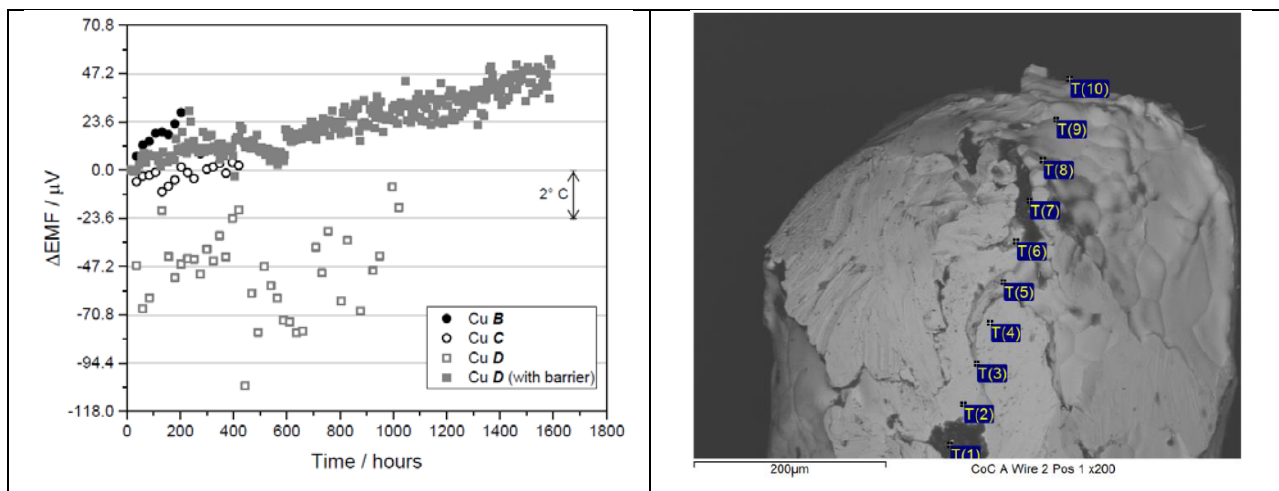


Figure 4.2.2: Left: EMF of the melting inflection point as a function of time during the testing of four Cu in-seva thermocouples at NPL. Right: SEM showing significant amounts of carbon (black regions) in the Pt wire following breakage.

Industrial trials at AFRC and ICPE-CA (copper)

AFRC (STRATH) and ICPE-CA (BRML) were each supplied with a self-validating thermocouple using the copper fixed point, and each placed the thermocouple in a process furnace. The process was then run normally for several months. In both facilities, clear melting and fr

eezing plateaus could be observed, permitting in-situ recalibration of the thermocouple. Figure 4.2.3 shows a typical melting plateau measured at ICPE-CA, and also the stability as a function of time in process.

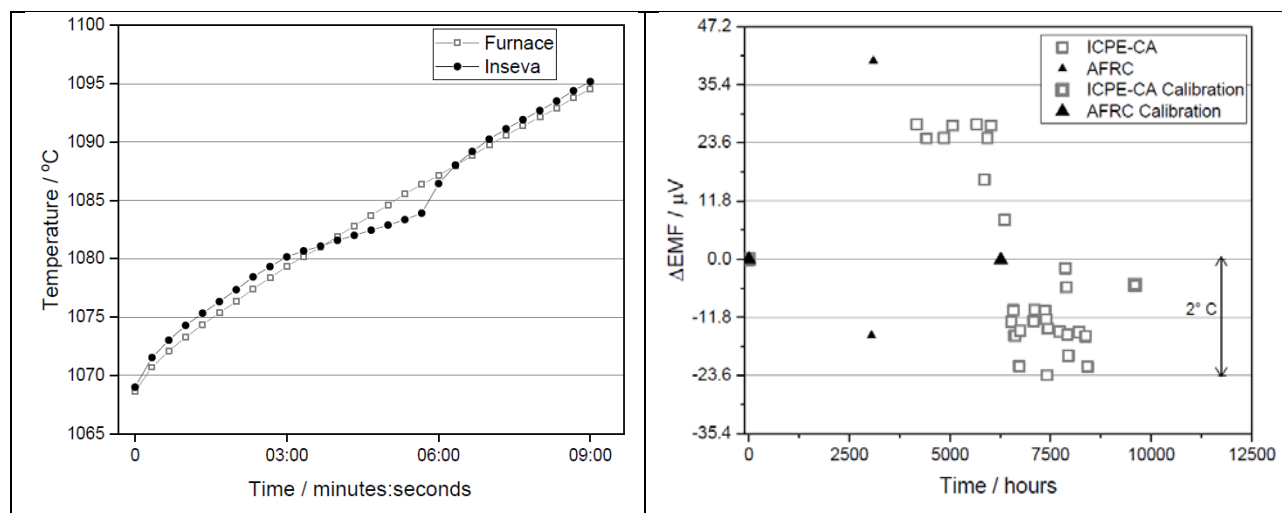


Figure 4.2.3: Left: Temperature recorded by the ICPE-CA furnace control sensor and the in-seva thermocouple, showing the clear melting plateau of the in-seva. Right: Melting inflection point of two Cu in-seva thermocouples trialed at AFRC and ICPE-CA as a function of time in process.

Tests at NPL (Co-C, 1324 °C and Ni-C, 1329 °C)

Three in-seva thermocouples were constructed with the Co-C cell; all broke due to cracking of the crucible and resulting leakage of the metal ingot. This was probably due to mechanical damage and oxidation. A fourth cell was constructed using graphite coated in an inert barrier material. This lasted 235 hours before failing. The

cause of failure is considered likely to be due to the Co-C, which may cause too much erosion of the graphite cell which necessarily has very thin (1 mm) walls.

A new in-seva was constructed using the Ni-C cell; this has a melting temperature very close to that of the Co-C cell (1329 °C instead of 1324 °C). This proved to be much more robust; it was tested for around 1600 hours and was still intact at the end of the tests.

A detailed assessment of the uncertainty associated with the in-situ calibration of the Ni-C in-seva was performed, yielding an expanded uncertainty of 1.95 °C.

4.2.2 Evaluation of mineral-insulated ultra-stable high temperature thermocouples

Previous work at the University of Cambridge resulted in the successful development of double wall MI thermocouples having a significantly reduced drift compared to conventional MI thermocouples. In conventional MI thermocouples operating at high temperatures, contamination of the thermoelements occurs during operation because of elemental transfer from the sheath to the thermoelements. In double wall MI thermocouples the outer wall can be made of alloys used for the sheath of conventional MI thermocouples (i.e. Inconel 600); the inner wall is made of customised alloys that avoid or minimise the contamination; this results in low drift MI thermocouples. For EMPRESS, a customised nickel alloy was chosen for the sheath to achieve low drift up to 1350 °C. Type K thermoelements were selected, again to achieve up to 1350 °C. A diameter of 4.5 mm was used. Two sets of tests were envisaged:

- Laboratory stability tests at the University of Cambridge and PTB
- Industrial tests at AFRC (vacuum heat treatment furnace) and Bodycote UK (long term tests in vacuum heat treatment furnace used for single crystal superalloys) to 1200 °C

Laboratory tests at University of Cambridge

In collaboration with Bodycote UK a simplified heat treatment cycle, reproducing the main features of the real heat treatment of superalloys at 1350 °C, was selected and agreed with PTB. The cycle was characterised by the following features:

- Ramp up from 300 °C to 1350 °C at ramp rate of 5 °C / min
- Hold on at 1350 °C for 25 h
- Ramp down from 1350 °C to 300 °C at ramp rate of 5 °C / min

The target for the tests was 90 cycles. To assess stability, calibration was performed using a Co-C fixed point cell at the start, end, and intermediate points during the tests, as well as full calibration before and after the tests. A miniature Co-C fixed point cell was manufactured by NPL; this was a custom size to accommodate the dimensions of the equipment at the University of Cambridge. A first batch of 15 customised Type K MI thermocouples were manufactured and supplied to University of Cambridge and PTB, and a new facility was set up at University of Cambridge to run tests in the thermal cyclic conditions and inert atmosphere representative of the conditions experienced in an industrial heat treatment furnace. The results of the thermal cyclic tests are shown in Figure 4.2.4.

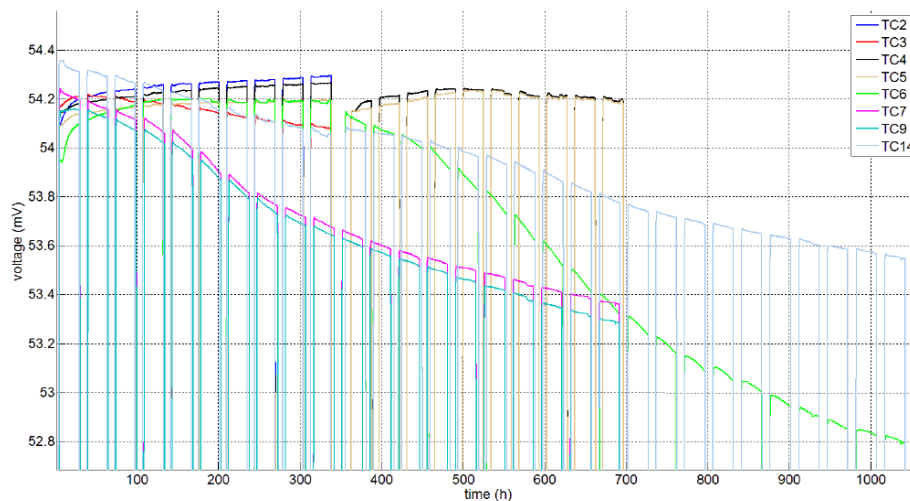


Figure 4.2.4: Thermal cyclic tests on customised Type K MI thermocouples (first batch).

Although the thermocouples were obtained from the same cable, a significant scatter of the results was observed. As a result, a second batch was manufactured which also performed below expectations.

Measurements of Type R thermocouple stability under comparable conditions were performed by PTB, and the results are compared with the MI thermocouples in Figure 4.2.5.

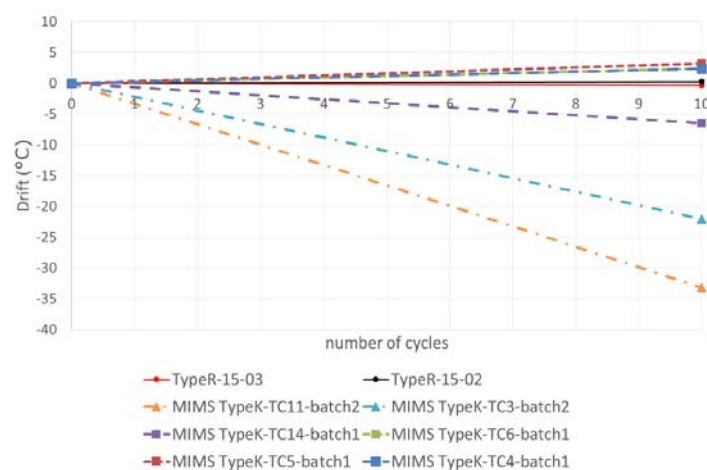


Figure 4.2.5: Comparison between Type R and customised Type K MI thermocouples after thermal cyclic tests at 1350 °C (comparison based on calibration in Co-C fixed point cells).

The tests at 1200 °C in the laboratory with a 3 mm double wall Inconel 600 sheathed Type N thermocouple and a 3 mm conventional Inconel 600 sheathed Type N thermocouple yielded considerably better results. This time the cycles were:

- Ramp up from 300 °C to 1200°C at ramp rate of 5 °C / min
- Hold on at 1200 °C for 4 h
- Ramp down from 1200 °C to 300 °C at ramp rate of 5 °C / min

Figure 4.2.6 shows the results of a 30 cycle test; the conventional thermocouple (blue curve) drifted continuously from 1200 °C to 1195 °C, while the double wall thermocouple (green curve) showed a very repeatable measurement (about 1204 °C) of the temperature plateau of the temperature cycle within about 1 °C for the whole duration of the test.

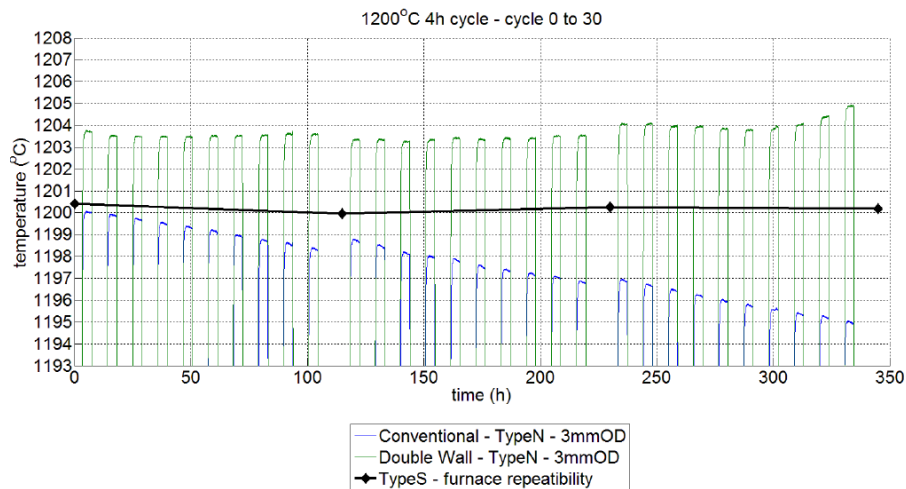


Figure 4.2.6: Comparison between the drift of 3 mm double wall Inconel 600 sheathed Type N thermocouples and the conventional equivalent with maximum temperature of 1200 °C.

Industrial test campaign

Figure 4.2.7 shows the industrial vacuum furnace at AFRC used for the installation of 3 mm double wall Type N thermocouples, also shown.



Figure 4.2.7: The industrial vacuum furnace at AFRC (left) and the thermocouples installed inside the furnace (right).

The test campaign at AFRC involved a short exposure for 5 cycles at high temperature (1200 °C). Each cycle consisted of:

- Ramp up to 1200 °C at 5 °C / min
- Hold at 1200 °C for 4 h
- Argon quenching (i.e. very rapid forced cooling) to ambient temperature

Four 3 mm double wall Type N thermocouples were tested in the AFRC vacuum furnace. The results are shown in Figure 4.2.8, in comparison with the furnace control thermocouple (Type R, green line in Figure 4.2.8).

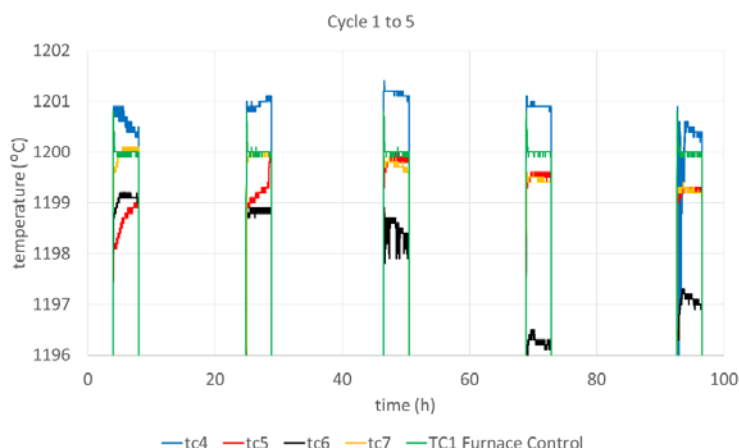


Figure 4.2.8: Thermal cyclic tests at AFRC.

The behaviour of the 3 mm double wall thermocouples was considered satisfactory as no drift was detected for the thermocouples, and good agreement with the furnace control thermocouple was achieved during the tests at AFRC.

Long term tests at Bodycote Romania in partnership with BRML were planned, but could not be performed due to difficulties in scheduling the work at Bodycote. Instead, an industrial furnace was identified at Bodycote UK and new thermocouples were sent. 3mm Type N thermocouples were compared. The results over 47 cycles accumulated during the test campaign were good, indicating reasonable stability, but it was difficult to distinguish the drift of the thermocouples under test from the inherent variability of the temperature associated with different heat treatment cycles, different locations and different temperature distributions caused by different furnace loads. Further tests are envisaged beyond the end of the project.

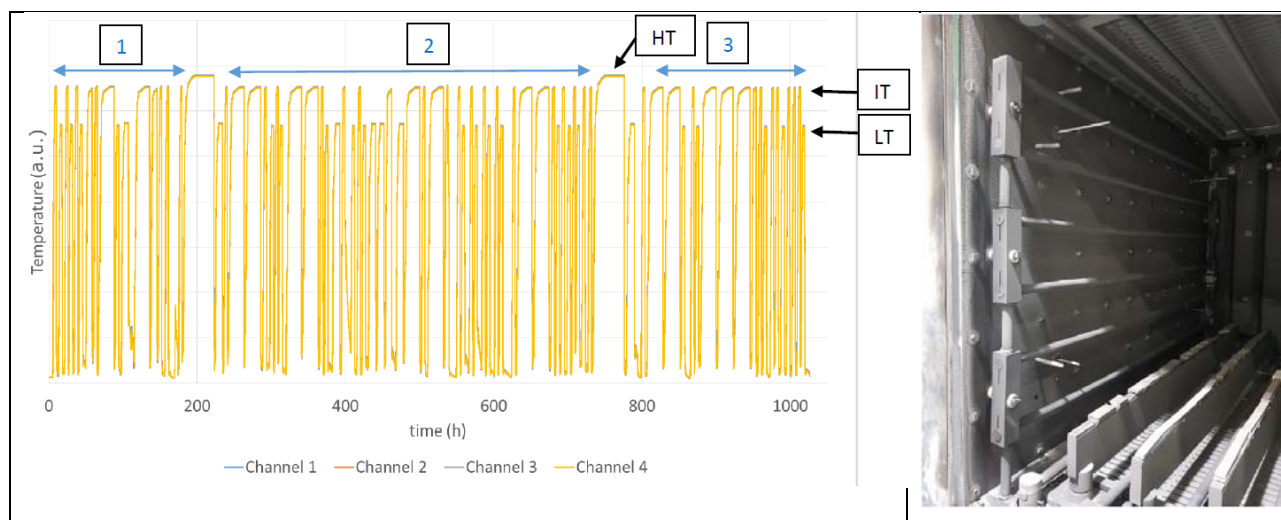


Figure 4.2.9: Test results from the test campaign at Bodycote UK on 4.5 mm customised double wall Type K MI thermocouples (left); installation showing thermocouples in the vacuum furnace (right).

The 4.5 mm customised double wall Type K MI thermocouples were installed in a high temperature vacuum furnace used for single crystal superalloy heat treatment at Bodycote UK from August 2017 to February 2018. Figure 4.2.9 shows the installation of the four thermocouples used in this test. The thermocouples were installed in fixed locations through the case of the furnace rather than being used as load thermocouples: this allowed a much better repeatability of the temperature measurement. The thermocouples were obtained from the first batch of the customised Type K MI thermocouple cable. Some of the test results are shown in Figure 4.2.9 where the thermocouples experienced over 80 heat treatments and over 1000 h of operation (note the temperature is indicated in arbitrary units, as information on the heat treatment temperature of the alloys cannot be disclosed due to confidentiality). The heat treatments experienced by the thermocouples in Figure 4.2.9 can be categorised as low temperature (LT), intermediate temperature (IT), very high temperature (HT).

The thermocouples appear to perform extremely well at temperatures exceeding 1300 °C, with stability between 1 °C and 2 °C for hundreds of hours in real-world industrial conditions.

Summary of results

- Self-validating thermocouples developed to 1329 °C and successfully trialled at AFRC (STRATH) and ICPE-CA (BRML)
- Double wall MI thermocouples trialled up to 1350 °C and showed excellent stability to 1200 °C; successfully trialled at AFRC and Bodycote UK

4.3 Traceable surface temperature measurement with contact sensors

State of the art

For temperatures up to about 500 °C, surface temperature measurement by contact thermometry is very difficult, yet critical for many processes. Examples of the state of the art include temperature sensitive crayons which are subjective and not traceable; surface contact sensors e.g. thermocouples are poorly characterised and prone to subjectivity, as well as perturbing the temperature of the surface to be measured (spurious heat flow effects). Infra-red thermometry is beset with emissivity problems causing large errors of up to hundreds of degrees Celsius; phosphor thermometry, prior to this project, was not widely available, being the preserve of research laboratories, not suitable for industrial use, and not properly traceable. Surface calibrators for calibration of conventional probes were beset with problems such as a poorly characterised surface temperature and a surface plate having a different material to that used in-process. Dynamically compensating sensors were available but again not well characterised. The state of the art has been advanced by the establishment of practical, traceable phosphor thermometry (both directly applied, and incorporated into a conventional surface probe calibrator unit), and trialled in-process. In addition, a dynamically compensated probe has been developed and rigorously characterised.

4.3.1 Development of phosphor thermometers – NPL

Surface temperatures can be measured using contact probes placed in good thermal contact with the surface. However, these measurements are prone to large and often difficult to quantify errors. When a thermometer is brought in to contact with a surface, heat will flow until the temperature of the probe tip and surface are equal. This process takes a finite time and will perturb the surface temperature considerably. To minimise these errors, surface thermometers are usually calibrated by bringing them in to contact with a surface calibrator. These devices provide a target of a similar material to that for which the probe will be used, of known temperature – usually measured by an embedded PRT or thermocouple. However, due to both the dynamic nature of the calibration and the perturbing nature of the probe, calibration uncertainties are typically conservative and can be as high as 10 °C to 20 °C over the temperature range 20 °C to 500 °C.

To reduce these uncertainties, NPL has developed validation targets. These employ additional embedded temperature sensors and a thermographic phosphor coating on the surface for non-contact thermometry, with the objective of reducing the surface probe calibration uncertainty to below 5 °C for temperatures up to 500 °C.

The surface calibrator

The new validation target makes use of a Fluke 3125 surface probe calibrator, modified for improved surface temperature measurement. It is pictured in Figure 4.3.1 in an unmodified state, with the heat guard removed. It has an aluminium block with an embedded PRT and the temperature is adjusted by a PID-controlled resistive heater below the block. The calibrator has been modified to accept new thermal validation targets made of different metals that can be inserted above the aluminium block.

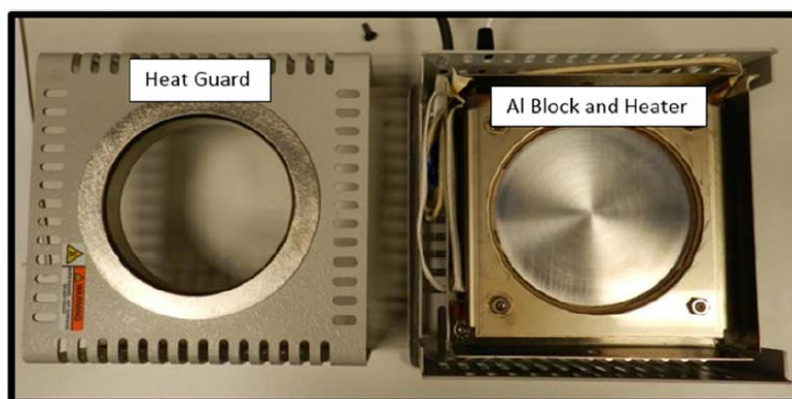


Figure 4.3.1: The Fluke 3125 surface probe calibrator, with the heat guard removed.

Validation

To provide temperature validation of the new targets, three different methods were implemented:

1. Embedded contact sensors – calibrated (to ITS-90) Type N mineral insulated thermocouples (1 mm diameter) were embedded at depths of 2 mm, 7 mm and 12 mm below the surface. The surface temperature was determined by linear extrapolation.
2. Phosphor thermometry – a thermographic phosphor coating was applied to the surface and following excitation with a violet light emitting diode (LED), the decay time of the emitted red light was measured and related to temperature via a suitable calibration.
3. Phase-change material – a small amount of indium foil was placed on the surface of the target and monitored optically for a change in its reflectance properties during its phase transition at 156.6 °C.

Figure 4.3.2 shows the final assembly of the modified calibrator plate – a stainless steel fixing plate is bolted to the top of the calibrator to ensure good thermal contact between the heater block and the interchangeable validation target. The alumina insulation ring limits heat losses through the stainless fixing plate, whilst also creating an air trap to help stabilise the surface temperature.

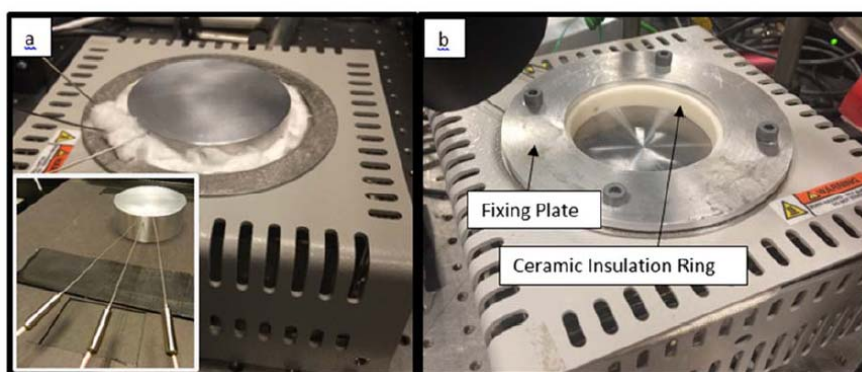


Figure 4.3.2: The surface probe calibrator with an instrumented removable block (see inset picture) installed. Figure 2b: Final modified calibrator, with fixing plate and ceramic insulation ring.

a. Embedded contact sensors

Extrapolation of the measured temperatures at a number of depths below the surface to determine the true surface temperature has been shown to be a robust and accurate method of surface temperature measurement [56-59]. The three Type N thermocouples were calibrated with an uncertainty of ± 0.37 °C ($k = 1$) from 20 °C to 500 °C in a dry block calibrator according to NPL procedure TPNPL/0068 (June 2017).

The thermocouples were inserted in to the validation target horizontally such that a) their tips were 2 mm, 7 mm and 12 mm below the surface of the block and b) they were displaced by an angle of 30 ° with respect to each other to minimise any perturbation to the vertical temperature profile. A Monte Carlo simulation was used to assess the propagation of the thermocouple calibration uncertainties to the surface temperature determination. Gradients measured experimentally were assessed for different target materials and within the

temperature range of the block, the magnitude of the gradient had a negligible effect on the extrapolated temperature. The uncertainty of the intercept measurement using the extrapolation method in this system was 0.42 °C ($k = 1$) for all measured temperatures.

b. Phosphor thermometry

Phosphor thermometry provides a robust method to determine the temperature of a surface remotely that is independent of both surface emissivity and background thermal radiation. A thin coating of thermographic phosphor is sprayed on the surface to be measured and interrogated optically. For this work the thermographic phosphor $\text{Mg}_4\text{FGeO}_6\text{:Mn}$ was used [60]. The phosphor coating is excited with violet light ($\lambda = 420 \text{ nm}$) and once the excitation is removed, the phosphorescence decay ($\lambda = 650 \text{ nm}$) is measured and the decay time determined, which can be directly related to temperature through calibration. The decay time τ can be found in a number of ways. Normally, it is determined from a least squares fit of the function $I(t) = I_0 e^{-t/\tau}$ to the measurement data and Figure 4.3.3 shows typical decay curves from $T = 75 \text{ °C}$ to $T = 375 \text{ °C}$.

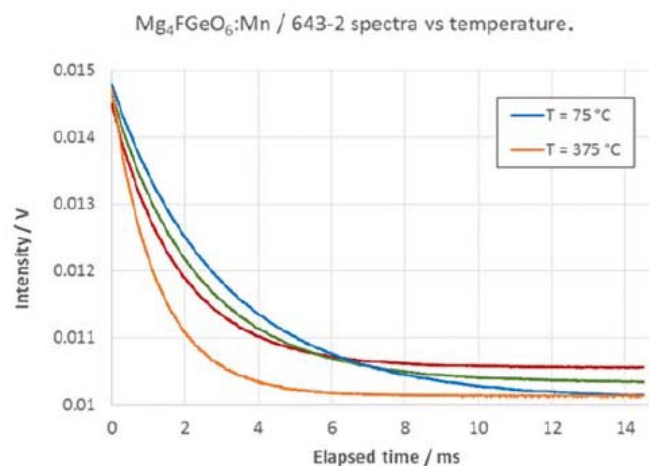


Figure 4.3.3: Typical phosphor emission signal versus time for a number of temperatures.

However, NPL have developed an equivalent method to determine the decay time based on the phase difference between the emitted and excitation signal, which yields a superior signal to noise ratio.

The measurement system: Figure 4.3.4 shows the phosphor thermometry system for the surface probe calibrator. A square-wave intensity modulated 1 mm diameter spot of violet light is focused onto the phosphor coating on the surface of the validation target and the phosphor is excited. A silicon detector measures the phosphorescent decay when the LED is off. The signal processing routine described above is performed to calculate the decay time of the phosphor, assuming a single exponential decay. The validity of this assumption is improved if the integration window employed is carefully selected.

Calibration: The phosphor is mixed with the binder *Ceramabind* 643-2 in the ratio 0.91:1 by weight and applied to the surface at ambient temperature. The calibration is performed by making a slow temperature ramp up to the maximum temperature, whilst logging the extrapolated surface temperature τ values. To validate the calibration and examine the stability of the phosphor coating, the temperature difference between the phosphor and extrapolated surface temperature are recorded on a subsequent ramp down to ambient temperature, denoted as a 'validation ramp'. Figure 4.3.4 shows the measured calibration curves t vs T for steel and aluminium targets. Differences between the calibration and validation ramp measurements were less than 0.3 °C.

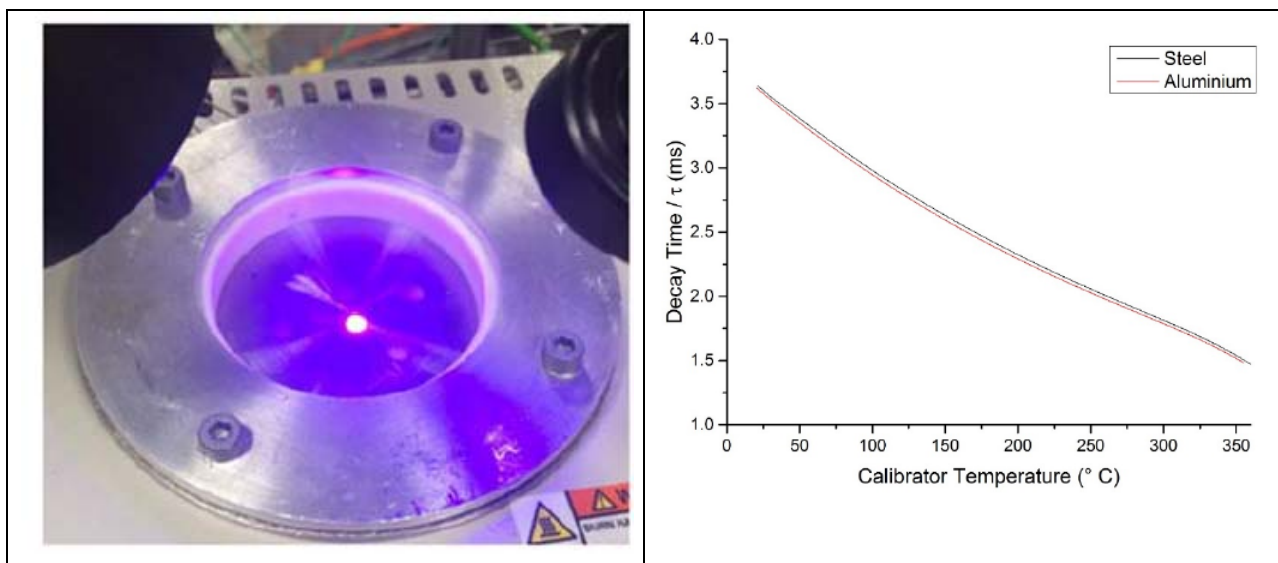


Figure 4.3.4 Left: UV-LED excited phosphor on the surface of the calibrator. Right: Calibration curves for steel and aluminium validation targets.

c. Phase-change material – phosphor validation

The phosphor thermometry system was validated by placing a small amount of indium foil on the surface of the target alongside the phosphor coated region and observing its phase transition at 156.6° C. This transition was monitored optically with a silicon detector / lens combination observing a change in the reflected light from a collimated green laser beam (1 mW) incident on the indium foil. The cooling rate of the target was varied by changing the lower set-point from 7° C to 1° C below the indium freezing point temperature. The reflectivity fell by greater than 20 % when the molten indium froze and served as a good indicator for the phase transition.

Figure 4.3.5 shows the measured phosphor temperature versus the calibrator off-set set-point (relative to the indium freezing temperature), with the ITS-90 indium freezing fixed-point temperature indicated. We see that there is excellent agreement between the phosphor and indium freezing point temperature – with agreement improving as the target set-point temperature is reduced relative to the indium freezing temperature.

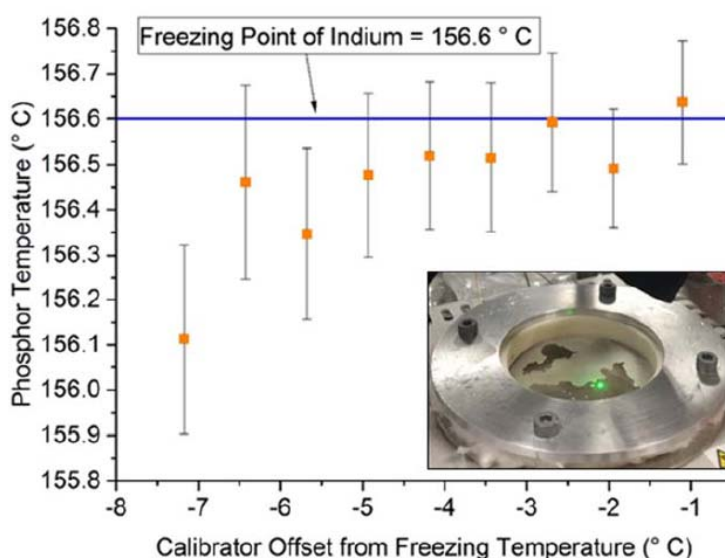


Figure 4.3.5: Measured phosphor temperature versus calibrator off-set set-point during the indium freeze. Inset: Green diode laser, monitoring the phase change of indium foil on the surface calibrator alongside a phosphor coating.

The advantage of this technique is the simplicity of installation, offering a source of traceability on the reference surface, rather than an extrapolation. The disadvantage is the range of ITS-90 fixed point materials that can be used in this way. Similar tests with tin have been unsuccessful due to increased surface oxidation.

Perturbation of the surface temperature due to phosphor coating

The temperature gradient across the phosphor coating needs to be understood and corrected for if a calibration is being transferred between difference calibrators. Assuming a maximum coating thickness of 50 μm (determined experimentally) and a phosphor/binder thermal conductivity of 1 $\text{W m}^{-1} \text{K}^{-1}$. The maximum temperature gradient is 0.3 $^{\circ}\text{C}$.

The phosphor/binder combination used in this work is known to be semi-transparent, so it cannot be assumed that the excitation light is completely absorbed on the surface of the coating. If temperature gradients exist across the coating, this may lead to spurious phosphor temperatures. This can be examined by using the peak phosphor emission brightness as a proxy for the amount of absorption and examine the emission intensity as a function of phosphor coating thickness.

The absorption is expected to follow a Beer-Lambert relationship $B(x) = B_0(1 - e^{-\alpha x})$ where α and x are the absorption coefficient and coating thickness respectively and $B(x)$ is the excitation signal measured for a phosphor coating of thickness x . A number of phosphor coatings were prepared, varying in thickness from 200 μm to 2500 μm , and under a constant excitation intensity, the emission strength was measured. This coating thickness x was measured with a capacitive thickness gauge.

Figure 4.3.6 shows the results of the emission strength (brightness) versus coating thickness, with the Beer-Lambert model fitted to the data; the model is quite a good fit. The absorption coefficient α is 300 μm^{-1} , which means that the excitation intensity approximately falls by 1/e through this thickness of phosphor. With this in mind, the excitation absorption over a 'thin' (< 50 μm) coating can be assumed to be linear, and thus the measured temperature on average will be in the middle of a coating, reducing the maximum temperature difference in this setup to 0.15 $^{\circ}\text{C}$. If it is possible to accurately measure the phosphor coating thickness, this uncertainty contribution can be reduced. However, for this work, we simply include it in the overall uncertainty.

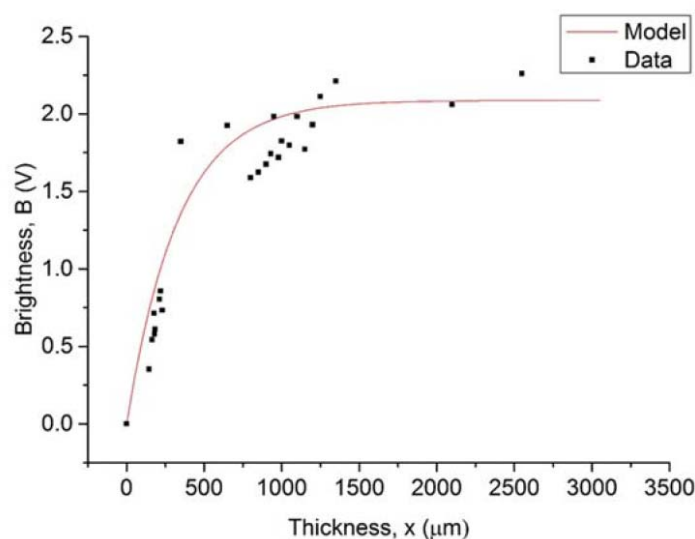


Figure 4.3.6: Phosphor emission strength (brightness) as a function of coating thickness: experimental data and theoretical fit of the Beer-Lambert model.

Coating stability

Reproducibility of the temperature determined with the phosphor thermometer primarily depends on the stability of the phosphor coating applied to the surface. To determine this, measurements were made on a stainless steel validation target. Following calibration the phosphor temperature was determined during 7 thermal cycles from 30 $^{\circ}\text{C}$ to 400 $^{\circ}\text{C}$. At first, there is evidence of drift, particularly at elevated temperatures, although this stabilises after about six thermal cycles. This represents the largest component of uncertainty in the phosphor thermometry system.

Calibration shift with target material

One of the biggest challenges when using phosphor based thermometry systems is that the decay lifetime of the phosphor is influenced by the surrounding environment. This means that a combination of phosphor, binder, surface material, coating application conditions and subsequent treatment can all have an effect on the lifetime decay characteristics for a given temperature. These processes need to be extensively evaluated in order to gain confidence in the ability to transfer a known decay lifetime vs. temperature characteristic between

different phosphor coatings. Figure 4.3.7 provides an example of this. The calibration from a phosphor coating on stainless steel is applied to aluminium and another proprietary material, a calibration ramp is then performed, and the differences between the new and previous calibration are recorded. Even though the binder and phosphor are the same, it is clear that the material the phosphor is coated on plays an important role in the calibration. In the case of aluminium, the calibration errors are as large as -6°C . This highlights the need for calibration to be specific to both the phosphor and material.

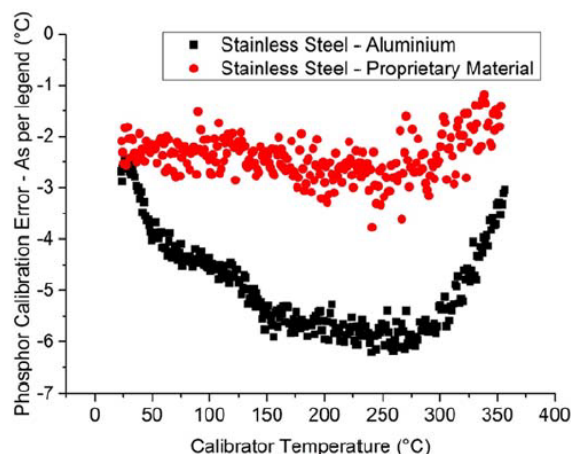


Figure 4.3.7: Transfer of calibration between materials and the resulting errors.

Calibration and validation of surface probes using phosphor thermometry

To assess the effectiveness of the surface calibrator and the phosphor to calibrate a contact surface probe, a number of different thermal scenarios encountered during the calibration of surface probes are studied. The contact surface probe examined is a TME KS11. It is a Type K thermocouple with an exposed coil/junction at the tip which has been engineered to minimise heat conduction errors. Figure 4.3.8 shows a) the probe assembly and b) a close-up of the probe tip. The probe is shown in operation alongside the phosphor thermometer on the surface calibrator in Figure 4.3.9. This configuration allows simultaneous surface thermometry measurement using conventional extrapolation methods and phosphor thermometry, during probe calibration.



Figure 4.3.8: TME contact thermometer KS11 showing the probe assembly (left) and a close-up of the probe tip (right).

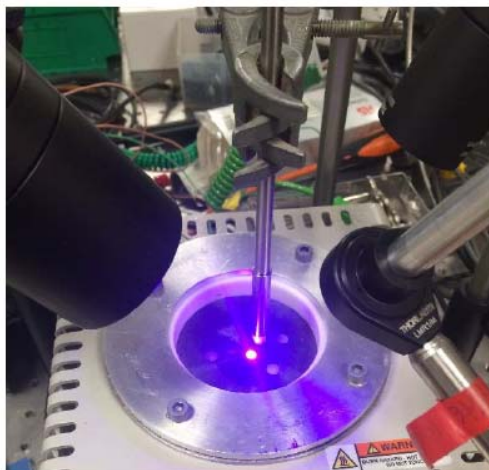


Figure 4.3.9: Commercial contact probe tested alongside the phosphor system.

Static test: the probe remains in contact with the surface, and the calibrator completes a temperature ramp from ambient to maximum, and back to ambient. This replicates a 'steady state' measurement with a contact probe for a range of temperatures. The temperature ramp rate is 0.5 °C/min from ambient up to a maximum temperature, which for aluminium is 340 °C, for stainless steel is 330 °C.

Dynamic test: the probe (initially at ambient temperature) is placed on to the surface (which is set at a number of fixed temperatures). This is representative of how the probe will be used in practice and provides information on both response times and temperature perturbation caused by the probe. For these dynamic tests, nominal surface temperatures of 60 °C, 115 °C, 220 °C and 300 °C were examined.

Figure 4.3.10 shows the results of the static test on the stainless steel surface (20 °C to 360 °C). The difference between the probe and block temperatures (steady-state) is shown in red and the difference between the phosphor and block temperatures is shown in black. Key points are:

- The steady-state probe perturbation to the surface temperature increases linearly with surface temperature. This clearly indicates the need for calibration of the surface probe.
- The phosphor temperature agrees with the block temperature (measured via extrapolation as described earlier). This demonstrates that phosphors can be used in place of embedded contact sensors with minimal perturbation or errors.

Figure 4.3.10 also shows the results of the dynamic test on the stainless steel surface at 300 °C. The time taken for the probe to reach stability is of the order of 15 minutes and the perturbation to the surface temperature is approximately 23 °C in this sample.

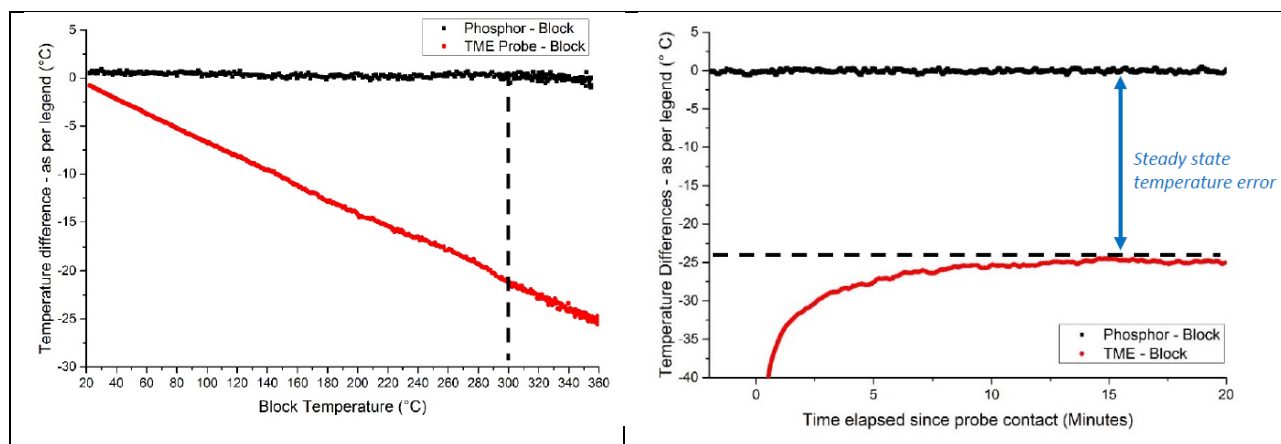


Figure 4.3.10: Left: Contact probe static test on stainless steel surface (20 °C to 360 °C) – steady-state temperature error compared to phosphor temperature. Right: Contact probe dynamic test on stainless steel surface at 300 °C – example of time taken for probe to reach stability and associated temperature error.

4.3.2 Development of phosphor thermometers – INRIM

The operating principle of the INRIM phosphor thermometer is based on the lifetime of a thin layer of thermographic phosphor coated on the surface under test. The phosphor and coating methodology was similar to that employed at NPL. The fluorescence was stimulated using excitation at 405 nm with a laser diode (LD). This LD emission was modulated in the form of repetitive rectangular pulses, focused into one branch of a 1x2 fibre coupler and delivered to the phosphor layer. The second branch of the fibre coupler was used to guide out the exponentially-decaying fluorescence response to a detection stage. Here, a silicon p-i-n photodiode converted the optical signal into an electrical signal. The latter was then sampled at 1 MS/s and converted by a 16-bit DAC module (NI DAQ), interfaced to a PC, for further processing [61,62]. The key parameter is the temperature-dependent fluorescence lifetime, whose change with temperature is characteristic of each phosphor. The fluorescent lifetime was then converted into a temperature through a pre-set calibration curve of the sensor investigated in a separate experiment. A scheme of the fibre-optic thermometer developed at INRIM, and this, together with the portable excitation/detection unit, is shown in Figure 4.3.11.

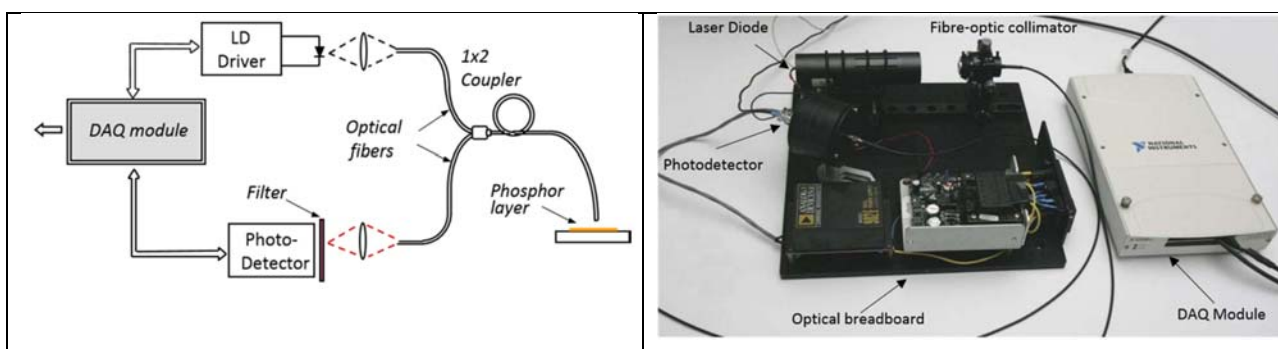
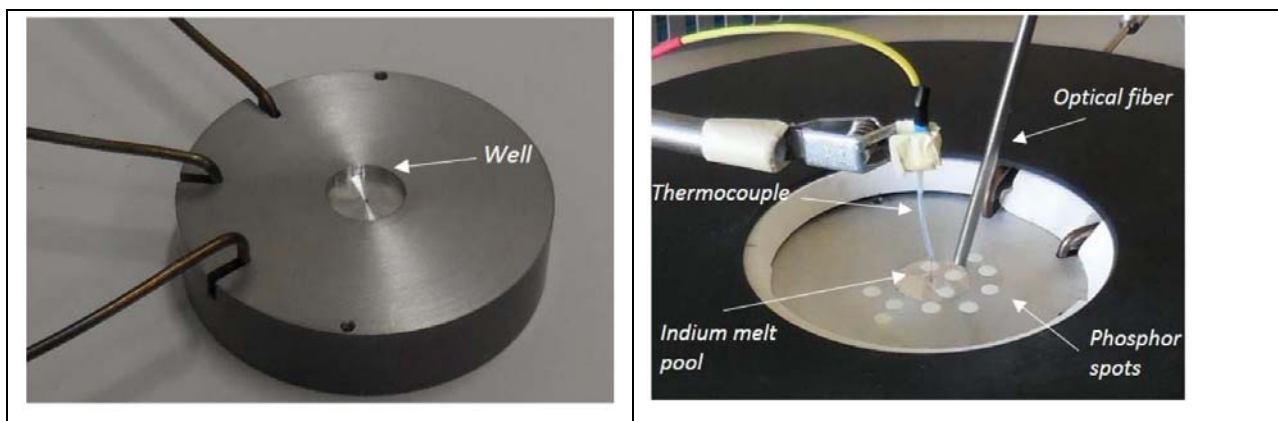


Figure 4.3.11: Phosphor-based thermometer developed at INRIM (left), and portable excitation/detection unit (right).

Phosphor calibration

In order to use the phosphor as a temperature sensor, it must be subjected to a traceable calibration. To ensure that the calibration conditions were as close as possible to the actual operating conditions of the phosphor, it was calibrated by contact on the INRIM reference calibrator system for surface sensors in the temperature range from 50 °C to 450 °C. This system is based on a temperature-controlled block, whose surface acts as a temperature reference, in a similar manner to that of the NPL system described above. The system was validated using the melting point of indium as for the NPL system. Figure 4.3.12 shows the block calibrator and the validation setup.



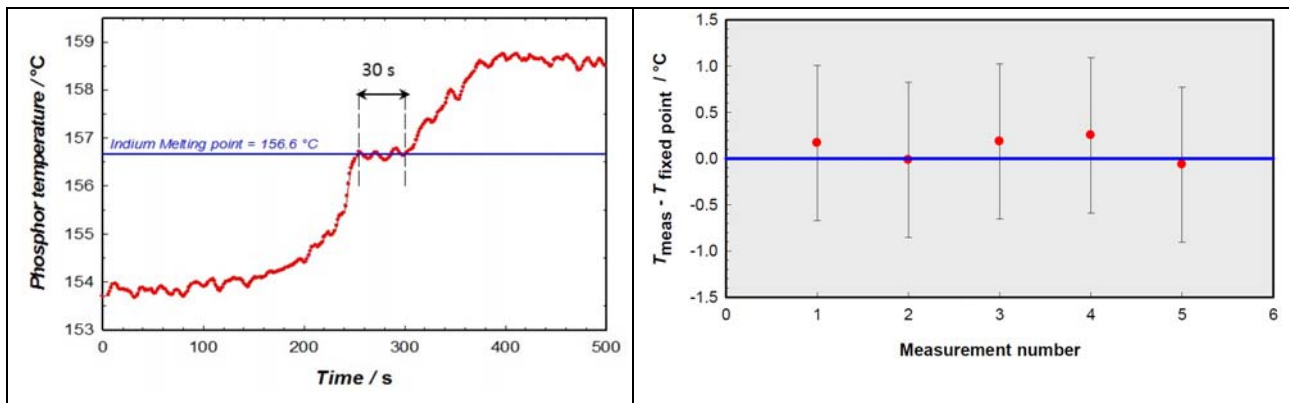


Figure 4.3.12: Top left: reference block with a well to house the indium. Top right: arrangement for the calibration of the phosphor. Bottom left: phosphor response during indium melting. Bottom right: difference between temperature measured by the phosphor and the indium melting temperature; error bars represent expanded uncertainty ($k = 2$, 95%).

Effect of IR background radiation

It is important to characterise the effect of significant IR background radiation which is commonly found in industrial applications. To do this, an IR lamp with incident power of 1 kW m^{-2} was used to generate background radiation on the hot plate reference surface, where a thin spot of phosphor was coated; this is shown in Figure 4.3.13.

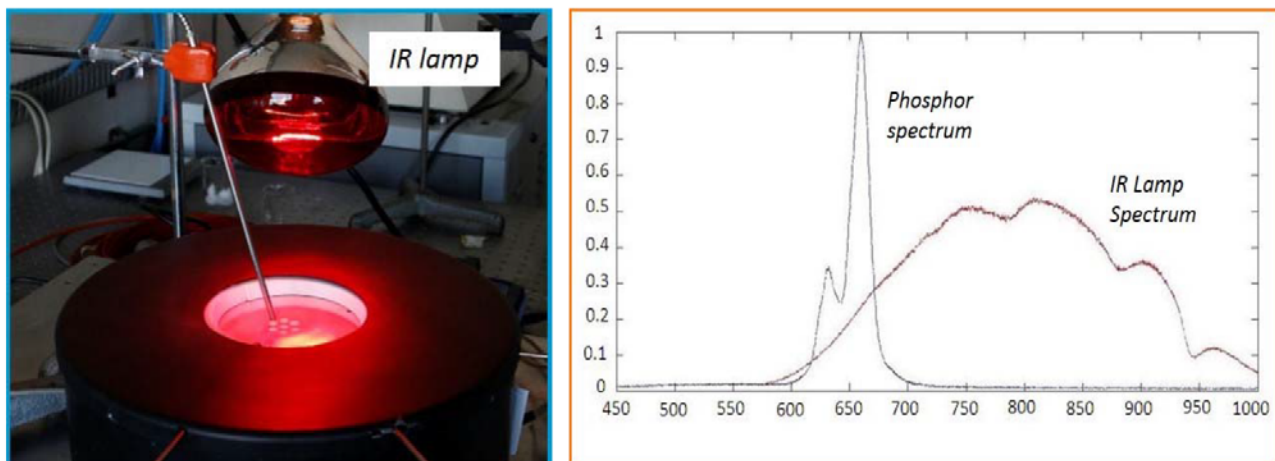


Figure 4.3.13: Experimental arrangement for assessing the effect of background IR radiation (left) and normalised power spectra of IR lamp and phosphor (right).

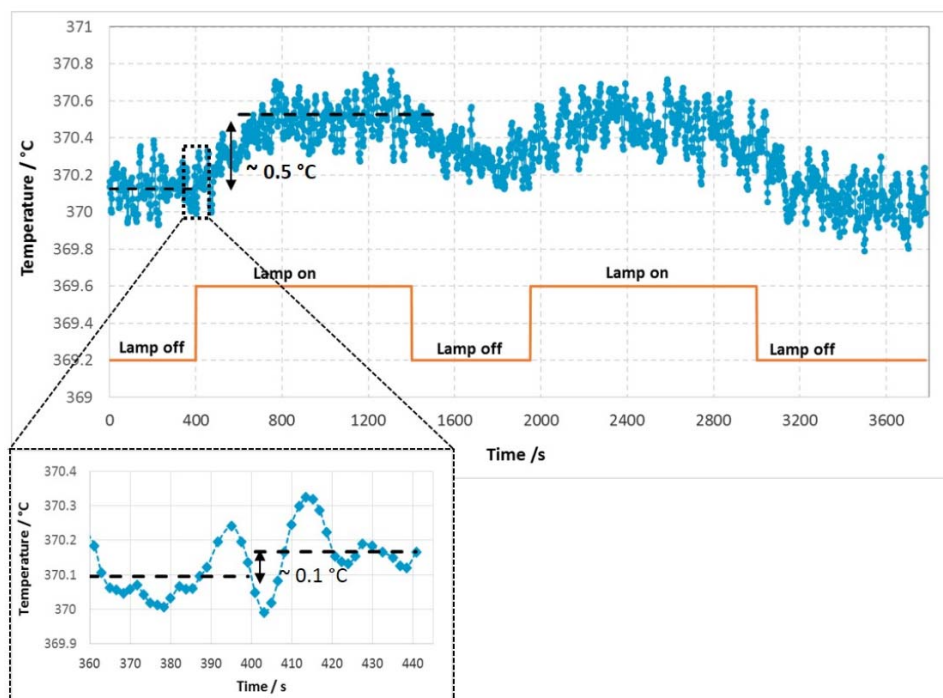


Figure 4.3.14: Phosphor response in the presence of a strong IR background radiation.

The IR lamp was repeatedly turned on and off and the phosphor response was recorded (Figure 4.3.14). The measurements indicate a slight long-term radiative warming of the surface due to the lamp of approximately 0.5 °C. The short-term radiative disturbance of the lamp on the electro-optic system was investigated by measuring the instantaneous variation of the fluorescence response when the lamp is switched on/off. A variation of about 0.1 °C, i.e. lower than the measurement repeatability, was observed. Thus, the phosphor-based thermometer is 'robust' enough to be unaffected by the strong radiative background.

Measurement uncertainty

A key difficulty of the technique is the production of a thin, robust and reproducible phosphor coating with good adhesion to the surface under test. The technique for preparing such a coating has been refined, by defining the most suitable mixing ratio of phosphor/binder, the thickness of coating, and the curing process. A deposition-based application process was employed. Nevertheless, the reproducibility associated with the coating must be taken into account if the calibration is transferred between different coatings. This contribution was experimentally evaluated by coating a two-dimensional array of phosphor spot sensors on the reference calibrator block and then measuring the fluorescence lifetime corresponding to the different spots. Over the whole temperature range from room temperature to 400 °C the spread of the temperatures measured by the spot sensors were within 0.5 °C both in the case of aluminium and stainless steel. The expanded uncertainty for the phosphor thermometer, including all relevant contributions, at 400 °C amounts to 1.168 °C ($k = 2$).

4.3.3 Development of phosphor thermometers – in-process trials at Gamma Forgiati (GF)

In the processing of aluminium alloy billets for the hot forming and forging of mechanical components, an accurate surface temperature control (within ± 5 °C) during the pre-heating is required. The INRIM optical fibre coupled phosphor thermometer was applied to the surface temperature measurement of aluminium alloy billets during pre-heating in hot forging at Gamma Forgiati using a large-scale industrial furnace; this was compared with conventional techniques both in static (i.e. billet stationary inside the furnace) and dynamic (i.e. during the extraction of the billet from the furnace) conditions. The phosphor thermometer was compared against a Type K thermocouple and a radiation thermometer.

Stationary conditions

The aluminium billet under test was equipped with a Type K thermocouple, introduced from the bottom, and with a series of fluorescent spots (Figure 4.3.15), and placed in a horizontal tube furnace. Simultaneous measurements were performed with the three thermometry techniques; all measurements are in agreement within the uncertainty, as shown in Figure 4.3.15.

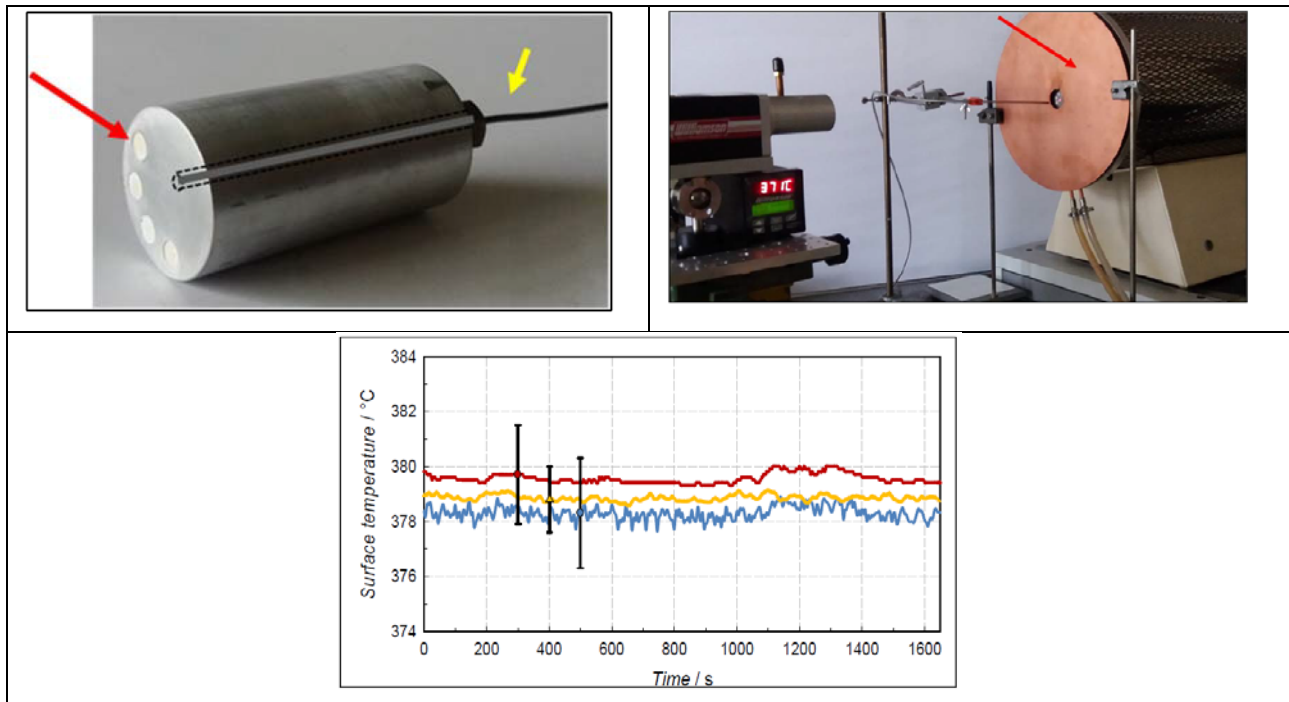


Figure 4.3.15: Aluminium billet (top left panel; red arrow indicates phosphor spots, yellow arrow indicates thermocouple). Top right panel shows the billet mounted in the horizontal tube furnace. Bottom panel shows agreement between the three measurement methods. Blue: radiation thermometer, yellow: phosphor thermometer, red; thermocouple.

Dynamic conditions

Measurements were also performed, with the same setup, in dynamic conditions i.e. during the extraction of the aluminium billet from the furnace, simulating the cooling to which the sample is subjected when it leaves the industrial pre-heating furnace before being forged. In this case, Figure 4.3.16 shows the temperature as a function of time indicates by the three methods, again showing good agreement.

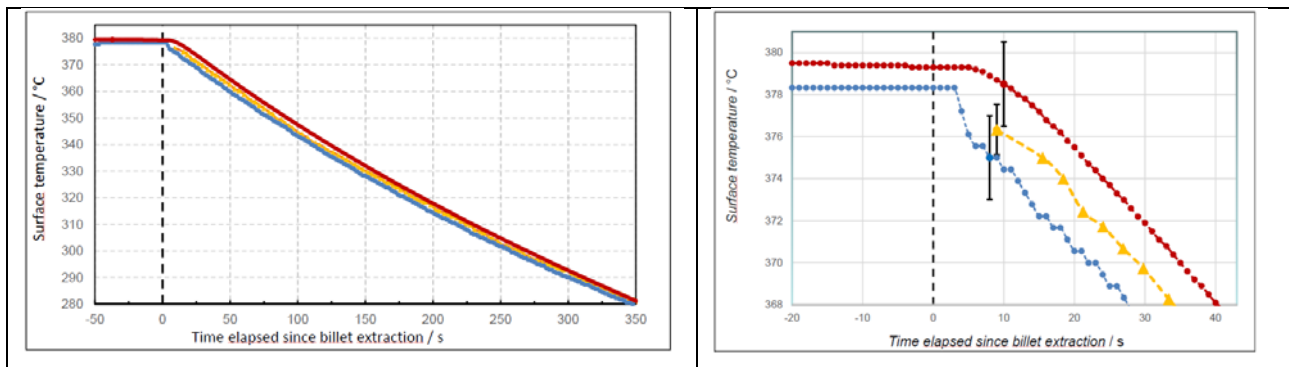


Figure 4.3.16: Surface temperature indicated by the three techniques under dynamic conditions. Colours as for Figure 4.3.15.

In-line measurements during manufacturing

The three techniques were shown to be equivalent under controlled conditions. For the in-line surface temperature measurements during manufacturing at Gamma Forgiati, radiation thermometry was chosen. This remote technique is better suited to this specific application, in which the billets on the conveyor belt are moving and are not readily accessible. In our experimental set-up four billets were placed inside the 4 m long furnace. One of the billets (billet 4) was equipped with a Type K thermocouple to give further validation of the radiation thermometry during the process. It takes about 20 minutes for the billets placed on the conveyor belt to reach the output of the furnace properly pre-heated and thus ready to be forged. The multi-wavelength radiation thermometer was placed at about 1 m from the furnace outlet, aimed at the billets leaving the oven. Figure 4.3.17 shows the industrial process setup.

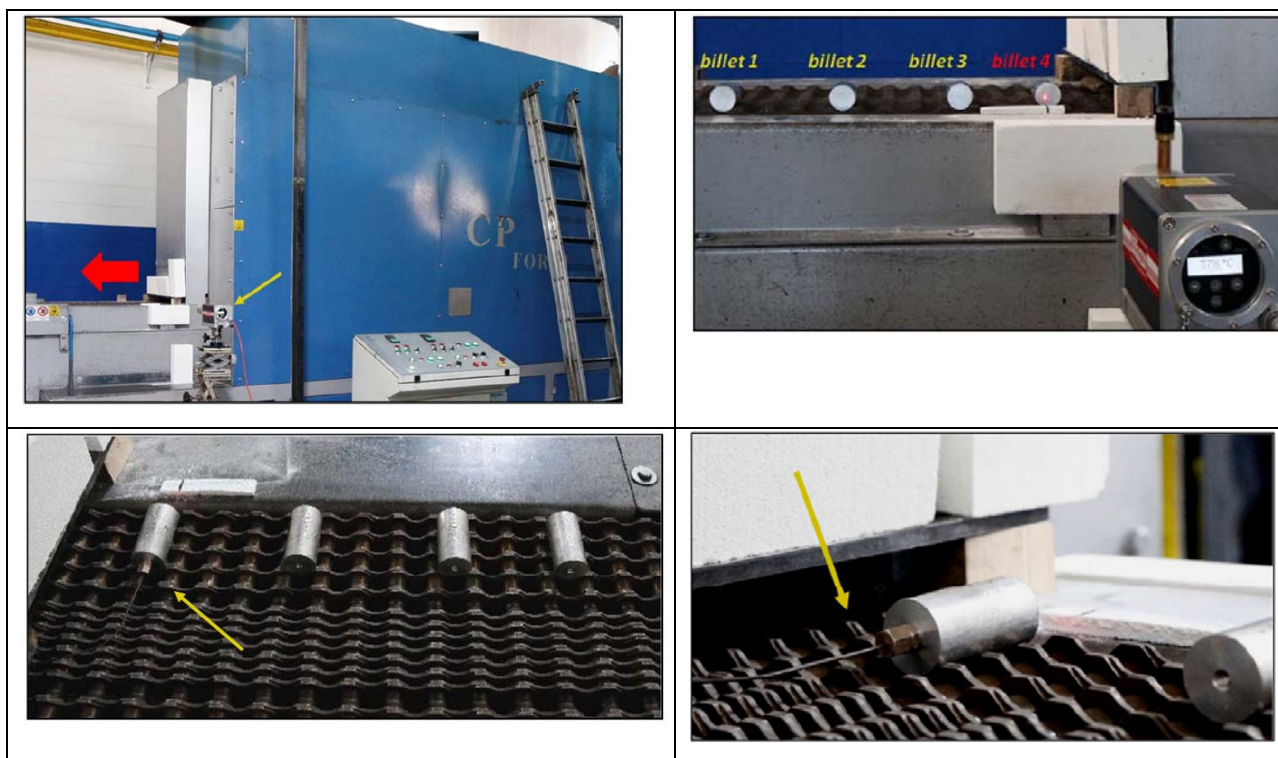


Figure 4.3.17: Top left: Industrial furnace for in-line manufacturing at Gamma Forgiati (the red and yellow arrows indicate the furnace outlet and the radiation thermometer, respectively). Top right: Aluminium billets in output from the pre-heating furnace (Billet 4 is equipped with a Type K thermocouple). Bottom: Aluminium billets on the conveyor belt at the output of the pre-heating furnace; arrow indicates Billet 4 with the thermocouple.

The surface temperature of the four billets as measured with the radiation thermometer are shown in Figure 4.3.18, together with a comparison of the radiation thermometer and the thermocouple; again good agreement is seen, even in this harsh industrial environment.

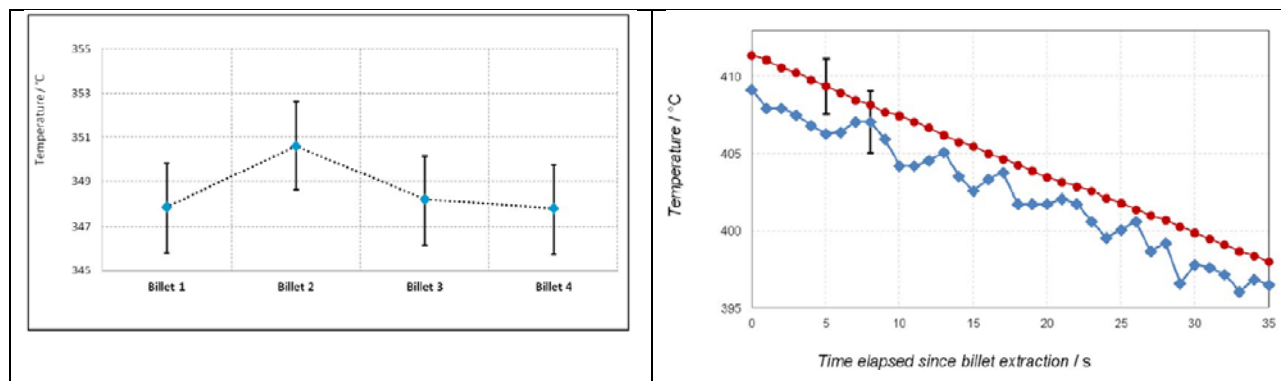


Figure 4.3.18: Left: Surface temperature of the four billets as measured with the radiation thermometer. Right: Surface temperature during the first few tens of seconds after removal from the furnace

The actual process considered here is best suited to radiation thermometry. However the radiation thermometer needs to be calibrated periodically to ensure in-process measurement traceability. Here, the phosphor-based technique can provide traceable, in-situ calibration in a comparatively simple way, being more suitable than contact thermometry.

4.3.4 Development of phosphor thermometers – in-process trials at BAE Systems

The strength of steel welds is critically dependent on the temperature of the steel parts to be joined pre- and post-welding. To improve the temperature measurements of the marine steel surfaces involved at BAE Systems, NPL adapted the phosphor thermometry setup described in the above sections by introducing an LED light source (20 mW, $\lambda = 420$ nm) and coupling it with an optical fibre to enable remote sensing which is more convenient for the industrial setting involved; this is shown in Figure 4.3.19.

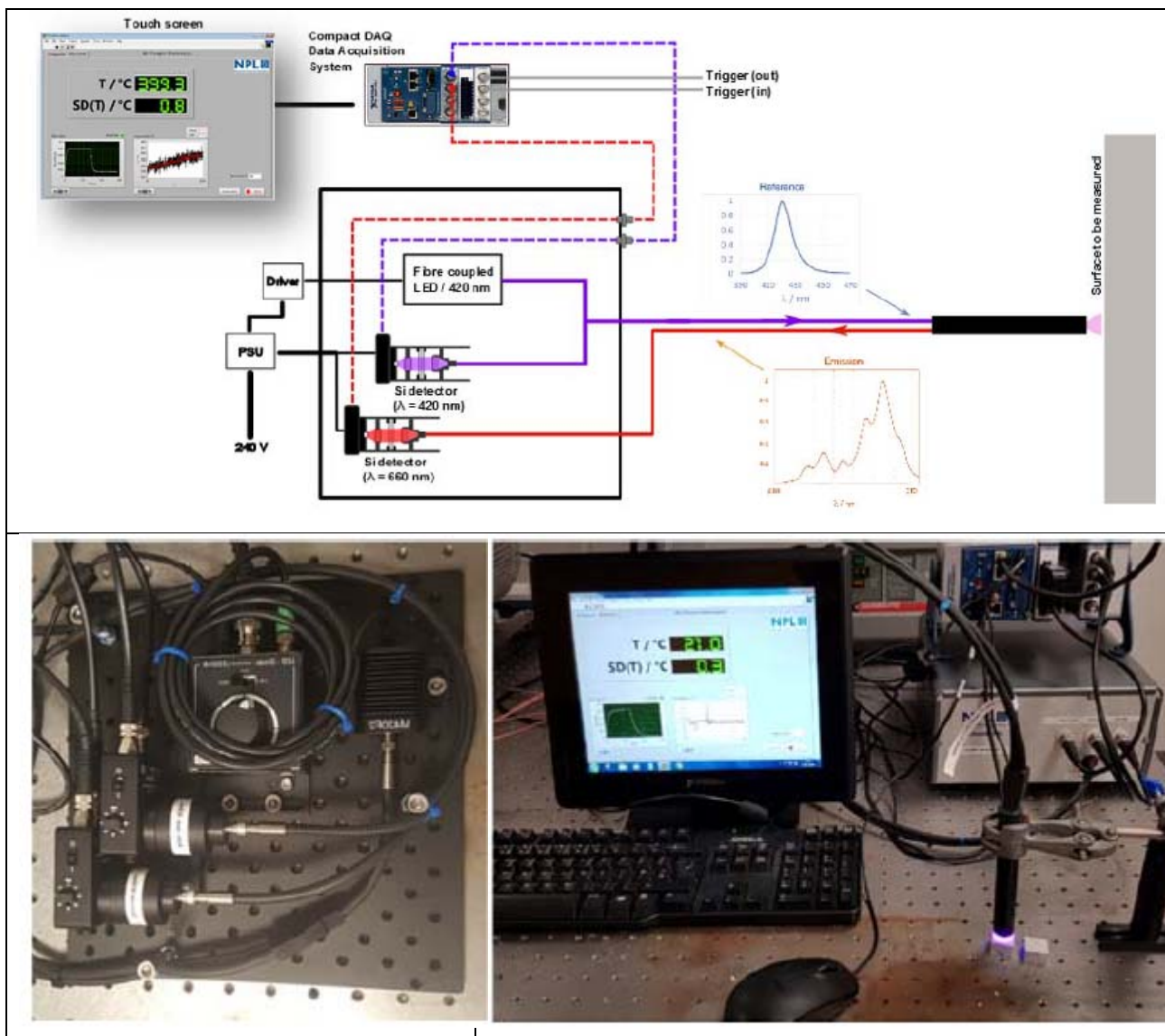


Figure 4.3.19: NPL portable phosphor thermometer design and construction.

The phosphor thermometry system was calibrated over the temperature 20 °C to 525 °C by placing the probe close to a phosphor coated steel (BAE supplied) thermal validation target installed into the end of a horizontal tube furnace. The validation process was as described in the previous section above.

Field trials were performed at BAE Systems, Barrow-in-Furness, Cumbria, in February 2018. This comprised two activities: a) measurements on a commercial surface probe calibrator provided by BAE and b) measurements on a pre-heated block of submarine steel before, during and after a simple welding procedure was applied.

Calibrator testing

BAE supplied an Isotech Jupiter calibration system, capable of reaching temperatures of approximately 140 °C. This was modified to accommodate an aftermarket block with a diameter of approximately 40 mm. One quarter of the block was covered with a phosphor coating (raw phosphor and binder supplied by NPL but applied by BAE) and the block was made with the same proprietary steel as used for BAE's construction purposes. To make an independent surface temperature reading, three 2 mm Pt100s are used to extrapolate a temperature to the surface. The tips of the probes were at the centre of the block, providing around 20 mm of immersion. A schematic is shown in Figure 4.3.20.

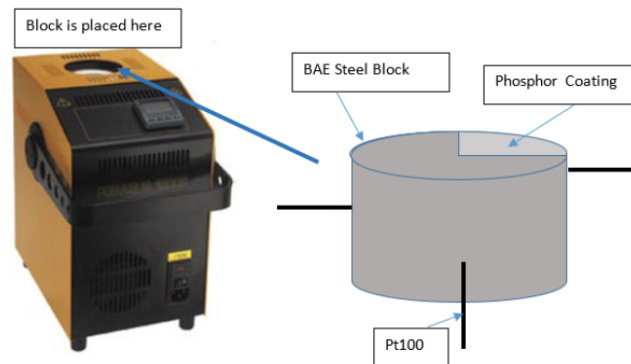


Figure 4.3.20: BAE steel block with phosphor coating.

A series of tests were performed to compare the phosphor thermometry against a conventional thermocouple surface probe (i.e. the conventional measurement device). The results were consistent with those found in the laboratory, namely that the phosphor thermometry is much more reproducible than the contact surface probe. Figure 4.3.21 shows the contact probe error as a function of surface temperature for different materials.

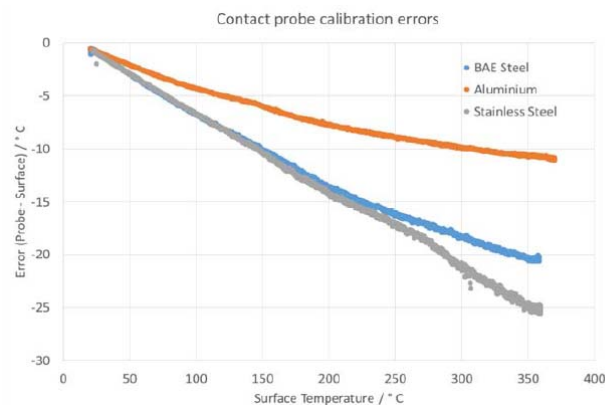


Figure 4.3.21: Contact probe conduction errors for different materials.

Industrial trials

The phosphor thermometer was used to assess the 'inter-pass temperature' during a welding process. This is a critical temperature band in which welding can be performed on steels used in the construction of the submarines made at BAE. The process is as follows:

- Pre-heat the steel to a defined temperature and measure it
- Perform the weld
- Monitor the temperature rise after the weld is complete
- Perform additional welding once the temperature falls within the 'inter-pass temperature' band

The steel block was instrumented with six Type-K thermocouples spot-welded to various positions. A sketch of the setup is shown in Figure 4.3.22, showing the sensor positions.

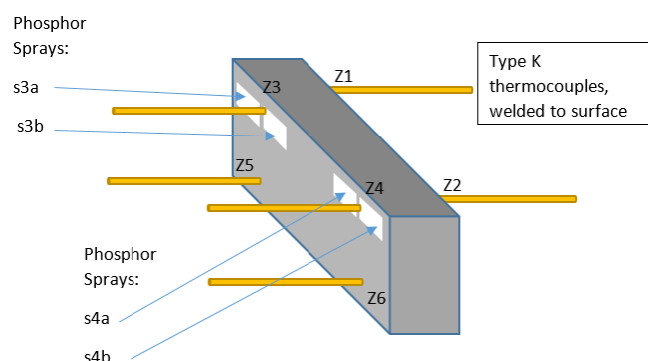


Figure 4.3.22: The BAE industrial trial setup.

In the first test, comparisons were made between the phosphor coatings, the welded Type K thermocouples, and the surface contact probe as described in earlier tests. This was done at a nominally constant pre-heated temperature, prior to any welding. It is unknown if the welded thermocouples are calibrated. As before, the phosphor measurements read consistently high. The contact probe and welded Type K thermocouples track well with the phosphor measurements, and there is a clearly identifiable temperature gradient from one portion of the block to the other. It should be noted that the phosphor measurements take about 0.5 s to be obtained, whereas the contact probe measurement takes about 30 s to stabilise.

Figure 4.3.23 shows transient temperature data from phosphor spray 4a, immediately after the weld. The probe was held with approximately 3 mm stand-off from the block. The phosphor tracks the temperature increase and subsequent cooling and, more importantly, is able to measure the temperature very quickly. The tracking of this temperature is key to reliable welding. In comparison, the long response time and perturbative nature of surface contact probes does not allow transient temperature information to be gathered in this way.

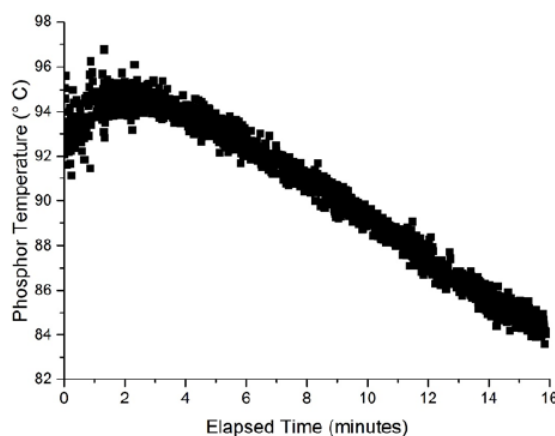


Figure 4.3.23: BAE steel sample – transient measurement of Zone 4a, immediately after weld completed.

4.3.5 Heat flux compensated probe and block calibrator

CMI have developed a surface temperature probe and evaluation unit with display called the 'Thermometer Tectra Master'. This work involved the extensive engagement of an RMG from BIM, Bulgaria. The principal scheme is shown in Figure 4.3.24. The stem contains two MI Type N thermocouples. One is connected to the brass layer in contact with the surface under test, while the second one measures the temperature about 10 mm above the surface. The difference arising from heat flow is computed and compensated for by the heater wound in the wall of the stem. The device operates from room temperature up to about 550 °C.

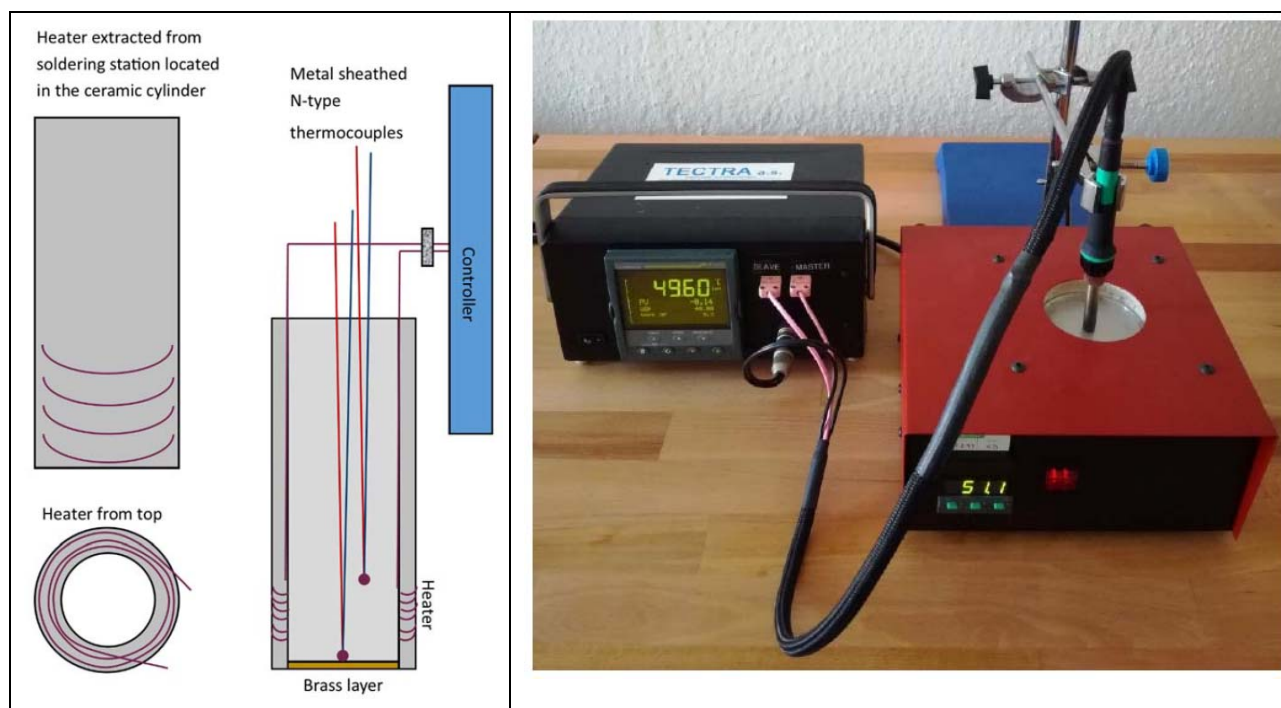


Figure 4.3.24: Scheme of the surface temperature probe.

A key feature of the device is that it is somewhat sensitive to the pressure used to hold it against the surface under test; for this reason most reproducible results are obtained when using a dedicated holder to apply a reproducible pressure. Above 400 °C, a radiation shield should be used to protect the probe from damage.

Three different surface temperature calibrators were used to validate the thermometer. The first was the commercially available Isotech 983 with aluminium surface; the second was the Pemit KT 550, and the third was the Pemit RKT-900 which permits interchangeable surfaces and operates to 900 °C. To validate the thermometer, all three calibrators were used, with aluminium surfaces. The differences between the various calibrators are smaller than the corresponding measurement uncertainty; this is shown in Figure 4.3.25.

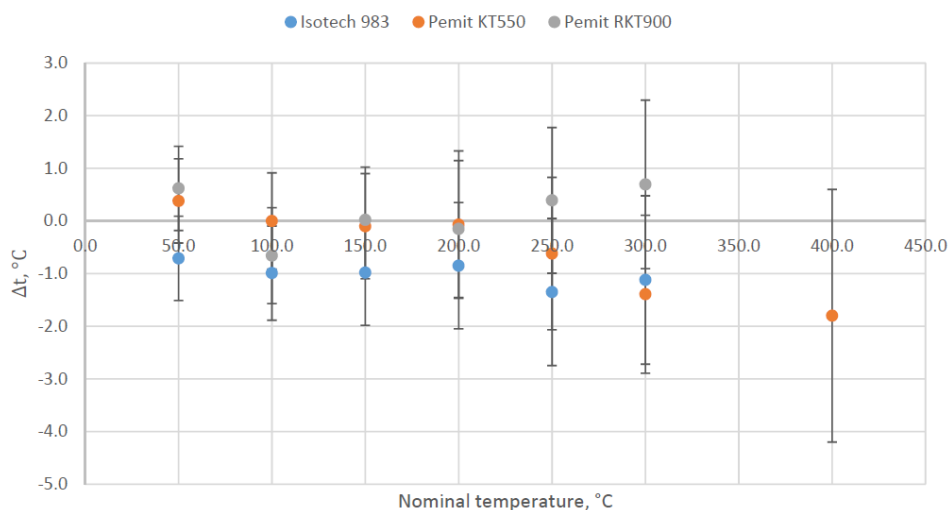


Figure 4.3.25: Results of the validation for the three calibrators; error bars show the uncertainty ($k = 2$).

To supplement the characterisation of the surface temperature probe calibrators, an RMG from BIM (Bulgaria) performed a series of experiments to systematically determine the effect of various parameters on the measurement accuracy. This included the effect of application pressure of the probe on the surface; orientation of the probe; influence of the probe/surface material; the difference between horizontal and vertical surfaces; the influence of the surrounding air velocity; short and long term drift of the sensors under typical use; and homogeneity of the surface temperature probe calibration devices. These parameters have been used to

inform the uncertainty budgets associated various aspects of the surface temperature measurement work. Examples of the measurements and corresponding results are shown in Figure 4.3.26.

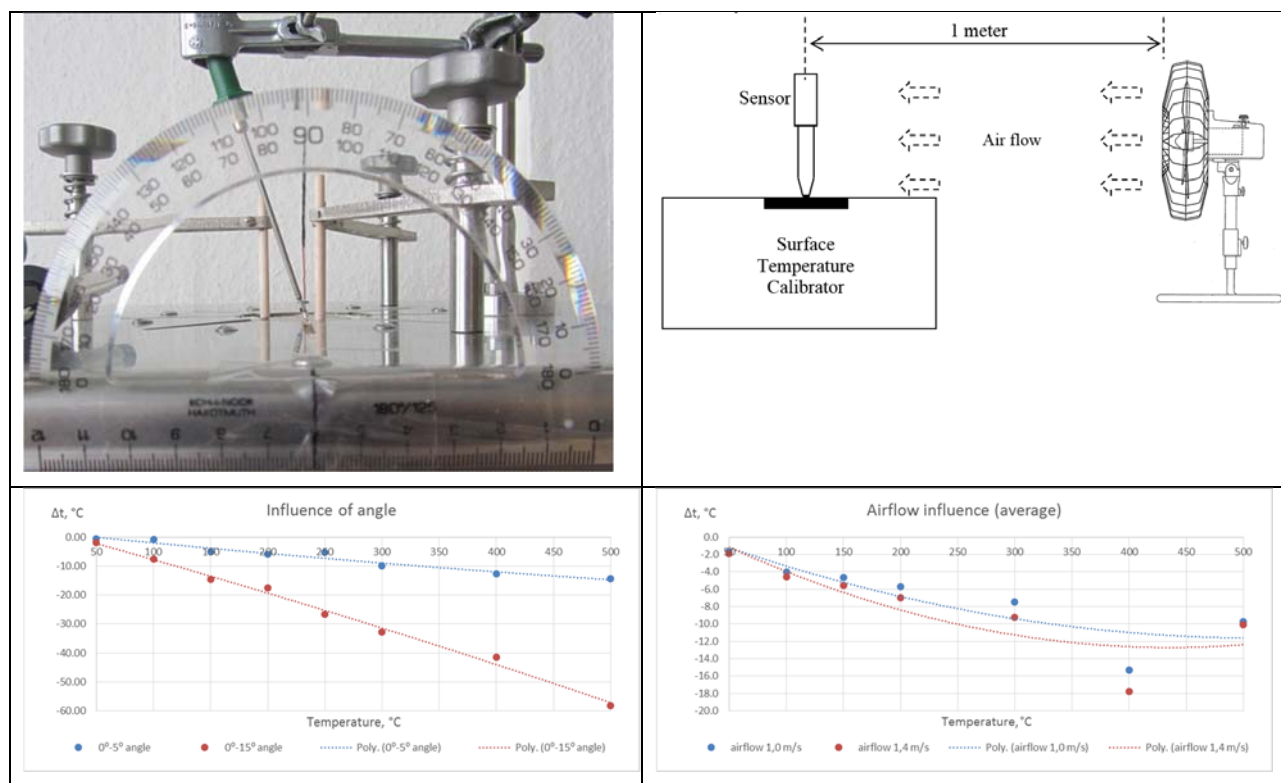


Figure 4.3.26: Top left: setup for measuring the angle dependence of the contact temperature probe measurements. Bottom left: temperature measurement error as a function of temperature, for different application angles. Top right: setup for systematic measurements of the error arising from airflow. Bottom right: temperature measurement error as a function of temperature, for different airflows.

4.3.6 Surface temperature probe calibrator at DTI

DTI has significantly developed its pre-existing surface temperature probe calibrator to operate from -20 °C to 500 °C, with five interchangeable materials for the surface itself. The system has been validated by comparison using the heat flux compensated probe, which has participated in measurements at INRIM, NPL and CMI at temperatures up to 370 °C. It is currently undergoing further validation in the Euramet intercomparison 1149 which involves a Europe-wide intercomparison of surface temperature calibrations. This will link the comparison performed in EMPRESS to a running Euramet intercomparison.

In addition, DTI has developed a system for phosphor thermometry by measuring the fluorescence lifetime, which has been locally validated up to 250 °C; in particular, the effect of the phosphor layer thickness has been evaluated systematically. DTI has also performed an assessment of the uncertainty associated with the phosphor thermometry system at INRIM, under different conditions including an isothermal setup, at a hot surface, and by comparison with the indium melting point (156 °C).

Summary of results

- Traceable phosphor thermometry developed to 500 °C – for direct application to surfaces, and to provide the reference temperature of surface probe calibrators; successfully trialled at BAE Systems and Gamma Forgiati
- Heat flux compensated probe developed to 500 °C and validated against embedded thermocouples

4.4 Traceable combustion temperature measurement

State of the art

Currently, the most accurate means of measuring temperature of combustion processes are with exotic laser-based apparatus such as CARS, DFWM or LIGS, however these are very complicated, and not generally accessible. Thermographic phosphors are sometimes deployed, but again despite the sophistication the uncertainty is typically between 5 % and 10 % of temperature. Thermocouples are sometimes used but such measurements are prone to under-reading by hundreds of degrees. None of these methods are traceable. To advance the state of the art, a standard flame has been commissioned, that has a known, validated temperature, as determined by characterisation at complementary facilities across Europe, and that can be transported to an end-user's site and used to validate the optical temperature measuring methods. The uncertainty of the portable standard flame has been reduced by a factor of 10 compared with that previously available.

4.4.1 Development of a portable standard flame system

The portable standard flame system has been fully commissioned and is available as a measurement service to external customers. Using laser Rayleigh scattering, it has been possible to determine the post-flame temperature with an uncertainty of less than 0.5 % of temperature – this is a factor of two less than the original target uncertainty of 1 % of temperature. The flame and laser interrogation are shown in Figure 4.4.1. Additionally, the system can provide a number of fixed and reproducible temperatures and species concentrations for propane/air equivalence ratios from $\phi = 0.8$ (lean flame) to $\phi = 1.4$ (rich flame). The range of fixed temperatures that can be attained (dependent on ϕ) is $\{2050 \text{ K} < T < 2250 \text{ K}\}$. This provides a robust mechanism to not only validate third party optical techniques but also assess their linearity. Measurements made by UC3M/CEM using a hyperspectral imager show excellent agreement with the STD portable standard flame, validating the technique and leading the way for development of a low-cost instrument in the EMPRESS 2 follow-on project. Measurements made by DTU using IR/UV spectroscopy are equally impressive, showing outstanding agreement with the NPL measurements. In one case, it was possible to improve on the NPL temperature profile measurements (provided in the user instructions) by comparison of the measured and synthesised IR emission spectral. This demonstrates that the collaboration between partners has been a two-way process, with each enhancing the other. The outputs from this work will feed in to the development of a fast scanning spectroscopic thermometer for industrial use in the EMPRESS 2 project.

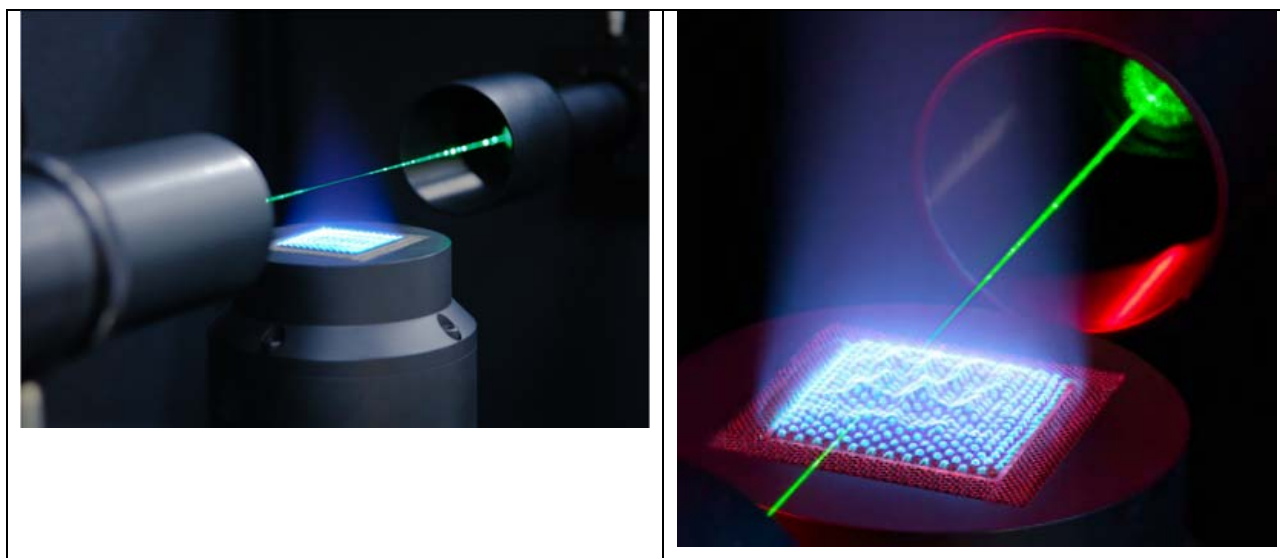


Figure 4.4.1: Portable standard flame, shown here with laser Rayleigh scattering interrogation.

Figure 4.4.2 shows the performance of the NPL portable standard flame: in a) the mean temperature measured, versus ϕ , for ten tests carried out over a three month period are shown; in b) the reproducibility of the system over the period May 2016 to Jan 2018 is shown – the system demonstrates a remarkable reproducibility of better than 0.5 % of temperature.

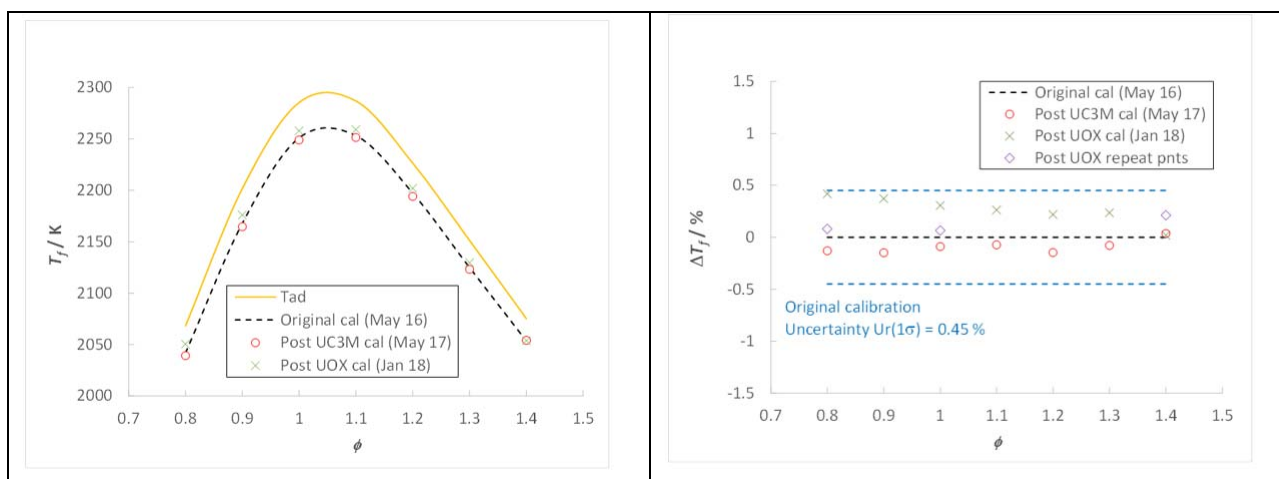


Figure 4.4.2: Portable standard flame - post UC3M/UOX trials performance: LHS - Rayleigh flame temperature 2 cm above the burner, RHS - reproducibility (percent of temperature), demonstrating that the system has remained stable to better than 0.5 % of temperature over a 2.5 year period.

4.4.2 Development of a FTIR flame thermometry system

The UC3M/CEM FTIR Hyperspectral Imaging System was the first optical technique used to obtain accurate temperature values of the NPL standard flame apart from the NPL Laser Rayleigh scattering technique. Its main advantages are the standoff and safer distance of measurement which is important for combustion processes and the possibility to get spatial and spectral information of the flame in the same measurement. The final temperature results have a very good agreement with the values obtained by NPL, which validates this technique as an excellent alternative to measure both accurate temperature and species concentration data for flames with a simple measurement setup. Following on from this work, in EMPRESS2, UC3M/CEM will develop a practical imaging spectrometer for industrial use.

Figure 4.4.3 shows a comparison of the flame temperatures measured by NPL (Rayleigh scattering) and UC3M/CEM (hyperspectral imaging). The agreement between the two techniques is excellent, particularly in the central region where the post-flame composition is well defined.

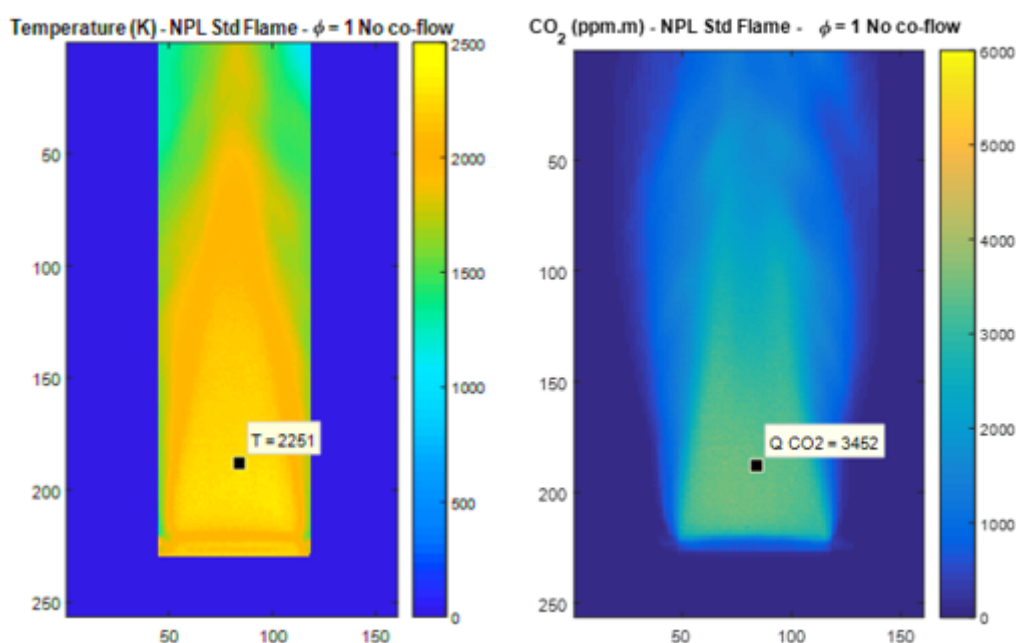
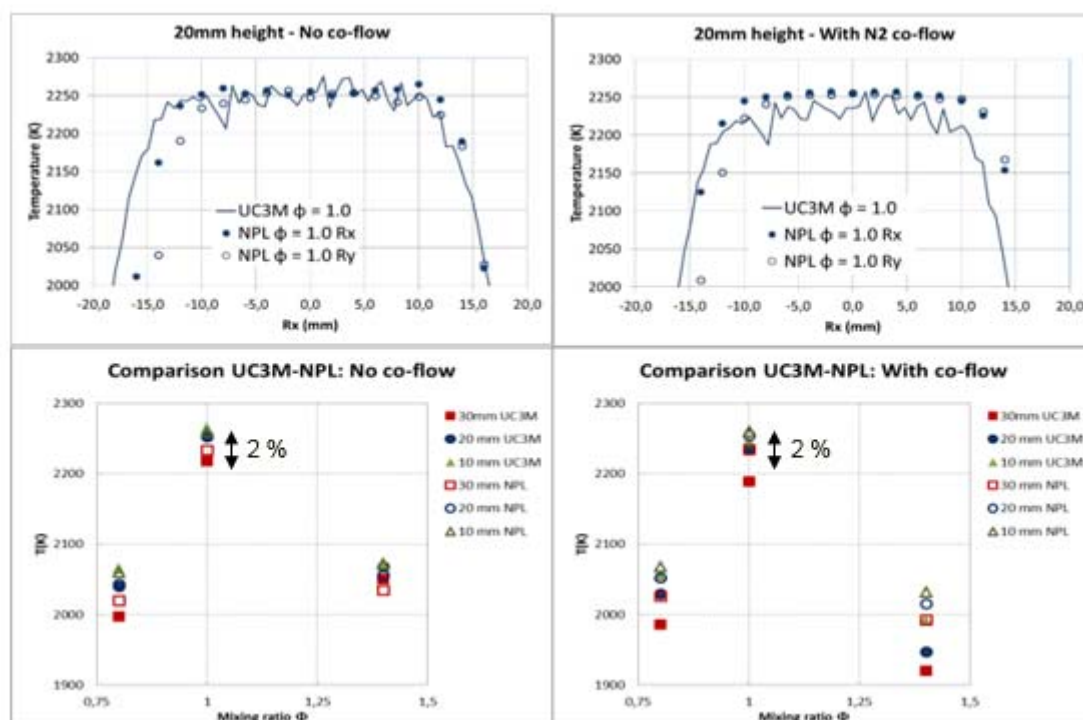


Figure 4.4.3: Comparison of the flame temperatures measured by NPL (Rayleigh scattering) and UC3M/CEM (hyperspectral imaging) - TOP: spatial temperature profile comparison and comparison of the mean temperatures versus ϕ ; BOTTOM: typical temperature and CO₂ species maps measured with the hyperspectral imager.

The DTU infra-red spectrometer is a FTIR-based system and has been adapted for measurements on the DTU small gas burner. A miniature FTIR fibre-optic probe has been designed. A small black-body light source for the FTIR fibre-optic system has been produced and tested. Due to a number of minor issues with the small gas burner, the FTIR system has been used on a second Hencken burner provided by NPL.

The measurements on NPL's spare burner were completed in October 2017 and the flame thermometry system was substantially updated. The FTIR spectrometer has been upgraded for a faster scanning in order to suppress flame flickering effects on measured FTIR spectra and a unified approach for IR and UV

measurements was selected. The approach utilises N_2 purge for all optical paths including FTIR/UV spectrometers and use the same close-to-burner optical path enclosures for both IR and UV measurements (also purged by N_2). This allowed single line-of-sight measurements with a well-defined field-of-view and minimises any side effects such as CO_2 self-absorption (IR), O_2 absorption (UV) and temperature variations in the system when the burner is in operation. In this way, additional (unwanted) light attenuation by other optical components such as that from fibres and lenses was eliminated.

Finally the measurements on the NPL standard burner were performed successfully at selected equivalence ratios 0.8, 1 and 1.4. The spectra were free from CO_2 self-absorption and flame flickering effects. Comparison of the measured emission spectra at various heights above the burner surface with forward radiative heat transfer models (using the latest HITEMP2010 spectral database and the NPL temperature profiles) show excellent agreement. It was also possible to optimise one of the NPL temperatures profiles at the flame boundary through this comparison.

Figure 4.4.4 shows the FTIR system interrogating the NPL standard flame, with the measurement geometry and FTIR optical probe shown on the LHS and the purged probe measuring close to the flame shown from a different angle on the RHS.



Figure 4.4.4: The DTU FTIR instrument measuring the temperature above the NPL STD flame. LHS: measurement geometry, with FTIR optical port visible (above indicated y-axis); RHS: FTIR purged optical probe measuring close to the burner.

It was shown that a single temperature reference point was not enough to model the measured IR emission spectrum, i.e. a whole temperature profile has to be used. It was also shown that the quality of the HITEMP2010 database for CO_2 and H_2O in selected spectral ranges is very good (better than 1 %). Therefore the NPL standard burner with DTU thermometry system can in the future be used for further validation/development of high-temperature spectral databases.

Figure 4.4.5 shows an example of the measured and synthesised spectra for the NPL standard flame for $\phi = 1.4$ and 32 mm height above the burner: Green line – synthesised spectra based on NPL provided temperature profile; Blue line – measured emission spectra; Red line – difference between the measured and synthesised spectra, showing excellent agreement.

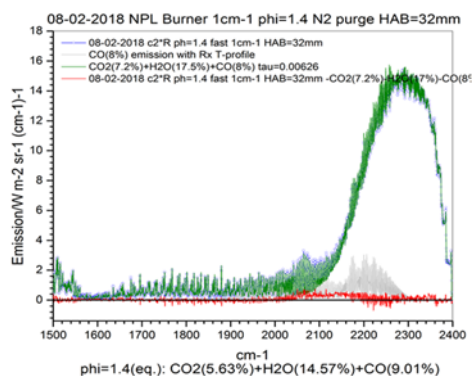


Figure 4.4.5: Measured and synthesize flame spectra of the NPL STD flame from DTU, for $\phi = 1.4$, 32 mm height above the burner. Green line – synthesised spectra based on NPL provided temperature profile. Blue line – measured emission spectra. Red line – difference between the measured and synthesised spectra, showing excellent agreement.

Additionally, a machine-learning approach (in collaboration with University California Merced (UCM), USA) for temperature retrievals from the DTU thermometry system has been investigated. The results show that

temperature profiles can also be obtained use low-resolution spectra (from 4 cm^{-1} and below) if sufficient training of the algorithm is performed. Figure 4.4.6 shows an example of how, using the machine learning approach, the temperature profile 20 mm above the burner (for $\phi = 1.0$) can be improved based on a comparison of the measured and synthesised emission spectra. The NPL measurements are shown by the black lines, and temperature profiles retrieved from the DTU measurements (8 cm^{-1} spectral resolution) are in red (labelled predicted I) and blue (predicted II) lines. The machine learning algorithm has minimised the difference between the measured and synthesised emission spectra by allowing the temperature profile of the burner to be asymmetric. This has improved the NPL profile at the edge of the flame where the Rayleigh scattering measurement has larger uncertainties. It is worthy of note that the agreement between the NPL and DTU results is outstanding, with differences in the central region (where the uncertainty of the NPL Rayleigh measurements is 0.45% of T) of 0.23% . The reproducibility of the DTU emission spectra measurements in the range 1800 cm^{-1} to 2500 cm^{-1} and 3000 cm^{-1} to 4200 cm^{-1} is better than 2% and 5% respectively, for time spans of minutes to days. This is because of $\text{CO}_2/\text{H}_2\text{O}$ concentration variations in the flame: measured emission spectra intensities depend on both concentrations and temperature. It should be noted that emission intensity in the range 3000 cm^{-1} to 4200 cm^{-1} is about seven times smaller than that in the range 1800 cm^{-1} to 2500 cm^{-1} . Considering 2% as a maximum scaling factor, the overall uncertainty of spectral measurements in the range 1800 cm^{-1} to 2500 cm^{-1} is better than 0.01% . Therefore uncertainty in the temperature retrievals is mainly defined by the quality of the HITEMP2010 database, namely 0.17% in the range 2150 cm^{-1} to 2500 cm^{-1} (this range has the most ‘weight’ in the retrievals).

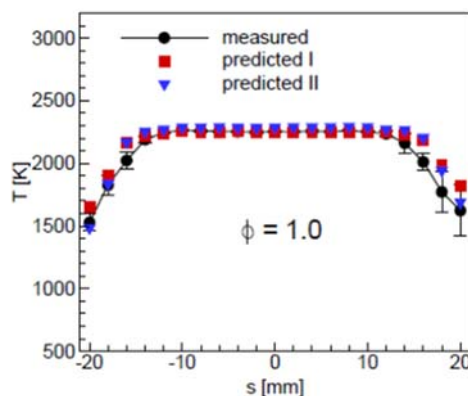


Figure 4.4.6: Temperature profile (for $\phi = 1.0$) 20 mm above the NPL burner measured by NPL (black) and predicted ones based on a machine learning approach with use in the spectral regions 1800 cm^{-1} to 2500 cm^{-1} (predicted I) and 3000 cm^{-1} to 4200 cm^{-1} (predicted II) in DTU's measured spectra at 8 cm^{-1} and 20 mm above the burner. The machine learning algorithm has minimised the difference between the measured and synthesised emission spectra by allowing the temperature profile of the burner to be asymmetric – this has improved the NPL profile at the edge of the flame where the Rayleigh scattering measurement has larger uncertainties.

4.4.3 Development of a UV flame thermometry system

The DTU single line-of-sight optical set-up developed and used for IR/UV gas absorption/emission measurements on the NPL standard burner can be exploited for other flame types and geometries. The set up minimises any ambient effects (for example, variations in ambient temperature and gas composition such as CO_2 and O_2) on the measurements, and significantly decreases the uncertainty of gas temperature measurements. The set up for the IR gas emission measurements together with the NPL standard flame can be exploited for future validations of the HITEMP spectral database. Measured high-temperature absorption cross-sections for CO_2 and H_2O can be used for gas temperature and composition measurements on other flame types or in other hot gas environments on Earth and in space.

Reference measurements of the UV high-resolution absorption cross-sections of CO_2 and H_2O from 500 °C to 1500 °C have been completed successfully, and represent novel measurement data. The absorption cross sections have been used in the analysis of the data obtained on UV flame thermometry system later.

The developed system includes a far UV spectrometer, UV light source and optical adapters (no UV light absorbing optical components) and can be used for narrow line-of-sight measurements typically in 180 nm to 330 nm (limited only by hot CO_2 and H_2O absorptions at low spectral range end). Preliminary measurements on DTU's small gas burner are now completed.

A few issues with burner operation (short and long term stability) have been experienced. Extra spectral features (excess of O_2 , appearance of NO) indicate issues and can be used for “problem solving” with burner operation. Measurements were completed in October 2017 with a unified approach used also for IR

measurements. It was shown that UV spectra have clear CO₂, H₂O and flame O₂ absorption features that can be used for effective gas temperature calculations (i.e. temperature in the middle of the burner). The spectra are free from ambient O₂ absorption. Because it is possible to measure flame O₂, the system can be used for precise control of the NPL and other burners (combustion optimisation).

The measurements on the NPL standard burner were completed recently (in April 2018). UV absorption thermometry can be used for an effective gas temperature (because high flame core-to-flame boundaries ratio) when CO₂/H₂O absorption features are used. The modelled spectra for different ϕ (i.e. equivalence ratios of 0.9, 1 and 1.4) with the use of new UV absorption CO₂/H₂O cross-section data) show effective gas temperature of 1780 K ($\phi = 0.8, 1.4$) and 1787 K for $\phi = 1$ (Figure 4.4.7).

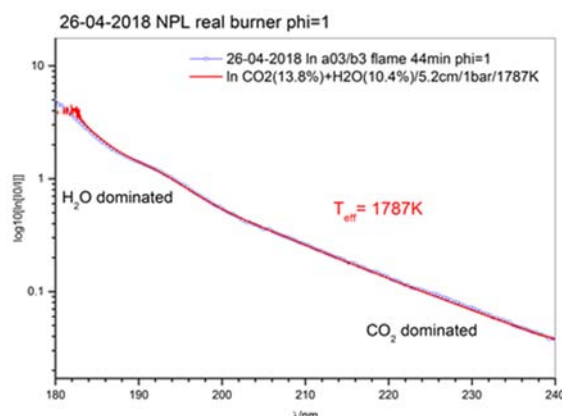


Figure 4.4.7: Measured and synthesized flame spectra of the NPL STD flame from DTU, for $\phi = 1$, 20 mm height above the burner. Red line – synthesised spectra at 1787 K based on new CO₂ and H₂O UV absorption cross section data. Blue line – measured absorption spectrum. Spectral regions with dominated H₂O and CO₂ absorptions are marked.

The measured temperatures are very similar to the *effective temperatures* (i.e. integrated and weighted over a single line of sight). In opposite use of the OH(0-0) absorption/emission band at 310 nm gives a gas temperature in the flame core (e.g. 2250 K for $\phi = 1$). Therefore the UV thermometry system is a valuable and efficient tool for single line of sight flame (hot gas)/boundaries (cold gas) investigations on various flames.

4.4.4 Development of the DFWM and LIGS laser based thermometers

Experiments using LIGS in NO in a O₂:N₂ (25:75 mass ratio) flame have been completed showing successful thermometry in this non-standard laboratory flame at 1 bar pressure yielding a value of 2294 K \pm 82 K i.e. an uncertainty of 3.5 % for only a modest degree of averaging (50 shots / 5 sec average at 10 Hz). A significant fraction of this uncertainty is ascribed to flame flicker with improved precision expected in the NPL standard flame. Using a standard combustion equilibrium code a detection limit for NO of <100 ppm is estimated from the S/N ratio of the LIGS data. The single-mode laser system for LIGS in H₂O at 3 μ m has been constructed and tested. Experiments in the standard flame using H₂O LIGS are complete. Measurements in NO remain a “fall-back” option for thermometry if the IR-LIGS in H₂O is unsuccessful.

Figure 4.4.8 shows examples of UOX measurements on an in-house methane/air burner. The agreement with the predicted temperatures is good.

However, measurements on the NPL standard flame operating at atmospheric pressure were challenging. Difficulties due to the short-lived signals and thermal grating contribution from H₂O absorption, when measuring under these conditions lead to inconsistent and unreliable results. More detailed information on the DFWM and LIGS measurements at UOXF are not available due to staffing issues at UOXF.

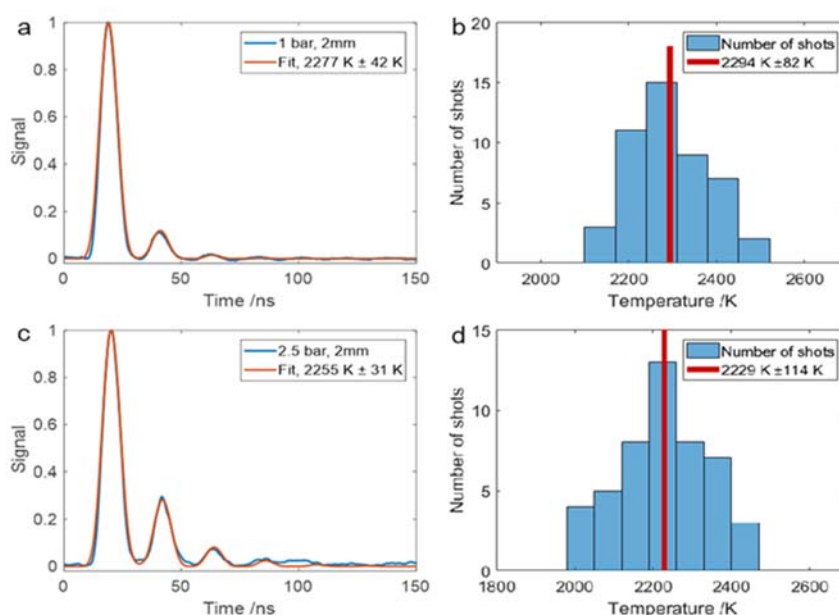


Figure 4.4.8: RIGS temperature measurements made at UOX (for $\phi = 1.0$) for an in-house methane/air burner at 1 Atm. (a and b) and 2.5 atm. (c and d).

Summary of results

- Portable standard flame commissioned and validated using laser Rayleigh scattering thermometry, FTIR thermometry, UV thermometry, DFWM and LIGS thermometry
- Creation of a new measurement service for providing a standard flame temperature

4.5 Overall summary of results

Low-drift contact temperature sensors to above 2000 °C

- Optimised Pt-Rh thermocouple between 1324 °C and 1492 °C identified at Pt-40%Rh/Pt-6%Rh and trialled in-process with satisfactory results in term of stability; preliminary reference function developed; trialled at AFRC and MUT
- Development of stable carbon thermocouples to 1500 °C has been achieved for the first time; trialled at MUT
- Development of a sapphire tube blackbody based sensor for silicon processing, and trialled in-situ at ELKEM. Robustness was excellent, but in-process calibration drift is so far unexplained

Zero-drift contact temperature sensors to 1350 °C

- Self-validating thermocouples developed to 1329 °C and successfully trialled at AFRC and ICPE-CA
- Double wall MI thermocouples trialled up to 1350 °C and showed excellent stability to 1200 °C; successfully trialled at AFRC and Bodycote UK

Traceable surface temperature measurement with contact sensors

- Traceable phosphor thermometry developed to 500 °C – for direct application to surfaces, and to provide the reference temperature of surface probe calibrators; successfully trialled at BAE Systems and Gamma Forgiati
- Heat flux compensated probe developed to 500 °C and validated against embedded thermocouples

Traceable combustion temperature measurement

- Portable standard flame commissioned and validated using laser Rayleigh scattering thermometry, FTIR thermometry, UV thermometry, DFWM and LIGS thermometry
- Creation of a new measurement service for providing a standard flame temperature

5 Impact

5.1 Summary of dissemination activities

To raise the profile of the project and publicise the activities there is a project website hosted by AFRC⁸ (Figure 5.1). A significant effort has been made to interact with relevant members of the high value manufacturing community. As a result the **stakeholder community interacting with the project has grown to 143 members** (Figure 5.1) and several companies have enquired about the results of the project and ways in which to commercially exploit them; this has been detailed below. Stakeholder community newsletters have been sent to the members approximately every 6 months to update members on current results and upcoming events. **Two stakeholder community workshops have been held**; the first was at the AFRC (Advanced Forming Research Centre at STRATH) in Glasgow in March 2017, which attracted around 70 delegates and featured a keynote speech by the Head of Measurement Engineering at Rolls-Royce. The second was held at NPL in April 2018, which again attracted around 65 delegates, and was featured on the Euramet website⁹. Both workshops were sponsored by the Institute of Physics and the Institute of Measurement & Control, both of which have wide membership¹⁰. The workshops were primarily used to bring together scientists and engineers from academia, research institutes and industrial establishments to present and discuss both the latest developments in the field of traceable temperature measurement for process control and end-users' requirements and challenges. These events were very successful and created significant promotion of the EMPRESS project, with very positive feedback received from the delegates.

The phosphor thermometry developments have been instrumental in the formation of the Inaugural International Conference on Phosphor Thermometry (ICPT-2018)¹¹, July 2018 at the University of Strathclyde; the consortium is represented on the organising committee.



Figure 5.1: Left: the project website. Right: the 143 EMPRESS Stakeholder community members.

An introductory paper on the project was presented at 'Metrologie' in Paris in September 2015 (and a more detailed review, as well as technical presentations, was given at Metrologie 2017); a summary paper was published in Measurement and Control, the widely read journal of the Institute for Measurement and Control. A more detailed description of EMPRESS, and several separate talks on more technical outputs, was presented at the XIII Symposium on Temperature and Thermal Measurements in Industry and Science

⁸ <https://www.strath.ac.uk/research/advancedformingresearchcentre/whatwedo/collaborativeprojects/empressproject/>

⁹ https://www.euramet.org/publications-media-centre/news/?tx_news_pi1%5Bnews%5D=667&tx_news_pi1%5Bcontroller%5D=News&tx_news_pi1%5Baction%5D=detail&cHash=84f4dce79da1f252cd4005ef9f76bc98

¹⁰ See the IoP Instrument Science and Technology newsletter http://www.iop.org/activity/groups/subject/isat/news/file_71518.pdf

¹¹ <https://www.icpt18.org/>

(Tempeko 2016) in Poland, and a review paper published in the International Journal of Thermophysics in 2017.

Other conferences at which the project outputs have been presented include Temperatur (PTB, May 2017), 6th Congreso Español de Metrología (Spain, June 2017), Annual XXVII Symposium on Metrology and Metrology Assurance 2017 (Bulgaria, September 2017), Australasian Measurement Conference 2015 (New Zealand, October 2015), 13th ASA/14th HITRAN Conference in Reims (France, August 2016), DKD conference (Berlin 2016), TC-T Workshop on surface thermometry with contact probes (February 2016). The project was featured at the 'ecssmet 2018' conference held at the European Space Agency in May 2018, both through a presentation and a metrology workshop, importantly, focusing on metrology and having an audience drawn from ESA's supply chain and customer base.

EMPRESS and its outputs were presented and discussed at the regular Euramet TC-T meetings¹² in 2015, 2016, 2017 and 2018. This also served as a platform for refining the project objectives and identifying new opportunities and sectors to improve outreach.

The project has also been presented widely at industrial-focused meetings e.g. EVI-GTI International gas turbine instrumentation conference (London 2015 and Amsterdam 2017); ecssmet2017 at ESTEC in the Netherlands; KTN meeting 'Sensing in Extreme Environments' in London 2015; Rolls-Royce measurement seminar 2015 in Manchester; Measurements for Low Carbon Engines (NPL, 2016); ERFA-group for temperature measurement (Denmark, February 2017), Metrologidagen 2017 (Denmark, May 2017), "Nové trendy v oblasti měření vysokých teplot" (New trends in the area of high temperature measurement) (Ostrava, Czech Republic, May 2018). An overview presentation was scheduled for presentation at the AFRC 'Thermal modelling and temperature measurement workshop' in June 2018, and the portable standard flame is scheduled to be a highlight at the Princeton Instruments Combustion Symposium (focused on internal combustion engines) at the Williams Conference Centre, UK in June 2018.

The project has been presented during visits to high value manufacturing companies and other interested parties; these are too numerous to itemise but highlights include Isotech (temperature metrology equipment and calibration), Oxsensis (aerospace fibre-optic based sensing), Esterline (aerospace sensing), University of Strathclyde (oil & gas exploration), Johnson Matthey (precious metal manufacturer), TRM (thermocouple manufacturer), Thermacore (heat pipes), Nature Physics magazine, High Temperature Research Centre (aerospace casting), Sellafield (nuclear decommissioning), Loughborough University (Rolls-Royce University Technical Centre, gas turbine sensing), Airbus Defence & Space, Huddersfield University, MIT (nuclear power sensing), Rolls-Royce (jet propulsion), Trescal (aerospace sensing and calibration), GKN Aerospace (wing spar manufacturing), CCPI Europe (aerospace sensing), University of Sheffield (IR imaging), and the international High Temperature Mechanical Testing Committee. AFRC have extensively promoted the project and its outputs to Tier 1 and Tier 2 members (mainly key aerospace companies e.g. Rolls-Royce, Boeing, Timet, Aubert & Duval)¹³.

Importantly, **the project has given rise to a new annual conference series**, entitled "Thermocouple Users and Manufacturers Conference", held at NPL each year since 2016. Each one-day conference aims to provide 'neutral territory' for users and manufacturers of thermocouples to discuss challenges and solutions in a benign forum without needing to consider commercial aspects, competition, etc. The 3rd conference is due to be held at NPL in December 2018.

Social media

Also associated with the project is the creation of a LinkedIn group "Thermocouples in Industry"¹⁴ which currently has approximately 130 members; the forum is also used for dissemination of outputs and is starting to be used by members for discussion and announcement of their own developments, challenges and events.

AFRC featured EMPRESS in its regular newsletter (May/June 2015), and have been tweeting regular updates on their Twitter and LinkedIn account¹⁵. The project also has its own Research Gate entry with periodic updates on technical developments¹⁶.

¹² Technical Committee for Thermometry

¹³ The Advanced Forming Research Centre (AFRC) is led by its industrial members. Both its governing and technical boards are made up of representatives from these companies: <https://www.strath.ac.uk/research/advancedformingresearchcentre/aboutus/members/>

¹⁴ <https://www.linkedin.com/groups/8588686>

¹⁵ <https://twitter.com/AFRCStrathclyde> and <https://www.linkedin.com/company/advanced-forming-research-centre/>

¹⁶ <https://www.researchgate.net/project/EMPIR-joint-research-project-EMPRESS-Enhancing-process-efficiency-through-improved-temperature-measurement>

Training

The two series of workshops described above (stakeholder community workshop and thermocouple users and manufacturers workshops) both contained a significant training component. Other training activities have also taken place during the project, both as a direct result of project outputs, and also where outputs have a bearing on pre-existing training courses.

These include the 18-monthly NPL Temperature Measurement and Calibration course (new material from EMPRESS included); one-to-one training between consortium members (PTB trained UCAM on the use of high temperature fixed points, NPL trained UC3M, CEM, UOXF and DTU on the use of the portable standard flame); CMI trained the RMG from BIM on surface temperature measurements; material will feature prominently in the Euramet Summer School on Thermal Metrology, Thessaloniki, Greece, 17-21 September 2018.

In addition, an RMG from BIM, Bulgaria collaborated with CMI on the development of the surface temperature probe, contributing a substantial effort to the characterisation of the surface probe calibrator, and benefitting from the expertise at CMI.

In summary, the dissemination, training and publicity for the project has enabled the stakeholder community to grow, opened up new opportunities for collaboration and trials of instrumentation, and should facilitate the uptake of the exploitable results from the project.

5.2 Impact on industrial and other user communities

This project has coordinated expertise distributed across a number of NMIs and enterprises to solve specific temperature measurement challenges. In solving these problems, the resulting improved energy efficiency will inevitably contribute to the goal of reducing carbon emissions. Through scaling these benefits, the impact at the European level is potentially very large. This project should lead to improvements for a wide range of EU enterprises, for example by facilitating better, more efficient manufacturing and lower energy use. Improved temperature measurement will result in tighter process control leading to better, more consistent quality products and so enhancing competitiveness. In addition the outcome of this project could well lead to the retention/creation of skilled high value manufacturing jobs within the EU.

The impact of the project will be very significant for the industrial participants, but would also have strong impact more generally on a broad front. Examples of wider users include the petrochemical industry, nuclear power industry, cement manufacture, iron and steel manufacture, automotive industry, consumer electronics industry, metals industries, food and beverages industry, and healthcare. The introduction of *in-situ* traceability to ITS-90 is embedded in all tasks of this project; this will ensure better consistency across the range of processes impacted.

In the EC Energy Efficiency Plan 2011 [7, page 11], it is stated that “At a time of increasingly scarce energy resources worldwide, expertise in energy efficient processes, technologies and services can also be turned into a new export business, giving a competitive edge to European industries.” A number of project partners in both high value manufacturing and sensor manufacturing are well positioned to realise this ambition.

To give a sense of scale, industrial consumption of electrical energy in Europe amounts to 3.4 PWh (3.4×10^{15} Wh) [63], corresponding to a total electricity cost for European industry of €300 billion per year. Small fractional efficiency improvements arising from improved temperature measurement and control affect large cost reductions, e.g. a 1 % improvement in energy efficiency across all European industry would save €3 billion per year and reduce greenhouse gas emissions by 3.4 million tonnes of CO₂ equivalent. A similar calculation can be done for transport, which is dominated by road users¹⁷ who contribute 20 % of all EU emissions. It can be shown that an efficiency saving of 1 % originating from improved measurement techniques saves Europeans about €3 billion per year. Shifting to a more energy efficient economy is identified as being essential for wide-ranging reasons by European Directive 2012/27/EU [64]. Compliance with environmental regulations [65] is a challenge e.g. the Integrated Pollution Prevention and Control (IPPC) Directive 2008/1/EC, recast as 2010/75/EU in 2010 which imposes a minimum efficiency level in energy use and emissions [66].

Europe currently has 41 % of the world market in aircraft turbine engines [2]. The efficiency is directly related to the combustion temperature, so improved measurement techniques are of great importance; these also have relevance to other energy-intensive industry relying on combustion processes e.g. iron and steel manufacture [67], which currently accounts for 18 % of all energy used in European industry [63]. New

¹⁷ There are about 300 million private automobiles in Europe and 3500 billion passenger-km are travelled each year, giving a mean distance of 11700 km travelled each year per person.

legislation to enforce emissions levels of new vehicles [8] by imposing fuel efficiency targets [9] present additional challenges to manufacturers; improving fuel efficiency is also prioritised in the EC Roadmap 'A Roadmap for moving to a competitive low carbon economy in 2050' [68]. There are few standards specific to flame or combustion thermometry and the development of a standard flame has laid the groundwork for discussions with standards bodies on improving the situation. Particular applications in need of improved standards have been identified, particularly in fire testing where there is a plethora of conflicting standards e.g. FAA Power Plant Engineering Report No. 3A [69], ISO 2685 [70], AC 20-135 [71], FAA Aircraft Material Fire Test Handbook [72], SAE AIR 1377A [73] and SAE AS 1055 [74]. This also applies to manufacture of aircraft and space vehicles. **Direct impact will be via a NPL-run standard flame for traceable calibration of flame thermometry systems.**

Reducing weight of aircraft and other vehicles by using new materials and composites can also significantly improve fuel efficiency and reduce emissions [75]. Despite the increasing popularity of composite materials, new and lighter aluminium alloys e.g. Al-Li [6,76,77] are also competitive but their strength is critically dependent on the heat treatment and subsequent cold work. It is also much more costly than conventional Al alloys, so reduced wastage is a high priority [6]. Forging and forming of these materials will benefit by **improved surface temperature measurement particularly via traceable calibration of users' contact surface temperature probes** [24].

Improved thermocouples will have wider applications to materials characterisation and testing, e.g. creep testing, where thermocouples need to be stable for >10,000 hours, materials processing (e.g. sintering of nuclear fuel >1800 °C), casting, heat treatment, power generation and semiconductor manufacture. Better sensors that can be left in-process for longer with longer maintenance intervals have less risk of breakage, less process interruption and down time and hence are more commercially advantageous. *In-situ* traceability via self-validation will result in a step change in long-term process efficiency and improvements are beneficial for sensor manufacturers in this large market [78]. **Direct impact is already occurring through the involvement of sensor manufacturers as project partners and collaborators**, and a two-pronged approach: licensing of know-how, and approaching the standardisation committees with evidence of the improved performance gained from the project.

Immediate industrial impact is a result of the direct involvement of industrial project partners. In addition, establishing a complete traceability link from industrial temperature measurements through to the SI will flow to end users via a number of routes, all of which have been progressed during the project:

- Commercialisation of new Pt-Rh, carbon and new format (double-walled) Type K/N thermocouples and sapphire based contact sensors via project partners, or other stakeholders, will enable end-users to realise the benefits of ultra-low drift thermocouples over a wide range of temperatures. External collaborators are involved in testing the newly developed thermocouples.
- During the project, partners CCPI and UCAM embarked on a commercial collaboration, with CCPI licensing the ground-breaking double wall MI thermocouple technology from UCAM¹⁸. The instrumentation will be available to end-users through direct sales in the next 12-24 months.
- Commercialisation of self-validating thermocouples will allow the user to realise *in-situ* calibration of thermocouples in-process. Early trials of this have garnered interest for licensing of the technology from CCPI; NPL and CCPI signed a licensing agreement with NPL in May 2018 to allow CCPI, as a large thermocouple manufacturer, to pursue commercial exploitation of the self-validating thermocouples (Figure 5.2).
- A central ISO 17025-ready calibration facility is available for users' contact surface temperature probes, or apparatus, using phosphor thermometry for traceable determination of the actual temperature of the surface.
- Discussions are underway between NPL and a UK metrology equipment manufacturer to license the phosphor thermometry technique for use in surface probe calibrators, which would create a new product line. BAE have expressed a strong desire to use it as soon as possible in order to solve outstanding manufacturing problems and, in particular, improve the efficiency of their welding processes.

¹⁸ <https://www.enterprise.cam.ac.uk/news/cambridge-enterprise-signs-licensing-agreement-revolutionary-thermocouple-cable-technology/>

- A portable standard flame for traceable calibration of users' flame/combustion thermometry systems has been developed and cross-validated at several European facilities; it is now a measurement service ready for provision to interested end-users. There is more information on the NPL website¹⁹. This has paved the way for development of a low-cost instrument in the EMPRESS2 follow-on project.
- The work on Pt-Rh thermocouples has given rise to the revision of the Euramet cg-8 guide on thermocouple calibration, led by NPL and co-authored by several EMPRESS partners. The main revisions are related to advice on how end-users can assess thermoelectric homogeneity – the most important contribution to the overall calibration uncertainty of thermocouples. An extensive survey of homogeneity results in the open literature and from European thermocouple manufacturers has resulted in a publication in the permanent record²⁰ that is cited in the guide. Euramet cg-8 is a particularly important guide as it is used as a *de-facto* reference guide by many accreditation bodies when auditing for compliance with ISO 17025 [79].
- A draft Euramet guide on best practice for surface temperature measurement is currently being prepared by the Euramet TC-T committee on best practice; submission for publication is expected in 2018. The document is expected to evolve further in EMPRESS2.
- The UC3M/CEM Hyperspectral Imaging System has been validated by the cross-comparison of the standard flame against other methods. Following on from this work, UC3M/CEM will develop a practical imaging spectrometer for industrial use in EMPRESS2.
- The DTU single line-of-sight optical setup developed and used for IR/UV gas absorption/emission measurements on the NPL standard flame can be exploited for future validations of the HITEMP spectral database²¹; also measured high temperature absorption cross-sections for CO₂ and H₂O can be used for gas temperature and composition measurements on other flame types or in other hot gas environments on the earth and in space.



Figure 5.2: Left: Jonathan Golding (MD, CCPI Europe) and Penny Owen (Commercial Director, NPL) signing the self-validating thermocouple licensing agreement. Right: post-signing photo opportunity.

5.3 Impact on the metrological and scientific communities

The consortium has representation on the Task Group 'Guides on Thermometry' of the BIPM Consultative Committee for Thermometry (CCT), who are responsible for promoting good thermometry practice and traceability to the SI, with a focus on secondary (i.e. practical) thermometry, and the EURAMET Technical Committee on Thermometry (TC-T). The representation are ensuring that CCT members are fully aware of the project outputs and that project outputs are widely disseminated via EURAMET TC-T activities, including by giving talks at the annual TC-T meeting.

¹⁹ <http://www.npl.co.uk/temperature-humidity/products-services/portable-standard-flame>

²⁰ A comprehensive survey of thermoelectric inhomogeneity of commonly used thermocouple types, J. Machin, D. Tucker, J.V. Pearce, Meas. Sci. Tech. 29 067002 (2018)

²¹ <https://www.cfa.harvard.edu/hitrans/HITEMP.html>; see also "HITEMP, the high-temperature molecular spectroscopic database, L.S. Rothman *et al.*, Spectrosc. and Rad. Transfer 111, 2139-2150 (2010)"

The newly developed sensors will make a substantial impact on the ability of NMIs to effectively disseminate the temperature scale to users up to at least 1800 °C; it is expected that there will be an impact on the Calibration and Measurement Capability of at least one NMI as a result of the project activities, as recorded in the BIPM key comparisons database (KCDB), boosting the technical and economic competitiveness of European NMIs and their customers.

Impact on relevant standards

- Informed IEC/SC65B/WG5 convenor (Masahiko Gotoh) of progress on the development of Pt-40%Rh/Pt-6%Rh thermocouples, and the key findings; a provisional draft reference function has been developed which is under consideration for publication in *Metrologia*
- UCAM/CCPI presentation of the double wall MI thermocouple results at the SAE International Aerospace Electrical Interconnect Systems Symposium (AEISS) meeting to AMEC²² committee (responsible for the AMS2750E aerospace heat treatment standard) in October 2016
- UCAM/CCPI invited to present the double wall MI thermocouple developments to the IEC/SC65B/WG5 committee on IEC 61515 thermocouple specifications at the next meeting in Berlin 26-28 September 2018; a document will be sent beforehand to prepare the ground
- CCPI presenting the double wall MI thermocouple developments to the ASTM May 2018 Committee Week in San Diego, 20-24 May 2018, specifically the E20 committee responsible for ASTM E 585/E 585M – 04 on MI thermocouple cable (the American equivalent to IEC 61515)
- UCAM presenting the double wall MI thermocouple developments to the NADCAP committee in London, June 2018

Further collaborations

- University of Sheffield as collaborator in EMPRESS2 on phosphor thermometry
- CCPI/UCAM – further development and optimisation of double wall MI thermocouples via commercial partnership
- CCPI/NPL – further development of self-validating thermocouples to the point of being ready for offer as a product
- UCAM have embarked on further collaborations with Bodycote UK, Bodycote Romania, and SAFRAN (France) on opportunities for further proving of the double wall MI thermocouples
- University of Loughborough will be a collaborator in EMPRESS2 on phosphor thermometry
- HTRC have expressed an interest in the thermocouple developments for casting of single crystal nickel alloy turbine blades in their RR-sponsored test facility; they have signed the collaborator agreement at a late stage in EMPRESS and hope to offer trials in EMPRESS2
- INRIM have developed a collaboration with ITT (manufacture of automotive braking equipment) and CNR (tribology) and will partner in EMPRESS2
- NPL, STRAT, DTI and BAE will collaborate on development and testing of phosphor thermometry for marine manufacturing applications
- NPL, DTU, B&W Volund, Sensia and UC3M will collaborate on putting the portable standard flame into practice for development of practical imaging flame thermometry that can be commercialised
- PTB, JV, MUT, IPHT and Elkem will collaborate on a hybrid blackbody/fibre Bragg grating thermometer for practical thermometry in high value manufacturing applications where thermocouples are not suitable
- NPL and Southampton will collaborate on the development of optical fibre thermometry using hollow core fibre bundles
- CEM, CSIC and Acerinox will collaborate on development of distributed fibre optic sensing

²² AMS AMEC Aerospace Metals and Engineering Committee

- AFRC and its parent University of Strathclyde are collaborating further via a CATP (EPSRC) 'Pathways to Impact' funded project involving applied phosphor thermometry
- A number of the collaborations listed above will feed into development activities in EMPRESS2

The project has, and will have, impact on a broad front. Through improved facilities at NMIs and the resulting propagation of lower uncertainties, as well as through new products which are in the process of being commercialised, better efficiency and consistency across a wide range of processes will be achievable. The efficiency of almost every process depends on its accurate temperature control; furthermore, improving energy efficiency is inextricably linked to reduced carbon emissions. Sectors that are vulnerable to rising energy prices and EU policies aimed at reducing greenhouse gases, with the resulting threat to international competitiveness, will benefit from improved process control. As sensors become more reliable in the longer term, safety will also increase. Shifting to a more energy efficient economy will accelerate the spread of technological innovations and boost economic growth, creating high quality jobs. Finally, the population of the EU is increasingly affected by climate change; energy efficiency is a key factor in the reduction of the causative greenhouse gases.

6 List of publications

1. Extra points for thermometry, J.V. Pearce, Nature Physics Vol. 13, January 2017, p. 104
2. Relating composition and thermoelectric stability of Pt-Rh alloy thermocouples, J.V. Pearce, A. Smith, C.J. Elliott, A. Greenen, Int. J. Thermophys. 38, 26 (2017)
3. EMPRESS: A pan-European project to enhance manufacturing process efficiency through improved temperature control, J.V. Pearce, Measurement and Control, Vol. 49 No. 8 pp. 252-255, October 2016
4. Optimising Pt-Rh thermocouple wire composition to minimise composition change due to evaporation of oxides, J.V. Pearce, Johnson Matthey Technology Review 60(4) 238-242 (2016)
5. EMPRESS – A European Project to enhance process efficiency through improved temperature measurement, J.V. Pearce, F. Edler, C.J. Elliott, L. Rosso, G. Sutton, S. MacKenzie, G. Machin, Proc. 17th International Congress of Metrologie (2015), EDP Sciences, DOI: 10.1051/metrology/20150008001 (2015)
6. Major Step Forward in Type K and Type N Thermocouple Performance, T. Ford, Industrial Heating, 8 January 2018, <https://www.industrialheating.com/articles/93965-major-step-forward-in-type-k-and-n-thermocouple-performance>
7. Thermoelemente auf Graphitbasis - Möglichkeiten und Grenzen; Graphite-based thermocouples – possibilities and limitation, F. Edler, S. Haupt, tm – Technisches Messen, Volume 84, Issue 12, Pages 779–786 (2017) doi.org/10.1515/teme-2017-0073
8. The NPL Standard Flame: operating instructions, NPL Report ENG 65, November 2016, ISSN 1754-2987 <http://www.npl.co.uk/content/ConPublication/7281>

7 Website address and contact details

Coordinator:

Jonathan Pearce
National Physical Laboratory
Hampton Road
Teddington
TW11 0LW
United Kingdom
jonathan.pearce@npl.co.uk
+44 20 8943 6886

Website:

<https://www.strath.ac.uk/research/advancedformingresearchcentre/whatwedo/collaborativeprojects/empressproject/>

8 References

[1] The World Bank:

<http://data.worldbank.org/indicator/NV.IND.MANF.CD/countries/1W-EU-XC?display=graph>

[2] FWC Sector Competitiveness Studies – Competitiveness of the EU Aerospace Industry with focus on Aeronautics Industry, ENTR/06/054 (ECORYS study for European Commission)

http://ec.europa.eu/enterprise/sectors/aerospace/files/aerospace_studies/aerospace_study_en.pdf

[3] Strategic Research Agenda, Volume 1, Advisory Council for Aeronautics in Europe, October 2004

<http://www.acare4europe.com/sites/acare4europe.org/files/document/ASD-volume1-2nd-final-ss%20illus-171104-out-asd.pdf>

[4] 2008 Addendum to the Strategic Research Agenda, Advisory Council for Aeronautics in Europe

http://www.acare4europe.com/sites/acare4europe.org/files/document/ACARE_2008_Addendum_1.pdf

[5] H.B. Callen, Thermodynamics and an Introduction to Thermostatistics, 2nd Ed., John Wiley & Sons, Inc. ISBN 0-471-86245-8 (1985)

[6] Aerospace Materials, Edited by B. Cantor, P. Grant, H. Assender, Taylor & Francis 2001. ISBN 987-1-4200-3472-1

[7] European Commission communication COM(2011) 109 final, Energy Efficiency Plan 2011

http://eur-lex.europa.eu/resource.html?uri=cellar:441bc7d6-d4c6-49f9-a108-f8707552c4c0.0002.03/DOC_1&format=PDF

[8] European Commission COM(2007) 19 final, Results of the review of the Community Strategy to reduce CO₂ emissions from passenger cars and light-commercial vehicles

<http://eur-lex.europa.eu/legal-content/EN/TXT/PDF/?uri=CELEX:52007DC0019&from=EN>

[9] European Commission COM(2010) 656 final, Progress report on implementation of the Community's integrated approach to reduce CO₂ emissions from light-duty vehicles

<http://eur-lex.europa.eu/legal-content/EN/TXT/PDF/?uri=CELEX:52010DC0656&from=EN>

[10] Aerospace Material Specification (AMS) 2750 REV. E – Pyrometry

[11] Thermocouple Temperature Measurement, P.A. Kinzie, John Wiley & Sons, 1973. ISBN 0-471-48080-0

[12] ASTM E1751/E1751M – 09 Standard Guide for Temperature Electromotive Force (emf) Tables for Non-Letter Designated Thermocouple Combinations

[13] J.V. Pearce, C.J. Elliott, G. Machin, O. Ongrai, Self-validating Type C thermocouples using high temperature fixed points, 9th International Temperature Symposium, AIP Conf. Proc. 1552, 595 (2013)

[14] M. Scervini and C. Rae, An Improved Nickel Based MIMS Thermocouple for High Temperature GasTurbine Applications, Journal of Engineering for Gas Turbines and Power, September 2013, Vol. 135, p. 091601. DOI: 10.1115/1.4024420.

<http://gasturbinespower.asmedigitalcollection.asme.org/article.aspx?articleid=1723418>

Patent number WO2011121313A1.

[15] Factories of the future: European Commission multi-annual roadmap for the contractual PPP under Horizon 2020, Policy Research document prepared by EFFRA

<http://bookshop.europa.eu/en/factories-of-the-futurepbKl0213266/?CatalogCategoryID=9cQKABstREYAAAEjKJEY4e5L>

- [16] A Review of DRA Work on Marine Strength Steels, Offshore Technology Report – OTO 97 066, Health and Safety Executive, November 1997
<http://www.hse.gov.uk/research/otopdf/1997/oto97066.pdf>
- [17] BS EN 13445-1:2009 Unfired pressure vessels Part 1: General & BS EN 13445-4:2009+A1:2011 Unfired pressure vessels Part 4: Fabrication
- [18] ASME Boiler and Pressure Vessel Code (BPVC) Section VIII – Rules for Construction of Pressure Vessels
- [19] PD 5500:2012+A2:2013 Specification for unfired fusion welded pressure vessels
- [20] ISO 15614-1 (2004) Specification and qualification of welding procedures for metallic metals – Welding procedure test – Part 1: Arc and gas welding of steels and arc welding of nickel and nickel alloys
- [21] EUROMET Project No. 635 Final Report: Comparison of the reference surface temperature apparatus atNMLs by comparison of transfer surface temperature standards, E. András, November 2003
- [22] R. Morice, E. András, E. Devin, T. Kovacs, “Contribution for the calibration and the use of surface temperature sensors”, in Proceedings of TEMPMEKO 2001, 8th International Symposium on Temperature and Thermal Measurements in Industry and Science, ed. By B. Fellmuth, J. Seidel, G. Scholz (VDE Verlag, Berlin, 2002), pp. 1111-1116
- [23] BS EN ISO 8502-4:2000 Preparation of steel substrates before application of paints and related products – Tests for the assessment of surface cleanliness – Part 4: Guidance on the estimation of the probability of condensation prior to paint application.
- [24] Enhancements of Aluminum Alloy Forgings through Rapid Billet Heating, Final Technical Report ORNL/TM-2006/30, June 2006
https://www.forging.org/system/files/field_document/Enhancement.pdf
- [25] R.T.E. Hermanns, A.A. Konnov, R.J.M. Bastiaans, L.P.H. de Goey, K. Lucka, H. Köhne, Effects of temperature and composition on the laminar burning velocity of CH₄ + H₂ + O₂ + N₂ flames, Fuel, 89 (2010) 114-121
- [26] Reduction of emissions and energy utilisation of coke oven underfiring heating systems through advanced diagnostics and control (Ecocarb), European Commission Research Fund for Coal and Steel, M. Saiepour, J. Delinchant, J. Soons, F. Huhn, J. Morris, Final Report. ISBN 978-92-79-29187-6
<http://bookshop.europa.eu/en/reduction-of-emissions-and-energy-utilisation-of-coke-oven-underfiringheating-systems-through-advanced-diagnostics-and-control-ecocarb--pbKINA25902/?CatalogCategoryID=w2wKABst3XAAAEjfJEY4e5L>
- [27] G. Sutton, A. Levick, G. Edwards, and D. Greenhalgh, A combustion temperature and species standard for the calibration of laser diagnostic techniques, Combustion and Flame 147 (2006) 39-48
- [28] J.C. Jones, Suggestions Towards Improved Reliability of Thermocouple Temperature Measurement in Combustion Tests, in Thermal Measurements: The Foundation of Fire Standards, Gritz LA, Alvares N, ASTM STP1427 (2003)
http://www.astm.org/DIGITAL_LIBRARY/STP/SOURCE_PAGES/STP1427.htm
- [29] Euramet TC-T Temperature Roadmap and explanatory notes
<http://www.euramet.org/index.php?id=1652>
- See also: G. Machin, J. Bojkovski, D. del Campo, A.K. Dogan, J. Fischer, Y. Hermier, A. Merlone, J. Nielsen, A. Peruzzi, J. Ranostaj, R. Strnad, A European Roadmap for Thermometry, Int. J. Thermophys. 35, 385-394 (2014)
- [30] H. Preston-Thomas, The International Temperature Scale of 1990 (ITS-90), Metrologia 27 (1990) 3-10; erratum: Metrologia 27 (1990) 107
- [31] Manual on The Use of Thermocouples in Temperature Measurement, American Society for Testing and Materials, 4th Edition, Ann Arbor, Michigan, USA, 1993

- [32] R.E. Bedford, Reference tables for platinum-40% rhodium / platinum-20% rhodium thermocouples, *Rev. Sci. Instrum.* 36 1571-80
- [33] J.V. Pearce, C.J. Elliott, A. Greenen, D. del Campo, M.J. Martin, C. Garcia Izquierdo, P. Pavlasek, P. Nemecek, G. Failleau, T. Deuze, M. Sadli, G. Machin, A pan-European investigation of the Pt-40%Rh/Pt-20%Rh (Land-Jewell) thermocouple reference function, *Meas. Sci. Technol.* 26 015101 (2015)
- [34] F. Edler and P. Ederer, Thermoelectric homogeneity and stability of platinum-rhodium alloyed thermoelements of different compositions, *AIP Conf. Proc.* 1552 532 (2013)
- [35] J.V. Pearce, Optimising Platinum-Rhodium Thermocouple Wire Composition to Minimise Composition Change Due to Evaporation of Oxides, *Johnson Matthey Technology Review*, 60(4) 238-242 (2016)
- [36] J.C. Chaston, The Oxidation of the Platinum Metals, *Platin. Metals Rev.* 19 135 (1975)
- [37] C.B. Alcock and G.W. Hooper, Thermodynamics of the gaseous oxides of the platinum-group metals, *Proc. R. Soc.* 254 551 (1960)
- [38] E.S. Webster, A.G. Greenen, J.V. Pearce, Measurement of the Inhomogeneity in Type B and Land-Jewell Noble-Metal Thermocouples, *Int. J. Thermophys.* 37 70 (2016)
- [39] J.V. Pearce, Extra points for thermometry, *Nature Physics* Vol. 13, January 2017, p. 104
- [40] Y. Yamada, H. Sakate, E. Sakuma, A. Ono, Radiometric observation of melting and freezing plateaus for a series of metal-carbon eutectic points in the range 1330 °C to 1950 °C, *Metrologia* 36 207-209 (1999)
- [41] Investigation of Co-C cells for improved thermocouple calibration, F. Edler, R. Morice, H. Ogura, and J.V. Pearce, *Metrologia* 90 47 (2010)
- [42] Investigation of Pd-C cells to improve thermocouple calibration, J.V. Pearce, F. Edler, C.J. Elliott, G. Failleau, R. Morice, and H. Ogura, *Metrologia* 48 375-381 (2011)
- [43] J.V. Pearce, A.D. Greenen, A. Smith and C.J. Elliott, Relating composition and thermoelectric stability of Pt-Rh alloy thermocouples, *Int. J. Thermophys.*, 38 26 (2017)
- [44] Relating composition and thermoelectric stability of Pt-Rh alloy thermocouples, J.V. Pearce, A. Smith, C.J. Elliott, A. Greenen, *Int. J. Thermophys.* 38, 26 (2017)
- [45] The research outcomes of the European Metrology Research Programme Project: HiTeMS – High Temperature Measurement Solutions for Industry, G. Machin, E. Vuelban, M. Sadli, F. Edler, R. Strnad, K. Anhalt, J. Pearce, M. Siefert, *Measurement* 78 pp. 168-179 (2016)
- [46] Y. Yamada, H. Sakate, F. Sakuma and A. Ono, "A possibility of practical high temperature fixed points above the copper point," in 7th International Symposium on Temperature and Thermal Measurements in Industry and Science, Delft, 1999
- [47] Extra points for thermometry, J.V. Pearce, *Nature Physics* Vol. 13, January 2017, p. 104
- [48] C. J. Elliott, A. D. Greenen, D. J. L. Tucker and J. V. Pearce, "A Slimline Integrated Self-Validating Thermocouple: Initial Results," *International Journal of Thermophysics*, vol. 38, no. 9, p. 141, 2017
- [49] F. Edler, S. Haput, S. -A. Mokdad, G. Failleau and M. Sadli, "Investigation of self-validating thermocouples with integrated fixed-point units," *International Journal of Metrology and Quality Engineering*, vol. 6, no. 1, 2015
- [50] G. Krapf, T. Froehlich, S. Augustin, H. Mannen, G. Blumroeder, M. Schalles and F. Hilbrunner, "Long Term Stability of Miniature Fixed-Point Cells Used in Self-Calibrating Thermometers," in *Proceedings SENSOR 2011, Nürnberg*, 2011.
- [51] M. Tischler and M. J. Korembli, "Miniature thermometric fixed points for thermocouple calibrations," *Temperature: Its Measurement and Control in Science and Industry*, vol. 5, p. 383–90, 1982.
- [52] O. Ongrai, J. V. Pearce, G. Machin and S. J. Sweeney, "Miniature Co-C eutectic fixed-point cells for self-validating thermocouples," *Measurement Science and Technology*, vol. 22, 2011.
- [53] G. Failleau, C. J. Elliott, T. Deuzé, J. V. Pearce, G. Machin and M. Sadli, "Miniature Fixed-Point Cell Approaches for In-Situ Monitoring Of Thermocouple Stability," *Download PDF*, vol. 35, no. 6-7, pp. 1223-1238, 2014.

- [54] H. Lehmann, "Fixed-Point Thermocouple in Power Plants: Long-Term Operational Experiences," *International Journal of Thermophysics*, vol. 31, pp. 1599-1607, 2010.
- [55] Self-validating Type C thermocouples using high temperature fixed points, J.V. Pearce, C.J. Elliott, G. Machin, O. Ongrai, 9th International Temperature Symposium, AIP Conf. Proc. 1552, 595 (2013)
- [56] L. Michalski, K. Eckersdorf, J. Kucharski, J. McGhee, *Temperature Measurement of Solid Bodies by Contact Method*, Temperature Measurement, John Wiley & Sons, Ltd 2002, pp. 333-360.
- [57] M. Lidbeck, J. Ivarsson, E. András, J.E. Holmen, T. Weckström, F. Andersen, *Interlaboratory Comparison of Reference Surface Temperature Apparatus at NMIs*, *International Journal of Thermophysics*, 29 (2008) 414-422
- [58] I. Saito, T. Nakano, J. Tamba, *Estimating Surface Temperature of a Calibration Apparatus for Contact Surface Thermometers from Its Internal Temperature Profile*, *International Journal of Thermophysics*, 38 (2017) 156
- [59] E. Turzo-Andras, *Calibration of Contact Surface Thermometers*, *International Journal of Thermophysics*, 39 (2017) 15.
- [60] L. Thorington, *Temperature Dependence of the Emission of an Improved Manganese-Activated Magnesium Germanate Phosphor*, *J. Opt. Soc. Am. A*, DOI (1950).
- [61] M.A. Everest, D.B. Atkinson, Discrete sums for the rapid determination of exponential decay constants, *Rev. Sci. Instr.* 79, 023108 (2008)
- [62] J. Brübach, J. P. Feist and A. Dreizle, Characterization of manganese-activated magnesium fluorogermanate with regards to thermographic phosphor thermometry, *Meas. Sci. Technol.* 19, 025602 (2008)
- [63] Energy, transport and environment indicators, Eurostat (European Commission), 2012 edition, ISSN 1725-4566
http://epp.eurostat.ec.europa.eu/cache/ITY_OFFPUB/KS-DK-12-001/EN/KS-DK-12-001-EN.PDF
- [64] Directive 2012/27/EU of the European Parliament and of the Council of 25 October 2012, on energy efficiency
http://ec.europa.eu/energy/efficiency/eed/eed_en.htm
- [65] FWC Sector Competitiveness Studies – Competitiveness of the EU Non-ferrous Metals Industries, KR/NZ FN97624 (ECORYS study for European Commission)
http://ec.europa.eu/enterprise/sectors/metals-minerals/files/fn97624_nfm_final_report_5_april_en.pdf
- [66] Directive 2008/1/EC of the European Parliament and of the Council of 15 January 2008, concerning integrated pollution prevention and control
<http://eur-lex.europa.eu/legal-content/EN/TXT/PDF/?uri=CELEX:32008L0001&from=EN>
- Recast in 2010: Directive 2010/75/EU of the European Parliament and of the Council of 24 November 2010 on industrial emissions (integrated pollution prevention and control) (Recast)
<http://eur-lex.europa.eu/LexUriServ/LexUriServ.do?uri=OJ:L:2010:334:0017:0119:en:PDF>
- [67] Green Jobs: Towards decent work in a sustainable, low-carbon world, United Nations Environment Programme, September 2008
http://www.unep.org/PDF/UNEPGreenjobs_report08.pdf
- [68] European Commission COM(2011) 112 final, A Roadmap for moving to a competitive carbon economy in 2050
http://eur-lex.europa.eu/resource.html?uri=cellar:5db26ecc-ba4e-4de2-ae08-dba649109d18.0002.03/DOC_1&format=PDF
- [69] FAA Power Plant Engineering Report No. 3A: Standard Fire Test Apparatus and Procedure (For Flexible Hose Assemblies), Revised March 1978
- [70] ISO 2685:1998(E) Aircraft – Environmental test procedure for airborne equipment – Resistance to fire in designated fire zones

- [71] AC 20-135: Powerplant Installation and Propulsion System Component Fire Protection Test Methods, Standards and Criteria, Revised 1990
- [72] FAA Aircraft Material Fire Test Handbook: Chapter 11 Powerplant Hose Assemblies Test and Chapter 12 Powerplant Fire Penetration Test - used to determine the fire resistance components used in designated fire zones to damage due to flame and vibration for showing compliance with TSO C42, C53A, and C75. April 2000
- [73] SAE AIR 1377A: Fire Test Equipment for Flexible Hose and Tube Assemblies, Revised January 1980
- [74] SAE AS 1055: Fire Testing of Flexible Hose, Tube Assemblies, Coils, Fittings and Similar System Components, Revised 1978
- [75] European Commission COM(2011) 144 final, WHITE PAPER: Roadmap to a Single European Transport Area – Towards a more competitive and resource efficient transport system
<http://eur-lex.europa.eu/legal-content/EN/TXT/PDF/?uri=CELEX:52011DC0144&from=EN>
- [76] Al-Li Alloys: Processing, Properties, and Applications, N.E. Prasad, A. Gokhale, R.J.H. Wanhill, Butterworth-Heinemann (7 Nov 2013), ISBN 978-0124016989
- [77] C. Giummarra, B. Thomas, R. Rioja, New Aluminum Lithium Alloys for Aerospace Applications, Proceedings of the 3rd Light Metals Technology Conference 2007, September 24-26, 2007, Saint-Saveur, Quebec, Canada
http://alcoa.com/global/en/innovation/papers_patents/pdf/lmt2007_110.pdf
- [78] Self-Validating Thermocouples: Technology Assessment, A Report for the National Physical Laboratory, Prepared by Frost & Sullivan, December 2008
- [79] ISO/IEC 17025:2005 General requirements for the competence of testing and calibration laboratories